



McDONALD INSTITUTE MONOGRAPHS

Temple landscapes

Fragility, change and resilience of Holocene environments in the Maltese Islands

By Charles French, Chris O. Hunt, Reuben Grima,
Rowan McLaughlin, Simon Stoddart & Caroline Malone



Volume 1 of Fragility and Sustainability – Studies on Early Malta,
the ERC-funded *FRAGSUS Project*

Temple landscapes



McDONALD INSTITUTE MONOGRAPHS

Temple landscapes

Fragility, change and resilience of Holocene environments in the Maltese Islands

By Charles French, Chris O. Hunt, Reuben Grima,
Rowan McLaughlin, Simon Stoddart & Caroline Malone

With contributions by

Gianmarco Alberti, Jeremy Bennett, Maarten Blaauw, Petros Chatzimpaloglou,
Lisa Coyle McClung, Alan J. Cresswell, Nathaniel Cutajar, Michelle Farrell,
Katrin Fenech, Rory P. Flood, Timothy C. Kinnaird, Steve McCarron,
Rowan McLaughlin, John Meneely, Anthony Pace, Sean D.F. Pyne-O'Donnell,
Paula J. Reimer, Alastair Ruffell, George A. Said-Zammit, David C.W. Sanderson,
Patrick J. Schembri, Sean Taylor, David Trumpp, Jonathan Turner, Nicholas C. Vella
& Nathan Wright

Illustrations by

Gianmarco Alberti, Jeremy Bennett, Sara Boyle, Petros Chatzimpaloglou,
Lisa Coyle McClung, Rory P. Flood, Charles French, Chris O. Hunt, Michelle Farrell,
Katrin Fenech, Rowan McLaughlin, John Meneely, Anthony Pace, David Redhouse,
Alastair Ruffell, George A. Said-Zammit & Simon Stoddart



Volume 1 of Fragility and Sustainability – Studies on Early Malta,
the ERC-funded *FRAGSUS Project*



This project has received funding from the European Research Council (ERC) under the European Union's Seventh Framework Programme (FP7-2007-2013) (Grant agreement No. 323727).

Published by:

McDonald Institute for Archaeological Research
University of Cambridge
Downing Street
Cambridge, UK
CB2 3ER
(0)(1223) 339327
eaj31@cam.ac.uk
www.mcdonald.cam.ac.uk



McDonald Institute for Archaeological Research, 2020

© 2020 McDonald Institute for Archaeological Research.

Temple landscapes is made available under a Creative Commons Attribution-NonCommercial-NoDerivatives 4.0 (International) Licence:
<https://creativecommons.org/licenses/by-nc-nd/4.0/>

ISBN: 978-1-902937-99-1

Cover design by Dora Kemp and Ben Plumridge.
Typesetting and layout by Ben Plumridge.

On the cover: *View towards Nadur lighthouse and Ghajnsielem church with the Gozo Channel to Malta beyond, from In-Nuffara (Caroline Malone).*

Edited for the Institute by James Barrett (*Series Editor*).

CONTENTS

Contributors		xi
Figures		xiii
Tables		xvi
Preface and dedication		xix
Acknowledgements		xxi
Foreword		xxiii
<i>Introduction</i>	CAROLINE MALONE, SIMON STODDART, CHRIS O. HUNT, CHARLES FRENCH, ROWAN McLAUGHLIN & REUBEN GRIMA	1
0.1. Introduction		1
0.2. Background to <i>FRAGSUS</i> as an archaeological project		3
0.3. Environmental research in Malta and the Mediterranean		5
0.4. The development of the <i>FRAGSUS Project</i> and its questions		6
0.5. Archaeological concerns in Maltese prehistory and the <i>FRAGSUS Project</i>		8
0.6. The research programme: the sites and their selection		9
0.7. Investigating the palaeoenvironmental context		10
0.8. Archaeological investigations		11
Part I	The interaction between the natural and cultural landscape – insights into the fifth–second millennia BC	17
<i>Chapter 1</i>	The geology, soils and present-day environment of Gozo and Malta PETROS CHATZIMPALOGLOU, PATRICK J. SCHEMBRI, CHARLES FRENCH, ALASTAIR RUFFELL & SIMON STODDART	19
1.1. Previous work		19
1.2. Geography		19
1.3. Geology		21
1.4. Stratigraphy of the Maltese Islands		23
1.4.1. Lower Coralline Limestone Formation		23
1.4.2. Globigerina Limestone Formation		23
1.4.3. Chert outcrops		25
1.4.4. Blue Clay Formation		26
1.4.5. Greensand Formation		28
1.4.6. Upper Coralline Limestone Formation		28
1.4.7. Quaternary deposits		29
1.5. Structural and tectonic geology of the Maltese Islands		29
1.6. Geomorphology		29
1.7. Soils and landscape		31
1.8. Climate and vegetation		32
<i>Chapter 2</i>	Chronology and stratigraphy of the valley systems CHRIS O. HUNT, MICHELLE FARRELL, KATRIN FENECH, CHARLES FRENCH, ROWAN McLAUGHLIN, MAARTEN BLAAUW, JEREMY BENNETT, RORY P. FLOOD, SEAN D. F. PYNE-O'DONNELL, PAULA J. REIMER, ALASTAIR RUFFELL, ALAN J. CRESSWELL, TIMOTHY C. KINNAIRD, DAVID SANDERSON, SEAN TAYLOR, CAROLINE MALONE, SIMON STODDART & NICHOLAS C. VELLA	35
2.1. Methods for dating environmental and climate change in the Maltese Islands		35
2.1.1. Data sources for chronology building		35
2.1.2. Pottery finds		41

2.2. Basin infill ground penetrating radar surveys	41
ALASTAIR RUFFELL, CHRIS O. HUNT, JEREMY BENNETT, RORY P. FLOOD, SIMON STODDART & CAROLINE MALONE	
2.2.1. <i>Rationale</i>	41
2.2.2. <i>Geophysics for basin fill identification</i>	41
2.2.3. <i>Valley locations</i>	43
2.3. The sediment cores	43
CHRIS O. HUNT, MICHELLE FARRELL, RORY P. FLOOD, KATRIN FENECH, ROWAN McLAUGHLIN, NICHOLAS C. VELLA, SEAN TAYLOR & CHARLES FRENCH	
2.3.1. <i>Aims and methods</i>	43
2.3.2. <i>The core descriptions</i>	49
2.3.3. <i>Magnetic susceptibility and XRF analyses of the cores</i>	59
2.4. Age-depth models	64
MAARTEN BLAUW & ROWAN McLAUGHLIN	
2.4.1. <i>Accumulation rates</i>	64
2.5. A local marine reservoir offset for Malta	65
PAULA J. REIMER	
2.6. Major soil erosion phases	65
RORY P. FLOOD, ROWAN McLAUGHLIN & MICHELLE FARRELL	
2.6.1. <i>Introduction</i>	65
2.6.2. <i>Methods</i>	66
2.6.3. <i>Results</i>	67
2.6.4. <i>Discussion</i>	68
2.6.5. <i>Conclusions</i>	71
Chapter 3 The Holocene vegetation history of the Maltese Islands	73
MICHELLE FARRELL, CHRIS O. HUNT & LISA COYLE McCLUNG	
3.1. Introduction	73
CHRIS O. HUNT	
3.2. Palynological methods	74
LISA COYLE-McCLUNG, MICHELLE FARRELL & CHRIS O. HUNT	
3.3. Taxonomy and ecological classification	75
CHRIS O. HUNT	
3.4. Taphonomy	75
CHRIS O. HUNT & MICHELLE FARRELL	
3.5. The pollen results	87
MICHELLE FARRELL, LISA COYLE-McCLUNG & CHRIS O. HUNT	
3.5.1. <i>The Salina cores</i>	87
3.5.2. <i>Wied Żembaq</i>	87
3.5.3. <i>Xemxija</i>	87
3.5.4. <i>In-Nuffara</i>	87
3.5.5. <i>Santa Verna</i>	95
3.5.6. <i>Ġgantija</i>	105
3.6. Synthesis	107
3.6.1. <i>Pre-agricultural landscapes (pre-5900 cal. BC)</i>	107
3.6.2. <i>First agricultural colonization (5900–5400 cal. BC)</i>	108
3.6.3. <i>Early Neolithic (5400–3900 cal. BC)</i>	109
3.6.4. <i>The later Neolithic Temple period (3900–2350 cal. BC)</i>	110
3.6.5. <i>The late Neolithic–Early Bronze Age transition (2350–2000 cal. BC)</i>	111
3.6.6. <i>The Bronze Age (2000–1000 cal. BC)</i>	112
3.6.7. <i>Late Bronze Age, Punic and Classical periods (c. 1000 cal. BC to AD 1000)</i>	112
3.6.8. <i>Medieval to modern (post-AD 1000)</i>	113
3.7. Conclusions	113

<i>Chapter 4</i>	Molluscan remains from the valley cores	115
	KATRIN FENECH, CHRIS O. HUNT, NICHOLAS C. VELLA & PATRICK J. SCHEMBRI	
	4.1. Introduction	115
	4.2. Material	117
	4.3. Methods	117
	4.4. Radiocarbon dates and Bayesian age-depth models	117
	4.5. Results	117
	4.5.1. Marsaxlokk (MX1)	127
	4.5.2. Wied Żembaq (WŻ)	127
	4.5.3. Mġarr ix-Xini (MĠX)	128
	4.5.4. Marsa 2	128
	4.5.5. Salina Deep Core	133
	4.5.6. Xemxija 1 and 2	152
	4.6. Interpretative discussion	153
	4.6.1. Erosion – evidence of major events from the cores	153
	4.7. Environmental reconstruction based on non-marine molluscs	155
	4.7.1. Early Holocene (c. 8000–6000 cal. BC)	155
	4.7.2. Mid-Holocene (c. 6000–3900 cal. BC)	155
	4.7.3. Temple Period (c. 3900–2400 cal. BC)	155
	4.7.4. Early to later Bronze Age (2400–c. 750 cal. BC)	155
	4.7.5. Latest Bronze Age/early Phoenician period to Late Roman/Byzantine period (c. 750 cal. BC–cal. AD 650)	156
	4.8. Concluding remarks	156
	4.9. Notes on selected species	157
	4.9.1. Extinct species	157
	4.9.2. Species with no previous fossil record	158
	4.9.3. Other indicator species	158
<i>Chapter 5</i>	The geoarchaeology of past landscape sequences on Gozo and Malta	161
	CHARLES FRENCH & SEAN TAYLOR	
	5.1. Introduction	161
	5.2. Methodology and sample locations	164
	5.3. Results	165
	5.3.1. Santa Verna and its environs	165
	5.3.2. Ġgantija temple and its environs	174
	5.3.3. Skorba and its immediate environs	183
	5.3.4. Taċ-Ċawla settlement site	188
	5.3.5. Xaġhra town	190
	5.3.6. Ta' Marżiena	192
	5.3.7. In-Nuffara	192
	5.3.8. The Ramla valley	193
	5.3.9. The Marsalforn valley	195
	5.3.10. Micromorphological analyses of possible soil materials in the Xemxija 1, Wied Żembaq 1, Marsaxlokk and Salina Deep (SDC) cores	196
	5.4. The Holocene landscapes of Gozo and Malta	213
	5.5. A model of landscape development	217
	5.6. Conclusions	221
<i>Chapter 6</i>	Cultural landscapes in the changing environments from 6000 to 2000 BC	223
	REUBEN GRIMA, SIMON STODDART, CHRIS O. HUNT, CHARLES FRENCH, ROWAN McLAUGHLIN & CAROLINE MALONE	
	6.1. Introduction	223
	6.2. A short history of survey of a fragmented island landscape	223
	6.3. Fragmented landscapes	225

	6.4. The Neolithic appropriation of the landscape	227
	6.5. A world in flux (5800–4800 cal. BC)	227
	6.6. The fifth millennium BC hiatus (4980/4690 to 4150/3640 cal. BC)	228
	6.7. Reappropriating the landscape: the ‘Temple Culture’	230
	6.8. Transition and decline	236
	6.9. Conclusion	237
Part II	The interaction between the natural and cultural landscape – insights from the second millennium BC to the present: continuing the story	239
<i>Chapter 7</i>	Cultural landscapes from 2000 BC onwards SIMON STODDART, ANTHONY PACE, NATHANIEL CUTAJAR, NICHOLAS C. VELLA, ROWAN McLAUGHLIN, CAROLINE MALONE, JOHN MENEELY & DAVID TRUMPT	241
	7.1. An historiographical introduction to the Neolithic–Bronze Age transition into the Middle Bronze Age	241
	7.2. Bronze Age settlements in the landscape	243
	7.3. The Bronze Age Phoenician transition and the Phoenician/Punic landscape	246
	7.4. Entering the Roman world	250
	7.5. Arab	250
	7.6. Medieval	251
	7.7. The Knights and the entry into the modern period	251
<i>Chapter 8</i>	The intensification of the agricultural landscape of the Maltese Archipelago JEREMY BENNETT	253
	8.1. Introduction	253
	8.2. The <i>Annales</i> School and the Anthropocene	254
	8.3. The Maltese Archipelago and the <i>longue durée</i> of the Anthropocene	255
	8.4. Intensification	257
	8.5. Population	258
	8.5.1. <i>Sub-carrying capacity periods</i>	258
	8.5.2. <i>Post-carrying capacity periods</i>	260
	8.6. The agrarian archipelago	262
	8.6.1. <i>The agricultural substrate</i>	262
	8.6.2. <i>The development of agricultural technology</i>	262
	8.7. Discussion: balancing fragility and sustainability	264
<i>Chapter 9</i>	Locating potential pastoral foraging routes in Malta through the use of a Geographic Information System GIANMARCO ALBERTI, REUBEN GRIMA & NICHOLAS C. VELLA	267
	9.1. Introduction	267
	9.2. Methods	267
	9.2.1. <i>Data sources</i>	267
	9.2.2. <i>Foraging routes and least-cost paths calculation</i>	268
	9.3. Results	271
	9.3.1. <i>Garrigue to garrigue least-cost paths</i>	271
	9.3.2. <i>Stables to garrigues least-cost paths</i>	273
	9.4. Discussion	276
	9.4. Conclusions	283
<i>Chapter 10</i>	Settlement evolution in Malta from the Late Middle Ages to the early twentieth century and its impact on domestic space GEORGE A. SAID-ZAMMIT	285
	10.1. The Medieval Period (AD 870–1530)	285
	10.1.1. <i>Medieval houses</i>	288

10.1.2. <i>Giren and hovels</i>	289
10.1.3. <i>Cave-dwellings</i>	292
10.1.4. <i>Architectural development</i>	292
10.2. The Knights' Period (AD 1530–1798)	293
10.2.1. <i>The phase AD 1530–1565</i>	293
10.2.2. <i>The phase AD 1565–1798</i>	293
10.2.3. <i>Early modern houses</i>	294
10.2.4. <i>Lower class dwellings</i>	297
10.2.5. <i>Cave-dwellings and hovels</i>	298
10.2.6. <i>The houses: a reflection of social and economic change</i>	298
10.3. The British Period (AD 1800–1900)	298
10.3.1. <i>The houses of the British Period</i>	299
10.3.2. <i>The effect of the Victorian Age</i>	300
10.3.3. <i>Urban lower class dwellings</i>	301
10.3.4. <i>Peasant houses, cave-dwellings and hovels</i>	301
10.4. Conclusions	302
Chapter 11 Conclusions	303
CHARLES FRENCH, CHRIS O. HUNT, MICHELLE FARRELL, KATRIN FENECH, ROWAN McLAUGHLIN, REUBEN GRIMA, NICHOLAS C. VELLA, PATRICK J. SCHEMBRI, SIMON STODDART & CAROLINE MALONE	
11.1. The palynological record	303
CHRIS O. HUNT & MICHELLE FARRELL	
11.1.1. <i>Climate</i>	303
11.1.2. <i>Farming and anthropogenic impacts on vegetation</i>	307
11.2. The molluscan record	308
KATRIN FENECH, CHRIS O. HUNT, NICHOLAS C. VELLA & PATRICK J. SCHEMBRI	
11.3. The soil/sediment record	310
CHARLES FRENCH	
11.4. Discontinuities in Maltese prehistory and the influence of climate	313
CHRIS O. HUNT	
11.5. Environmental metastability and the <i>longue durée</i>	314
CHRIS O. HUNT	
11.6. Implications for the human story of the Maltese Islands	316
CHARLES FRENCH, CHRIS O. HUNT, CAROLINE MALONE, KATRIN FENECH, MICHELLE FARRELL, ROWAN McLAUGHLIN, REUBEN GRIMA, PATRICK J. SCHEMBRI & SIMON STODDART	
References	325
Appendix 1	
How ground penetrating radar (GPR) works	351
ALASTAIR RUFFELL	
Appendix 2	
Luminescence analysis and dating of sediments from archaeological sites and valley fill sequences	353
ALAN J. CRESSWELL, DAVID C.W. SANDERSON, TIMOTHY C. KINNAIRD & CHARLES FRENCH	
A2.1. Summary	353
A2.2. Introduction	354
A2.3. Methods	355
A2.3.1. <i>Sampling and field screening measurements</i>	355
A2.3.2. <i>Laboratory calibrated screening measurements</i>	355
A2.4. Quartz OSL SAR measurements	356
A2.4.1. <i>Sample preparation</i>	356
A2.4.2. <i>Measurements and determinations</i>	356

A2.5. Results	357
A2.5.1. <i>Sampling and preliminary luminescence stratigraphies</i>	357
A2.5.2. <i>Gozo</i>	357
A2.5.3. <i>Skorba</i>	363
A2.5.4. <i>Tal-Istabal, Qormi</i>	363
A2.6. Laboratory calibrated screening measurements	363
A2.6.1. <i>Dose rates</i>	367
A2.6.2. <i>Quartz single aliquot equivalent dose determinations</i>	367
A2.6.3. <i>Age determinations</i>	371
A2.7. Discussion	372
A2.7.1. <i>Ġgantija Temple (SUTL2914 and 2915)</i>	372
A2.7.2. <i>Ramla and Marsalforn Valleys (SUTL2917–2923)</i>	373
A2.7.3. <i>Skorba Neolithic site (SUTL2925–2927)s</i>	373
A2.7.4. <i>Tal-Istabal, Qormi (SUTL2930)</i>	376
A2.7. Conclusions	376
<i>Appendix 2 – Supplements A–D</i>	379
<i>Appendix 3</i> Deep core borehole logs	401
CHRIS O. HUNT, KATRIN FENECH, MICHELLE FARRELL & ROWAN McLAUGHLIN	
<i>Appendix 4</i> Granulometry of the deep cores	421 (online edition only)
KATRIN FENECH	
<i>Appendix 5</i> The molluscan counts for the deep cores	441 (online edition only)
KATRIN FENECH	
<i>Appendix 6</i> The borehole and test excavation profile log descriptions	535
CHARLES FRENCH & SEAN TAYLOR	
<i>Appendix 7</i> The detailed soil micromorphological descriptions from the buried soils and Ramla and Marsalforn valleys	549
CHARLES FRENCH	
A7.1. Santa Verna	549
A7.2. Ġgantija Test Pit 1	551
A7.3. Ġgantija WC Trench 1	552
A7.4. Ġgantija olive grove and environs	553
A7.5. Skorba	553
A7.6. Xagħra town	554
A7.7. Taċ-Ċawla	555
A7.8. In-Nuffara	555
A7.9. Marsalforn Valley Profile 626	556
A7.10. Ramla Valley Profile 627	556
A7.11. Dwerja	556
<i>Appendix 8</i> The micromorphological descriptions for the Malta deep cores of Xemxija 1, Wied Żembaq 1, Marsaxlokk and the base of the Salina Deep Core (21B)	557
CHARLES FRENCH & SEAN TAYLOR	
<i>Appendix 9</i> The charcoal data	563
NATHAN WRIGHT	
Index	565

CONTRIBUTORS

DR GIANMARCO ALBERTI

Department of Criminology, Faculty for Social Wellbeing, University of Malta, Msida, Malta
Email: gianmarco.alberti@um.edu.mt

JEREMY BENNETT

Department of Archaeology, University of Cambridge, Cambridge, UK
Email: jmb241@cam.ac.uk

DR MAARTEN BLAAUW

School of Natural and Built Environment, Queen's University, University Road, Belfast, Northern Ireland
Email: marten.blaauw@qub.ac.uk

DR PETROS CHATZIMPALOGLOU

Department of Archaeology, University of Cambridge, Cambridge, UK
Email: pc529@cam.ac.uk

DR LISA COYLE McCLUNG

School of Natural and Built Environment, Queen's University, University Road, Belfast, Northern Ireland
Email: l.coylemccclung@qub.ac.uk

DR ALAN J. CRESSWELL

SUERC, University of Glasgow, East Kilbride, University of Glasgow, Glasgow, Scotland
Email: alan.cresswell@glasgow.ac.uk

NATHANIEL CUTAJAR

Deputy Superintendent of Cultural Heritage, Heritage Malta, Valletta, Malta
Email: nathaniel.cutajar@gov.mt

DR MICHELLE FARRELL

Centre for Agroecology, Water and Resilience, School of Energy, Construction and Environment, Coventry University, Coventry, UK
Email: ac5086@coventry.ac.uk

DR KATRIN FENECH

Department of Classics & Archaeology, University of Malta, Msida, Malta
Email: katrin.fenech@um.edu.mt

DR RORY P. FLOOD

School of Natural and Built Environment, Queen's University, University Road, Belfast, Northern Ireland
Email: r.flood@qub.ac.uk

PROF. CHARLES FRENCH

Department of Archaeology, University of Cambridge, Cambridge, UK
Email: caif2@cam.ac.uk

DR REUBEN GRIMA

Department of Conservation and Built Heritage, University of Malta, Msida, Malta
Email: reuben.grima@um.edu.mt

DR EVAN A. HILL

School of Natural and Built Environment, Queen's University, University Road, Belfast, Northern Ireland
Email: ehill08@qub.ac.uk

PROF. CHRIS O. HUNT

Faculty of Science, Liverpool John Moores University, Liverpool, UK
Email: c.o.hunt@ljmu.ac.uk

DR TIMOTHY C. KINNAIRD

School of Earth and Environmental Sciences, University of St Andrews, St. Andrews, Scotland
Email: tk17@st-andrews.ac.uk

PROF. CAROLINE MALONE

School of Natural and Built Environment, Queen's University, University Road, Belfast, BT7 1NN, Northern Ireland
Email: c.malone@qub.ac.uk

DR STEVE McCARRON

Department of Geography, National University of Ireland, Maynooth, Ireland
Email: stephen.mccarron@mu.ie

DR ROWAN McLAUGHLIN

School of Natural and Built Environment, Queen's University, University Road, Belfast, Northern Ireland
Email: r.mclaughlin@qub.ac.uk

JOHN MENEELY
School of Natural and Built Environment, Queen's
University, University Road, Belfast, Northern
Ireland
Email: j.meneely@qub.ac.uk

DR ANTHONY PACE
UNESCO Cultural Heritage, Valletta, Malta
Email: anthonypace@cantab.net

DR SEAN D.F. PYNE-O'DONNELL
Earth Observatory of Singapore, Nanyang
Technological University, Singapore
Email: sean.1000@hotmail.co.uk

PROF. PAULA J. REIMER
School of Natural and Built Environment, Queen's
University, University Road, Belfast, Northern
Ireland
Email: p.j.reimer@qub.ac.uk

DR ALASTAIR RUFFELL
School of Natural and Built Environment, Queen's
University, University Road, Belfast, Northern
Ireland
Email: a.ruffell@qub.ac.uk

GEORGE A. SAID-ZAMMIT
Department of Examinations, Ministry for
Education and Employment, Government of Malta,
Malta
Email: george.said-zammit@gov.mt

PROF. DAVID C.W. SANDERSON
SUERC, University of Glasgow, East Kilbride,
University of Glasgow, Glasgow, Scotland
Email: david.sanderson@glasgow.ac.uk

PROF. PATRICK J. SCHEMBRI
Department of Biology, University of Malta,
Msida, Malta
Email: patrick.j.schembri@um.edu.mt

DR SIMON STODDART
Department of Archaeology, University of
Cambridge, Cambridge, UK
Email: ss16@cam.ac.uk

DR SEAN TAYLOR
Department of Archaeology, University of
Cambridge, Cambridge, UK
Email: st435@cam.ac.uk

DR DAVID TRUMPT

DR JONATHAN TURNER
Department of Geography, National University
of Ireland, University College, Dublin, Ireland
Email: jonathan.turner@ucd.ie

PROF. NICHOLAS C. VELLA
Department of Classics and Archaeology, Faculty
of Arts, University of Malta, Msida, Malta
Email: nicholas.vella@um.edu.mt

DR NATHAN WRIGHT
School of Social Science, The University of
Queensland, Brisbane, Australia
Email: n.wright@uq.edu.au

Figures

0.1	<i>Location map of the Maltese Islands in the southern Mediterranean Sea.</i>	2
0.2	<i>Location of the main Neolithic archaeological and deep coring sites investigated on Malta and Gozo.</i>	11
0.3	<i>Some views of previous excavations on Malta and Gozo.</i>	12–13
0.4	<i>Some views of recent excavations.</i>	14
1.1	<i>The location of the Maltese Islands in the southern Mediterranean Sea with respect to Sicily and North Africa.</i>	20
1.2	<i>Stratigraphic column of the geological formations reported for the Maltese Islands.</i>	22
1.3	<i>Geological map of the Maltese Islands.</i>	22
1.4	<i>Typical coastal outcrops of Lower Coralline Limestone, forming sheer cliffs.</i>	23
1.5	<i>Characteristic geomorphological features developed on the Lower Coralline Limestone in western Gozo (Dwerja Point).</i>	24
1.6	<i>The Middle Globigerina Limestone at the Xwejni coastline.</i>	24
1.7	<i>An overview of the area investigated in western Malta.</i>	25
1.8	<i>The end of the major fault system of Malta (Victorian Lines) at Fomm Ir-Rih.</i>	26
1.9	<i>An overview of the western part of Gozo where the chert outcrops are located.</i>	27
1.10	<i>Chert outcrops: a) and c) bedded chert, and b) and d) nodular chert.</i>	27
1.11	<i>Four characteristic exposures of the Blue Clay formation on Gozo and Malta.</i>	28
1.12	<i>Map of the fault systems, arranged often as northwest–southeast oriented graben, and strike-slip structures.</i>	30
2.1	<i>Summary of new radiocarbon dating of Neolithic and Bronze Age sites on Gozo and Malta.</i>	36
2.2	<i>Summed radiocarbon ages for the main sediment cores.</i>	36
2.3	<i>The location of the Birzebbuga Ghar Dalam and Borġ in-Nadur basins and their GNSS-located GPR lines.</i>	42
2.4	<i>The core locations in Malta and Gozo.</i>	44
2.5	<i>Radiocarbon activity in settlement cores.</i>	48
2.6	<i>The Xemxija 2 core by depth.</i>	51
2.7	<i>The Wied Żembaq 1 and 2 cores by depth.</i>	52
2.8	<i>The Mġarr ix-Xini core by depth.</i>	54
2.9	<i>The Marsaxlokk 1 core and part of 2 by depth.</i>	55
2.10	<i>The resistivity and magnetic susceptibility graphs for Xemxija 1 core.</i>	60
2.11	<i>The resistivity and magnetic susceptibility graphs for Xemxija 2 core.</i>	60
2.12	<i>The multi-element data plots for Xemxija 1 core.</i>	61
2.13	<i>The multi-element data plots for Wied Żembaq 1 core.</i>	62
2.14	<i>The multi-element data plots for Marsaxlokk 1 core.</i>	63
2.15	<i>RUSLE models of soil erosion for the Maltese Islands in September and March.</i>	69
2.16	<i>R and C factors and their product.</i>	70
3.1	<i>Valley catchments and core locations in the Mistra area of Malta.</i>	79
3.2	<i>The modern pollen spectra.</i>	81
3.3	<i>Pollen zonation for the Salina Deep Core.</i>	82–3
3.4	<i>Pollen zonation for the Salina 4 core.</i>	88–9
3.5	<i>Pollen zonation for the Wied Żembaq 1 core.</i>	92–3
3.6	<i>Pollen zonation for the Xemxija 1 core.</i>	96–7
3.7	<i>Pollen zonation for the pit fills at In-Nuffara.</i>	101
3.8	<i>Pollen and palynofacies from the buried soils below the temple at Santa Verna.</i>	102
3.9	<i>Pollen and palynofacies from Test Pit 1 on the southwestern edge of the Ġgantija platform.</i>	104
3.10	<i>Photomicrographs (x800) of key components of the palynofacies at Santa Verna and Ġgantija.</i>	106
4.1	<i>Marsaxlokk 1 molluscan histogram.</i>	120
4.2	<i>Wied Żembaq 1 molluscan histogram.</i>	122
4.3	<i>Mġarr ix-Xini molluscan histogram.</i>	129
4.4	<i>Marsa 2 molluscan histogram.</i>	134
4.5	<i>Salina Deep Core molluscan histogram.</i>	138
4.6	<i>Marine molluscan histogram for the Salina Deep Core.</i>	139

4.7	<i>Xemxija 1 molluscan histogram.</i>	144
4.8	<i>Base of Xemxija 2 molluscan histogram.</i>	145
5.1	<i>Location map of the test excavation/sample sites and geoarchaeological survey areas on Gozo and Malta.</i>	164
5.2	<i>Plan of Santa Verna temple and the locations of the test trenches.</i>	166
5.3	<i>Santa Verna excavation trench profiles all with sample locations marked.</i>	167
5.4	<i>The red-brown buried soil profiles in Trench E, the Ashby and Trump Sondages within the Santa Verna temple site.</i>	170
5.5	<i>Santa Verna soil photomicrographs.</i>	172–3
5.6	<i>Plan of Ġgantija temple and locations of Test Pit 1 and the WC Trench excavations, with as-dug views of the WC Trench and TP1.</i>	175
5.7	<i>Section profiles of Ġgantija Test Pit 1 on the southwest side of Ġgantija temple and the east-west section of the Ġgantija WC Trench on the southeast side.</i>	176
5.8	<i>Ġgantija TP 1 photomicrographs.</i>	178
5.9	<i>Ġgantija WC Trench 1 photomicrographs.</i>	180
5.10	<i>Section profiles of Trench A at Skorba showing the locations of the micromorphological and OSL samples.</i>	183
5.11	<i>Skorba Trench A, section 1, photomicrographs.</i>	185
5.12	<i>Skorba Trench A, section 2, photomicrographs.</i>	186
5.13	<i>Taċ-Ċawla soil photomicrographs.</i>	189
5.14	<i>A typical terra rossa soil sequence in Xagħra town at construction site 2.</i>	191
5.15	<i>Xagħra soil photomicrographs.</i>	191
5.16	<i>In-Nuffara photomicrographs.</i>	193
5.17	<i>The Marsalforn (Pr 626) and Ramla (Pr 627) valley fill sequences, with the micromorphology samples and OSL profiling/dating loci marked.</i>	194
5.18	<i>Ramla and Marsalforn valley profiles soil photomicrographs.</i>	195
5.19	<i>Photomicrographs of the Blue Clay and Greensand geological substrates from the Ramla valley.</i>	199
5.20	<i>Xemxija 1 deep valley core photomicrographs.</i>	202
5.21	<i>Wied Żembaq 1 deep valley core photomicrographs.</i>	206
5.22	<i>Marsaxlokk and Salina Deep Core photomicrographs.</i>	210
5.23	<i>Scrub woodland on an abandoned terrace system and garrigue plateau land on the north coast of Gozo.</i>	213
5.24	<i>Terracing within land parcels (defined by modern sinuous lanes) on the Blue Clay slopes of the Ramla valley with Xagħra in the background.</i>	216
6.1	<i>The location of the Cambridge Gozo Project survey areas.</i>	224
6.2	<i>Fieldwalking survey data from around A. Ta Kuljat, B. Santa Verna, and C. Ġhajnsielem on Gozo from the Cambridge Gozo survey and the FRAGSUS Project.</i>	227
6.3	<i>The first cycle of Neolithic occupation as recorded by the Cambridge Gozo survey using kernel density analysis for the Għar Dalam, Red Skorba and Grey Skorba phases.</i>	229
6.4	<i>The first half of the second cycle of Neolithic occupation as recorded by the Cambridge Gozo survey using kernel density analysis implemented for the Żebbuġ and Mġarr phases.</i>	232
6.5	<i>The second half of the second cycle of Neolithic occupation as recorded by the Cambridge Gozo survey using kernel density analysis for the Ġgantija and Tarxien phases.</i>	233
7.1	<i>Kernel density analysis of the Tarxien Cemetery, Borg in-Nadur and Bahrija periods for the areas covered by the Cambridge Gozo survey.</i>	244
7.2a	<i>The evidence for Bronze Age settlement in the Mdina area on Malta.</i>	245
7.2b	<i>The evidence for Bronze Age settlement in the Rabat (Gozo) area.</i>	245
7.3	<i>Distribution of Early Bronze Age dolmen on the Maltese Islands.</i>	246
7.4	<i>Distribution of presses discovered in the Mġarr ix-Xini valley during the survey.</i>	248
7.5	<i>The cultural heritage record of the Punic tower in Żurrieq through the centuries.</i>	249
7.6	<i>The changing patterns of social resilience, connectivity and population over the course of the centuries in the Maltese Islands.</i>	252
8.1	<i>An oblique aerial image of the northern slopes of the Magħtab land-fill site, depicting landscaping efforts including 'artificial' terracing.</i>	256
8.2	<i>RUSLE estimates of areas of low and moderate erosion for Gozo and Malta.</i>	259
9.1	<i>a) Sheep being led to their fold in Pwales down a track; b) Sheep grazing along a track on the Bajda Ridge in Xemxija, Malta.</i>	269

9.2	<i>Least-cost paths (LCPs), connecting garrigue areas, representing potential foraging routes across the Maltese landscape.</i>	271
9.3	<i>Density of LCPs connecting garrigue areas to random points within the garrigue areas themselves.</i>	272
9.4	<i>Location of ‘public spaces’, with size proportional to the distance to the nearest garrigue-to-garrigue LCP.</i>	273
9.5	<i>LCPs connecting farmhouses hosting animal pens to randomly generated points within garrigue areas in northwestern (A) and northeastern (B) Malta.</i>	274
9.6	<i>As for Figure 9.5, but representing west-central and east-central Malta.</i>	274
9.7	<i>As for Figure 9.5, but representing southern and southwestern Malta.</i>	275
9.8	<i>Location of ‘public spaces’, with size proportional to the distance to the nearest outbound journey.</i>	276
9.9	<i>a) Public space at Tal-Wei, between the modern town of Mosta and Naxxar; b) Tal-Wei public space as represented in 1940s survey sheets.</i>	277
9.10	<i>Approximate location of the (mostly disappeared) raħal toponyms.</i>	279
9.11	<i>Isochrones around farmhouse 4 representing the space that can be covered at 1-hour intervals considering animal walking speed.</i>	280
9.12	<i>Isochrones around farmhouse 2 representing the space that can be covered at 1-hour intervals considering animal walking speed (grazing while walking).</i>	281
9.13	<i>a) Isochrones around farmhouse 5 representing the space that can be covered at 1-hour intervals; b) Isochrones around farmhouse 6; c) Isochrones around farmhouse 7.</i>	282
10.1	<i>The likely distribution of built-up and cave-dwellings in the second half of the fourteenth century.</i>	286
10.2	<i>The lower frequency of settlement distribution by c. AD 1420.</i>	286
10.3	<i>The distribution of settlements just before AD 1530.</i>	288
10.4	<i>The late medieval Falson Palace in Mdina.</i>	289
10.5	<i>A girna integral with and surrounded by stone dry walling.</i>	290
10.6	<i>A hovel dwelling with a flight of rock-cut steps.</i>	291
10.7	<i>The hierarchical organisation of settlements continued, with the addition of Valletta, Floriana and the new towns around Birgu.</i>	295
10.8	<i>An example of a seventeenth century townhouse with open and closed timber balconies.</i>	296
10.9	<i>An example of a two-storey razzett belonging to a wealthier peasant family.</i>	297
10.10	<i>The distribution of built-up settlements in about AD 1900.</i>	299
10.11	<i>An example of a Neo-Classical house.</i>	301
11.1	<i>Summary of tree and shrub pollen frequencies at 10 sample sites.</i>	304
11.2	<i>Summary of cereal pollen frequencies at 14 sample sites.</i>	305
11.3	<i>Schematic profiles of possible trajectories of soil development in the major geological zones of Malta and Gozo.</i>	311
11.4	<i>The main elements of a new cultural-environmental story of the Maltese Islands throughout the last 10,000 years.</i>	317
A2.1	<i>Marsalforn valley, Gozo.</i>	360
A2.2	<i>Marsalforn valley, Gozo.</i>	361
A2.3	<i>Ramla valley, Gozo.</i>	361
A2.4	<i>Ġgantija Test Pit 1, Gozo.</i>	361
A2.5	<i>Skorba Neolithic site; trench A, East section; trench A, South section.</i>	362
A2.6	<i>Skorba, Trench A, South section.</i>	362
A2.7	<i>Tal-Istabal, Qormi, Malta.</i>	364
A2.8	<i>Tal-Istabal, Qormi, Malta.</i>	364
A2.9	<i>Photograph, showing locations of profile sample and OSL tubes, and luminescence-depth profile, for the sediment stratigraphy sampled in profile 1.</i>	365
A2.10	<i>Photograph, and luminescence-depth profile, for the sediment stratigraphy sampled in profile 3.</i>	365
A2.11	<i>Photograph, and luminescence-depth profile, for the sediment stratigraphy sampled in profile 2.</i>	366
A2.12	<i>Photograph, and luminescence-depth profile, for the sediment stratigraphy sampled in profiles 4 and 6.</i>	366
A2.13	<i>Photograph, and luminescence-depth profile, for the sediment stratigraphy sampled in profile 5.</i>	367
A2.14	<i>Apparent dose and sensitivity for laboratory OSL and IRSL profile measurements for SUTL2916 (P1).</i>	370
A2.15	<i>Apparent dose and sensitivity for laboratory OSL and IRSL profile measurements for SUTL2920 (P2).</i>	370
A2.16	<i>Apparent dose and sensitivity for laboratory OSL and IRSL profile measurements for SUTL2913 (P3).</i>	370
A2.17	<i>Apparent dose and sensitivity for laboratory OSL and IRSL profile measurements for SUTL2924 (P4).</i>	370

A2.18	<i>Apparent dose and sensitivity for laboratory OSL and IRSL profile measurements for SUTL2929 (P5).</i>	371
A2.19	<i>Apparent dose and sensitivity for laboratory OSL and IRSL profile measurements for SUTL2928 (P6).</i>	371
A2.20	<i>Apparent dose and sensitivity for laboratory OSL and IRSL profile measurements for SUTL2931 (P7).</i>	371
A2.21	<i>Probability Distribution Functions for the stored dose on samples SUTL2914 and 2915.</i>	374
A2.22	<i>Probability Distribution Functions for the stored dose on samples SUTL2917–2919.</i>	374
A2.23	<i>Probability Distribution Functions for the stored dose on samples SUTL2921–2923.</i>	375
A2.24	<i>Probability Distribution Functions for the stored dose on samples SUTL2925–2927.</i>	375
A2.25	<i>Probability Distribution Function for the stored dose on sample SUTL2930.</i>	376
SB.1	<i>Dose response curves for SUTL2914.</i>	385
SB.2	<i>Dose response curves for SUTL2915.</i>	385
SB.3	<i>Dose response curves for SUTL2917.</i>	386
SB.4	<i>Dose response curves for SUTL2918.</i>	386
SB.5	<i>Dose response curves for SUTL2919.</i>	387
SB.6	<i>Dose response curves for SUTL2921.</i>	387
SB.7	<i>Dose response curves for SUTL2922.</i>	388
SB.8	<i>Dose response curves for SUTL2923.</i>	388
SB.9	<i>Dose response curves for SUTL2925.</i>	389
SB.10	<i>Dose response curves for SUTL2926.</i>	389
SB.11	<i>Dose response curves for SUTL2927.</i>	390
SB.12	<i>Dose response curves for SUTL2930.</i>	390
SC.1	<i>Abanico plot for SUTL2914.</i>	391
SC.2	<i>Abanico plot for SUTL2915.</i>	391
SC.3	<i>Abanico plot for SUTL2917.</i>	392
SC.4	<i>Abanico plot for SUTL2918.</i>	392
SC.5	<i>Abanico plot for SUTL2919.</i>	392
SC.6	<i>Abanico plot for SUTL2921.</i>	393
SC.7	<i>Abanico plot for SUTL2922.</i>	393
SC.8	<i>Abanico plot for SUTL2923.</i>	393
SC.9	<i>Abanico plot for SUTL2925.</i>	394
SC.10	<i>Abanico plot for SUTL2926.</i>	394
SC.11	<i>Abanico plot for SUTL2927.</i>	394
SC.12	<i>Abanico plot for SUTL2930.</i>	395
SD.1	<i>Apparent ages for profile 1, with OSL ages.</i>	397
SD.2	<i>Apparent ages for profile 2, with OSL ages.</i>	397
SD.3	<i>Apparent ages for profile 3, with OSL ages.</i>	398
SD.4	<i>Apparent ages for profiles 4 and 6, with OSL ages.</i>	398
SD.5	<i>Apparent ages for profile 5, with OSL ages.</i>	399
SD.6	<i>Apparent ages for profile 7.</i>	399

Tables

1.1	<i>Description of the geological formations found on the Maltese Islands.</i>	21
2.1	<i>The cultural sequence of the Maltese Islands (with all dates calibrated).</i>	37
2.2	<i>Quartz OSL sediment ages from the Marsalforn (2917–2919) and Ramla (2921–2923) valleys, the Skorba temple/buried soil (2925–2927) and Tal-Istabal, Qormi, soil (2930).</i>	40
2.3	<i>Dating results for positions in the sediment cores.</i>	45
2.4	<i>Summary stratigraphic descriptions of the sequences in the deep core profiles.</i>	57
2.5	<i>Mean sediment accumulation rates per area versus time for the deep cores.</i>	64
2.6	<i>Radiocarbon measurements and ΔR values from early twentieth century marine shells from Malta.</i>	65
2.7	<i>Calibrated AMS ^{14}C dates of charred plant remains from Santa Verna palaeosol, Gozo.</i>	68
2.8	<i>Physical properties of the catchments.</i>	68
2.9	<i>Normalized Diffuse Vegetation Index (NDVI) for the catchments in 2014–15 and average rainfall data for the weather station at Balzan for the period 1985 to 2012.</i>	69
3.1	<i>Semi-natural plant communities in the Maltese Islands.</i>	76

3.2	<i>Attribution of pollen taxa to plant communities in the Maltese Islands and more widely in the Central Mediterranean.</i>	77
3.3	<i>Characteristics of the taphonomic samples from on-shore and off-shore Mistra Valley, Malta.</i>	80
3.4	<i>The pollen zonation of the Salina Deep Core with modelled age-depths.</i>	84
3.5	<i>The pollen zonation of the Salina 4 core with modelled age-depths.</i>	90
3.6	<i>The pollen zonation of the Wied Żembaq 1 core with modelled age-depths.</i>	94
3.7	<i>The pollen zonation of the Xemxija 1 core with modelled age-depths.</i>	98
3.8	<i>The pollen zonation of the fill of a Bronze Age silo at In-Nuffara, Gozo.</i>	103
3.9	<i>Summary of the pollen analyses of the buried soil below the Santa Verna temple structure.</i>	103
3.10	<i>Summary of the pollen analyses from the buried soil in Ġgantija Test Pit 1.</i>	105
3.11	<i>Activity on Temple sites and high cereal pollen in adjacent cores.</i>	105
4.1	<i>List of freshwater molluscs and land snails found in the cores, habitat requirement, palaeontological record and current status and conservation in the Maltese Islands.</i>	118
4.2	<i>Molluscan zones for the Marsaxlokk 1 core (MX1).</i>	121
4.3	<i>Molluscan zones for the Wied Żembaq 1 core (WŻ1).</i>	123
4.4	<i>Molluscan zones for the Wied Żembaq 2 core (WŻ2).</i>	125
4.5	<i>Integration of molluscan zones from the Wied Żembaq 1 and 2 cores.</i>	128
4.6	<i>Molluscan zones for the Mġarr ix-Xini 1 core (MĠX1).</i>	130
4.7	<i>Molluscan zones for the Marsa 2 core (MC2).</i>	135
4.8	<i>The non-marine molluscan zones for the Salina Deep Core (SDC).</i>	140
4.9	<i>Molluscan zones for the Salina Deep Core (SDC).</i>	142
4.10	<i>Molluscan zones for the Xemxija 1 core (XEM1).</i>	146
4.11	<i>Molluscan zones for the Xemxija 2 core (XEM2).</i>	148
4.12	<i>Correlation and integration of molluscan data from Xemxija 1 (XEM1) and Xemxija 2 (XEM2).</i>	151
5.1	<i>Micromorphology and small bulk sample sites and numbers.</i>	162
5.2	<i>Summary of available dating for the sites investigated in Gozo and Malta.</i>	163
5.3	<i>pH, magnetic susceptibility, loss-on-ignition, calcium carbonate and % sand/silt/clay particle size analysis results for the Ġgantija, Santa Verna and the Xagħra town profiles, Gozo.</i>	168
5.4	<i>Selected multi-element results for Ġgantija, Santa Verna and Xagħra town buried soils, and the Marsalforn and Ramla valley sequences, Gozo.</i>	169
5.5	<i>Summary of the main soil micromorphological observations for the Santa Verna, Ġgantija and the Xagħra town profiles, Gozo.</i>	181
5.6	<i>pH, magnetic susceptibility and selected multi-element results for the palaeosols in section 1, Trench A, Skorba.</i>	184
5.7	<i>Loss-on-ignition organic/carbon/calcium carbonate frequencies and particle size analysis results for the palaeosols in section 1, Trench A, Skorba.</i>	184
5.8	<i>Summary of the main soil micromorphological observations of the buried soils in sections 1 and 2, Trench A, Skorba.</i>	188
5.9	<i>Summary of the main soil micromorphological observations of the possible buried soils at Taç-Ċawla.</i>	189
5.10	<i>Field descriptions and micromorphological observations for the quarry and construction site profiles in Xagħra town.</i>	190
5.11	<i>Sample contexts and micromorphological observations for two silo fills at In-Nuffara.</i>	192
5.12	<i>Summary of the main soil micromorphological observations from the Ramla and Marsalforn valley fill profiles.</i>	196
5.13	<i>Main characteristics of the Upper and Lower Coralline Limestone, Globigerina Limestone, Blue Clay and Greensand.</i>	197
5.14	<i>Summary micromorphological descriptions and suggested interpretations for the Xemxija 1 core.</i>	200
5.15	<i>Summary micromorphological descriptions and suggested interpretations for the Wied Żembaq 1 core.</i>	207
5.16	<i>Summary micromorphological descriptions and suggested interpretations for the Marsaxlokk 1 core.</i>	209
5.17	<i>Summary micromorphological descriptions and suggested interpretations for the base zone of the base of the Salina Deep Core.</i>	211
8.1	<i>Carrying capacity estimates for the Neolithic/Temple Period of the Maltese Archipelago.</i>	258
8.2	<i>Summary of population changes in the Maltese Archipelago.</i>	261
11.1	<i>Summary of the environmental and vegetation changes in the Maltese Islands over the longue durée.</i>	306

11.2	<i>Summary of events revealed by the molluscan data in the deep cores.</i>	309
11.3	<i>Major phases of soil, vegetation and landscape development and change during the Holocene.</i>	312
11.4	<i>Occurrence of gypsum in FRAGSUS cores and contemporary events.</i>	314
A2.1	<i>Sample descriptions, contexts and archaeological significance of the profiling samples used for initial screening and laboratory characterization.</i>	358
A2.2	<i>Sample descriptions, contexts and archaeological significance of sediment samples SUTL2914–2930.</i>	360
A2.3	<i>Activity and equivalent concentrations of K, U and Th determined by HRGS.</i>	368
A2.4	<i>Infinite matrix dose rates determined by HRGS and TSBC.</i>	368
A2.5	<i>Effective beta and gamma dose rates following water correction.</i>	369
A2.6	<i>SAR quality parameters.</i>	369
A2.7	<i>Comments on equivalent dose distributions of SUTL2914 to SUTL2930.</i>	372
A2.8	<i>Quartz OSL sediment ages.</i>	372
A2.9	<i>Locations, dates and archaeological significance of sediment samples SUTL2914–2930.</i>	373
SA.1	<i>Field profiling data, as obtained using portable OSL equipment, for the sediment stratigraphies examined on Gozo and Malta.</i>	379
SA.2	<i>OSL screening measurements on paired aliquots of 90–250 µm 40% HF-etched ‘quartz’.</i>	380
SA.3	<i>OSL screening measurements on three aliquots of 90–250 µm 40% HF-etched ‘quartz’ for SUTL2924.</i>	382
SA.4	<i>IRSL screening measurements on paired aliquots of 90–250 µm 15% HF-etched ‘polymineral’.</i>	382
SA.5	<i>IRSL screening measurements on three aliquots of 90–250 µm 15% HF-etched ‘polymineral’ for SUTL2924.</i>	383
A3.1	<i>Stratigraphy and interpretation of the Salina Deep Core.</i>	401
A3.2	<i>Stratigraphy and interpretation of the Salina 4 core.</i>	405
A3.3	<i>Stratigraphy and interpretation of the Salina 2 core.</i>	407
A3.4	<i>Stratigraphy and interpretation of the Xemxija 1 core.</i>	408
A3.5	<i>Stratigraphy and interpretation of the Xemxija 2 core.</i>	411
A3.6	<i>Stratigraphy and interpretation of the Wied Żembaq 1 core.</i>	413
A3.7	<i>Stratigraphy and interpretation of the Wied Żembaq 2 core.</i>	413
A3.8	<i>Stratigraphy and interpretation of the Mgarr ix-Xini core.</i>	414
A3.9	<i>Stratigraphy and interpretation of the Marsaxlokk core.</i>	416
A3.10	<i>Stratigraphy and interpretation of the Marsa 2 core.</i>	417
A3.11	<i>Stratigraphy and interpretation of the Mellieħa Bay core.</i>	418
A3.12	<i>Key to the scheme for the description of Quaternary sediments.</i>	419
A4.1	<i>Marsa 2.</i>	421 (online edition only)
A4.2	<i>Mgarr ix-Xini.</i>	424 (online edition only)
A4.3	<i>Salina Deep Core.</i>	427 (online edition only)
A4.4	<i>Wied Żembaq 2.</i>	429 (online edition only)
A4.5	<i>Wied Żembaq 1.</i>	430 (online edition only)
A4.6	<i>Xemxija 1.</i>	432 (online edition only)
A4.7	<i>Xemxija 2.</i>	435 (online edition only)
A4.8	<i>Marsaxlokk 1.</i>	438 (online edition only)
A5.1	<i>Marsa 2.</i>	442 (online edition only)
A5.2	<i>Mgarr ix-Xini.</i>	456 (online edition only)
A5.3	<i>Salina Deep Core non-marine.</i>	466 (online edition only)
A5.4	<i>Salina Deep Core marine.</i>	478 (online edition only)
A5.5	<i>Wied Żembaq 2.</i>	490 (online edition only)
A5.6	<i>Wied Żembaq 1.</i>	496 (online edition only)
A5.7	<i>Xemxija 1.</i>	502 (online edition only)
A5.8	<i>Xemxija 2.</i>	516 (online edition only)
A5.9	<i>Marsaxlokk 1.</i>	528 (online edition only)
A8.1	<i>Xemxija 1 core micromorphology sample descriptions.</i>	557
A8.2	<i>Wied Żembaq 1 core micromorphology sample descriptions.</i>	559
A8.3	<i>Marsaxlokk core micromorphology sample descriptions.</i>	560
A8.4	<i>Salina Deep Core micromorphology sample descriptions.</i>	561
A9.1	<i>The charcoal data from the Skorba, Kordin, In-Nuffara and Salina Deep Core.</i>	563

Preface and dedication

Caroline Malone

The *FRAGSUS Project* emerged as the direct result of an invitation to undertake new archaeological fieldwork in Malta in 1985. Anthony Bonanno of the University of Malta organized a conference on ‘The Mother Goddess of the Mediterranean’ in which Colin Renfrew was a participant. The discussions that resulted prompted an invitation that made its way to David Trump (Tutor in Continuing Education, Cambridge University), Caroline Malone (then Curator of the Avebury Keiller Museum) and Simon Stoddart (then a post-graduate researcher in Cambridge). We eagerly took up the invitation to devise a new collaborative, scientifically based programme of research on prehistoric Malta.

What resulted was the original Cambridge Gozo Project (1987–94) and the excavations of the Xagħra Brochtorff Circle and the Ġhajnsielem Road Neolithic house. Both those sites had been found by local antiquarian, Joseph Attard-Tabone, a long-established figure in the island for his work on conservation and site identification.

As this and the two other volumes in this series report, the original Cambridge Gozo Project was the germ of a rich and fruitful academic collaboration that has had international impact, and has influenced successive generations of young archaeologists in Malta and beyond.

As the Principal Investigator of the *FRAGSUS Project*, on behalf of the very extensive *FRAGSUS* team I want to dedicate this the first volume of the series to the enlightened scholars who set up this now 35 year-long collaboration of prehistoric inquiry with our heartfelt thanks for their role in our studies.

We dedicate this volume to:

Joseph Attard Tabone
Professor Anthony Bonanno
Professor Lord Colin Renfrew

and offer our profound thanks for their continuing role in promoting the prehistory of Malta.

Acknowledgements

This volume records research undertaken with funding from the European Research Council under the European Union's Seventh Framework Programme (FP/2007-2013)/ERC Grant Agreement n. 323727 (*FRAGSUS Project: Fragility and sustainability in small island environments: adaptation, cultural change and collapse in prehistory* – <http://www.qub.ac.uk/sites/FRAGSUS/>). All the authors of this volume are indebted to the ERC for its financial support, and to the Principal Investigator of the *FRAGSUS Project*, Prof. Caroline Malone (Queen's University, Belfast, UK), for her central role in devising the project and seeing this research through to publication.

For Chapter 2, we extend warm thanks to the staff of the ¹⁴CHRONO centre at QUB, especially Stephen Hoper, Jim McDonald, Michelle Thompson and Ron Reimer, all of whom took a keen interest in the *FRAGSUS Project*. The success of the *FRAGSUS Project* in general and the radiocarbon dating exercise has depended on their work. We thank the Physical Geography Laboratory staff at the School of Geography, University College Dublin, for the use of their ITRAX XRF core scanner. In particular, we would like to thank Dr Steve McCarron, Department of Geography, National University of Ireland, Maynooth and Dr Jonathan Turner, Department of Geography, National University of Ireland, University College, Dublin. We thank Prof. Patrick Schembri for sourcing and collecting the *Acanthocardia* samples from the Natural Museum of Natural History. Sean Pyne O'Donnell thanks Dr Chris Hayward at the Tephrochronology Analytical Unit (TAU), University of Edinburgh, for help and advice during microprobe work. Dr Maxine Anastasi, Department of Classics and Archaeology, University of Malta, helped identify the pottery from the settlement cores. Dr Frank Carroll helped show us the way forward; but sadly is no longer with us. Chris Hunt, Rory Flood, Michell Farrell, Sean Pyne O'Donnell and Mevrick Spiteri were the coring team.

They were helped by Vincent Van Walt, who provided technical assistance. Al Ruffell and John Meneely did geophysical evaluation and GRP location of the cores. During fieldwork, Tim Kinnaird and Charles French were assisted by Sean Taylor, Jeremy Bennett and Simon Stoddart. We are grateful to the Superintendence of Cultural Heritage, Malta and Heritage Malta for permission to undertake the analyses and much practical assistance.

For Chapter 5, we would like to thank all at Heritage Malta, the Ġgantija visitor's centre and the University of Malta for their friendly and useful assistance throughout. In particular, we would like to thank George Azzopardi, Daphne Caruana, Josef Caruana, Nathaniel Cutajar, Chris Gemmell, Reuben Grima, Joanne Mallia, Christian Mifsud, Anthony Pace, Ella Samut-Tagliaferro, Mevrick Spiteri, Katya Stroud, Sharon Sultana and Nick Vella. We also thank Tonko Rajkovača of the McBurney Laboratory, Department of Archaeology, University of Cambridge, for making the thin section slides, the Physical Geography Laboratory, Department of Geography, University of Cambridge, and the ALS Global laboratory in Seville, Spain, for processing the multi-element analyses.

For Chapter 6, Reuben Grima wrote the first draft of this contribution, receiving comments and additions from the other authors.

For Chapter 7, Simon Stoddart wrote the first draft of this contribution, receiving comments and additions from the other authors.

For Chapter 9, we thank Sharlo Camilleri for providing us with a copy of the GIS data produced by the MALSIS (MALtese Soil Information System) project. We are grateful to Prof. Saviour Formosa and Prof. Timmy Gambin, both of the University of Malta, who facilitated the donation of LiDAR data, together with computer facilities, as part of the European project ERDF156 *Developing National Environmental Monitoring Infrastructure and Capacity*, from the former Malta

Environment and Planning Authority. A number of individuals were happy to share their recollections of shepherding practices in Malta and Gozo over the last sixty or seventy years; others facilitated the encounters. We are grateful to all of them: Charles Gauci, Grezzju Meilaq, Joseph Micallef, Louis Muscat, Ċettina and Anglu Vella, Ernest Vella and Renata Zerafa.

Simon Stoddart would like to thank Prof. Martin Jones and Rachel Ballantyne for their advice in constructing Figure 11.4. The editors would like to thank Emma Hannah for compiling the index.

Firstly, the FRAGSUS Project is the result of a very generous research grant from the European Research Council (Advanced Grant no' 323727), without which this and its two partner volumes and the research undertaken could not have taken place. We heartily thank the ERC for its award and the many administrators in Brussels who monitored our use of

the grant. The research team also wants to record our indebtedness to the administrators of the grant within our own institutions, since this work required detailed and dedicated attention. In particular we thank Rory Jordan in the Research Support Office, Stephen Hoper and Jim McDonald – CHRONO lab, and Martin Stroud (Queen's University Belfast), Laura Cousens (Cambridge University), Glen Farrugia and Cora Magri (University of Malta), the Curatorial, Finance and Designs & Exhibitions Departments in Heritage Malta and Stephen Borg at the Superintendence of Cultural Heritage. Finally, we thank Fr. Joe Inguanez (Emeritus Head of Department, Department of Sociology, University of Malta) for offering us the *leitmotif* of this volume while a visiting scholar in Magdalene College, Cambridge: '*Mingħajr art u ħamrija, m'hemmx sinjorija*' translating as 'without land and soil, there is no wealth'.

Foreword

Anthony Pace

Sustainability, as applied in archaeological research and heritage management, provides a useful perspective for understanding the past as well as the modern conditions of archaeological sites themselves. As often happens in archaeological thought, the idea of sustainability was borrowed from other areas of concern, particularly from the modern construct of development and its bearing on the environment and resource exploitation. The term sustainability entered common usage as a result of the unstoppable surge in resource exploitation, economic development, demographic growth and the human impacts on the environment that has gripped the World since 1500. Irrespective of scale and technology, most human activity of an economic nature has not spared resources from impacts, transformations or loss irrespective of historical and geographic contexts. Theories of sustainability may provide new narratives on the archaeology of Malta and Gozo, but they are equally important and of central relevance to contemporary issues of cultural heritage conservation and care. Though the archaeological resources of the Maltese islands can throw light on the past, one has to recognize that such resources are limited, finite and non-renewable. The sense of urgency with which these resources have to be identified, listed, studied, archived and valued is akin to that same urgency with which objects of value and all fragile forms of natural and cultural resources require constant stewardship and protection. The idea of sustainability therefore, follows a common thread across millennia.

It is all the more reason why cultural resource management requires particular attention through research, valorization and protection. The *FRAGSUS Project* (Fragility and sustainability in small island environments: adaptation, cultural change and collapse in prehistory) was intended to further explore and enhance existing knowledge on the prehistory of Malta and Gozo. The objective of the project as

designed by the participating institutional partners and scholars, was to explore untapped field resources and archived archaeological material from a number of sites and their landscape to answer questions that could be approached with new techniques and methods. The results of the *FRAGSUS Project* will serve to advance our knowledge of certain areas of Maltese prehistory and to better contextualize the archipelago's importance as a model for understanding island archaeology in the central Mediterranean. The work that has been invested in *FRAGSUS* lays the foundation for future research.

Malta and Gozo are among the Mediterranean islands whose prehistoric archaeology has been intensely studied over a number of decades. This factor is important, yet more needs to be done in the field of Maltese archaeology and its valorization. Research is not the preserve of academic specialists. It serves to enhance not only what we know about the Maltese islands, but more importantly, why the archipelago's cultural landscape and its contents deserve care and protection especially at a time of extensive construction development. Strict rules and guidelines established by the Superintendence of Cultural Heritage have meant that during the last two decades more archaeological sites and deposits have been protected in situ or rescue-excavated through a statutory watching regime. This supervision has been applied successfully in a wide range of sites located in urban areas, rural locations and the landscape, as well as at the World Heritage Sites of Valletta, Ġgantija, Ғaġar Qim and Mnajdra and Tarxien. This activity has been instrumental in understanding ancient and historical land use, and the making of the Maltese historic centres and landscape.

Though the cumulative effect of archaeological research is being felt more strongly, new areas of interest still need to be addressed. Most pressing are those areas of landscape studies which often become

peripheral to the attention that is garnered by prominent megalithic monuments. *FRAGSUS* has once again confirmed that there is a great deal of value in studying field systems, terraces and geological settings which, after all, were the material media in which modern Malta and Gozo ultimately developed. There is, therefore, an interplay in the use of the term sustainability, an interplay between what we can learn from the way ancient communities tested and used the very same island landscape which we occupy today, and the manner in which this landscape is treated in contested economic realities. If we are to seek factors of sustainability in the past, we must first protect its relics and study them using the best available methods in our times. On the other hand, the study of the past using the materiality of ancient peoples requires strong research agendas and thoughtful stewardship. The *FRAGSUS Project* has shown us how even small fragile deposits, nursed through protective legislation and guardianship, can yield significant information which the methods of pioneering scholars of Maltese archaeology would not have enabled access to. As already outlined by the Superintendence of Cultural Heritage, a national research agenda for cultural heritage and the humanities is a desideratum. Such a framework, reflected in the institutional partnership of the

FRAGSUS Project, will bear valuable results that will only advance Malta's interests especially in today's world of instant e-knowledge that was not available on such a global scale a mere two decades ago.

FRAGSUS also underlines the relevance of studying the achievements and predicaments of past societies to understand certain, though not all, aspects of present environmental challenges. The twentieth century saw unprecedented environmental changes as a result of modern political-economic constructs. Admittedly, twentieth century developments cannot be equated with those of antiquity in terms of demography, technology, food production and consumption or the use of natural resources including the uptake of land. However, there are certain aspects, such as climate change, changing sea levels, significant environmental degradation, soil erosion, the exploitation and abandonment of land resources, the building and maintenance of field terraces, the rate and scale of human demographic growth, movement of peoples, access to scarce resources, which to a certain extent reflect impacts that seem to recur in time, irrespectively of scale and historic context.

Anthony Pace
Superintendent of Cultural Heritage (2003–18).

Chapter 5

The geoarchaeology of past landscape sequences on Gozo and Malta

Charles French & Sean Taylor

5.1. Introduction

Geoarchaeological survey, test excavations and sampling on Gozo and Malta concentrated on the sites and landscapes associated with the Neolithic temple period of the fourth and third millennia BC. Targeted investigations were carried out at two Neolithic temple sites of Ġgantija and Santa Verna on the Xagħra plateau and the associated Ramla and Marsalforn valleys on Gozo. Sequences were also recovered from the excavations of the Neolithic Taċ-Ċawla settlement site in the modern town of Rabat and the later Bronze Age mesa-top site of In-Nuffara. On Malta, geoarchaeological work focused on the temple site of Skorba, and the nearby valley coring site of Xemxija, as well as the deep valley core sites of Wied Żembaq, Marsaxlokk and Salina (Figs. 2.4 & 5.1).

In the context of the on-site investigations, test excavations at the Santa Verna, Ġgantija and Skorba temple sites and at the Taċ-Ċawla settlement site all revealed old land surfaces beneath mixed soil and cultural deposits. For the off-site geoarchaeological work, some 200 hand-augered boreholes were made during the 2014/15/16 field seasons. Most boreholes were in the Santa Verna to Ġgantija areas on the margins of the modern town of Xagħra, across the intervening Ramla valley to In-Nuffara and down-valley to the sea, and also in the Marsalforn valley from Rabat northwards to the sea (Fig. 5.1). The areas around the Ta' Marżiena and Skorba temple sites were also investigated briefly for comparison using the hand auger, but no sample test pits were excavated. This geoarchaeological programme has provided sufficient soil/sediment sequence data to address several sets of aims as set out below, and in combination with the analysis of the deep valley cores (see Chapters 2 & 3), it is now possible to suggest a model for Holocene landscape development.

It has always been assumed that the seasonally dry and hot Mediterranean climate made the

Gozitan and Maltese landscapes quite 'marginal' in agricultural terms (Grima 2008a; Schembri 1997). As a consequence, it has also been presumed that terracing was adopted extensively from the Bronze Age onwards on both islands to conserve soils and moisture, and also to create a more suitable landscape for subsistence based agriculture (Grima 2004). Like many other parts of the southern Mediterranean, this landscape is prone to deforestation, drought and erosion combined with intensive human activity, and that this has been the case since Neolithic times (Bevan & Conolly 2013; Brandt & Thornes 1996; Hughes 2011; Grove & Rackham 2003). The *FRAGSUS Project* aimed to examine these assumptions and test them with a suite of archaeological science approaches that would shed new light on the nature and impact of Neolithic farming and on the degree of fragility of this island landscape.

Within the overall project, the main objectives of the geoarchaeological work were to:

- 1) investigate the deposit and soil catena sequence of the Xagħra plateau and its associated Ramla and Marsalforn valleys for the Holocene;
- 2) identify floors, floor deposits, old land surfaces and palaeosols associated with the Neolithic monuments, concentrating on the Santa Verna, Ġgantija and Skorba temple sites, as well as the Taċ-Ċawla settlement site;
- 3) create a model for the Holocene land-use sequence for Gozo and Malta, focusing on the impact of Neolithic agriculture and later landscape terracing, and
- 4) establish if there is any correlation between observed soil properties and prehistoric activities and/or longer-term climate change.

The results of the geoarchaeological analyses are discussed below, with the borehole logs and field

Table 5.1. Micromorphology and small bulk sample sites and numbers.

Site, profile and context	Micromorphology sample numbers	Small bulk sample numbers	Description
Ġgantija:			
Test Pit 1	28: terrace soil; 27 and 26: lower terrace/buried A; 25, 24, 23: buried B	16 and 17: terrace and buried A 18–22: buried soil	Terrace soil over <i>in situ</i> reddish brown palaeosol developed on Upper Coralline Limestone
WC Trench 1	Archaeological horizons: (top) 13, context 1016; 12, context 1015; 6, 7 and 11: contexts 1040, 1042 and 1004; Buried soil: 10, 9 and 8, context 1019 (base)	1–4: Archaeological horizons; 6–10: Buried soil	Later Neolithic stone structure collapse over <i>in situ</i> midden and soil aggradation over a reddish brown palaeosol developed on Upper Coralline Limestone
Xagħra town:			
Quarry; new house site 2; house site 3	5 and 6; 9 and 11; 12 and 13	4; 10; 15	<i>In situ</i> buried <i>terra rossa</i> soils on Upper Coralline Limestone beneath nineteenth century town houses
Santa Verna:			
Temple internal excavations	Buried soils: Ashby Pr2: 2/1–2/3; Cut 55 Pr3: 3/1–3/2; Tr E Pr4: 4/1–4/4 Pit fill in Cut 55: 3/3 and 3/4	1–3; 1 and 2; 1–4; 3 and 4	<i>In situ</i> brown to reddish-brown palaeosols on Upper Coralline Limestone beneath Neolithic temple floors
Trench B (outside temple to north)	Buried soil: Tr B Pr 1: 1/1–1/4	1: Terrace soil 2–4: Buried soil	<i>In situ</i> terrace soil over buried <i>terra rossa</i> soil on Upper Coralline Limestone
Transects & test pits in vicinity: L	L; Test Pit 5; BH54	3 spot samples	Possible of buried soils
Taċ-Ċawla:	9, 14, 139, 261, 301	-	Possible buried soils
In-Nuffara:	2 silos: 17 and 40, 503 and 509	-	Basal fills of Bronze Age storage silos
Marsalforn valley, Pr 626	Colluvial soil sequence: 626/1–626/3	626/1–626/3	Colluvial/soil valley fill sequence on Globigerina Limestone
Ramla valley, Pr 627	Alluvial aggradation sequence: 627/1–627/3	627/1–627/3	Alluvial aggradation valley fill sequence on Globigerina Limestone
Skorba:			
Section 1, Trench A	11, 20, 24, 28	11, 20, 24, 28	Cumulative buried soil
Section 2, Trench A	23, 26 (x2), 3–5, 75, 78	23, 26 (x2), 3–5	Cumulative buried soil; with 26 as plaster floor
Dwerja:	616	616	Possible buried soil under terraces
Deep cores:			
Xemxija 1	1–25	1–25	Spot samples through core sediments
Wied Żembaq 1	26–38	26–38	Spot samples through core sediments
Marsalokk 1	39–47	39–47	Spot samples through core sediments
Salina 21B	3 spot sub-samples	-	Spot samples of ? eroded soil at base (27.83–28.12 m)

profile descriptions (after FAO & ISRIC 1990) found in Appendix 6, the thin section descriptions in Appendices 7 and 8, the sample list in Table 5.1, the summary dating of the analysed profiles in Table 5.2, and the optically stimulated luminescence (OSL) dating report in Appendix 2. Note that the comprehensive

radiocarbon dating study is discussed in this volume (see Chapter 2), and the site-based geoarchaeological and micromorphological studies at Santa Verna, Ġgantija, Skorba, In-Nuffara and Taċ-Ċawla are reported on separately in the *FRAGSUS* excavation Volume 2.

The geoarchaeology of past landscape sequences on Gozo and Malta

Table 5.2. Summary of available dating (archaeological, radiocarbon and OSL) for the sites investigated in Gozo (after R. McLaughlin, pers. comm. and Cresswell et al. 2017) (Note: OSL dates in italics are poorly constrained due to low precision and large dispersion of equivalent doses as determined by OSL analysis).

Site and context	cal. BP date	cal. BC date (2σ)	Laboratory number	Quartz OSL sediment ages (years/ka)	BC/AD date	SUTL number
Santa Verna:						
Early Neolithic phase	6412±44; 6239±37; 6181±40; 6151±33	5500–5320; 5300–5070; 5290–5000;	UBA-31042; UBA-31044; UBA-31043; UBA-31048			
Temple build	4645±87; 4908±37	3790–3630	UBA-33706; UBA-31041			
Xaghra Brochtorff Circle:		c. 3650–3200	(see Malone <i>et al.</i> 2009)			
Ġgantija:						
Temple build		3510–3080				
Tarxien period		2840–2380				
Pre-temple midden soil in WC Trench, context 1021	3962±50	2580–2300	UBA-33707			
Base of terrace deposits/top of old land surface in TP1, 68–72 cm				3.16±0.25	1140±250 BC	2914
Lower horizon of buried soil in TP1, 92–96 cm		c. 2900–2350	presence of common Tarxien pottery	10.79±0.68	8560±630 BC	2915
Skorba:						
Base of buried soil				10.80±0.71	8780±710 BC	2927
Old land surface of buried soil				10.11±0.59	8090±590 BC	2926
Amended buried A horizon above				9.78±0.56	7760±560 BC	2925
Early Neolithic phase	6158±51; 6005±51	c. 5200–5000; 5000–4800	UBA-33710; UBA-33708			
Ramla valley Pr 66:						
Base of valley hillwash, 103–106 cm				0.10±0.03	1910±30 AD	2923
Mid-point in fill sequence, 62–66 cm				0.17±0.01	1850±12 AD	2922
Top of valley hillwash, 15–20 cm				0.14±0.02	1880±16 AD	2921
Marsalforn valley Pr 110:						
Base of valley hillwash fill, 320–325 cm				3.50±0.34	1480±340 BC	2919
Lower incipient soil horizon at mid-point of lower valley fill, 265–270 cm				3.58±0.24	1560±240 BC	2918
Top of upper incipient soil horizon at mid-point of valley fill, 175–180 cm				2.78±0.92	760±920 BC	2917
Xemxija 2 core, Malta: base at -9.9 m	8334±46	c. 7500–7200	UBA-29347			

5.2. Methodology and sample locations

The bulk of the geoaerchaeological work involved using hand-augered boreholes at both systematic and judgemental intervals across the landscape to assess the valley deposit sequences and check for the presence/absence of buried soils and former agricultural terrace soils, and to note the geological substrates present from high mesa plateau to valley bottom positions. Auger-hole positions were recorded with a hand-held Garmin GPS and measured descriptive profile records kept (Appendix 6).

Given the archaeological interest and efforts concentrated on the Neolithic temple sites of Santa Verna and Ġgantija and Santa Verna and the Taċ-Ċawla Neolithic settlement site, all on the Xagħra plateau, and the Bronze Age use of the In-Nuffara plateau to the south, it was also essential to investigate the intervening Ramla valley and the sediment/soil sequences between Xagħra and the sea. In addition, the Marsalforn valley to the west of Xagħra, running from Rabat town northwards to the sea, was also investigated. These valley systems were investigated using a series of hand-auger borehole transects undertaken by the authors (Fig. 5.1). Some

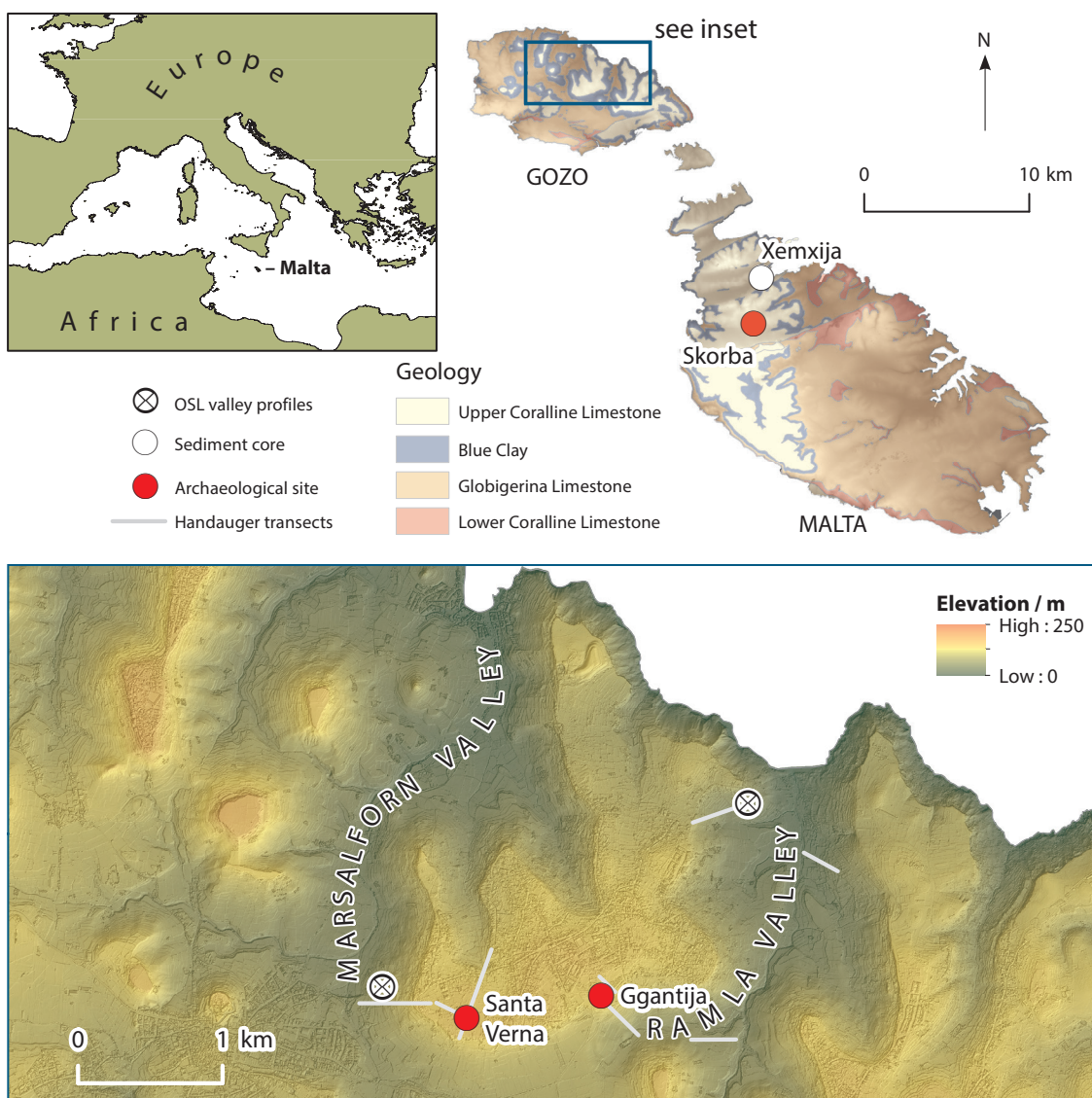


Figure 5.1. Location map of the test excavation/sample sites and geoaerchaeological survey areas on Gozo and Malta, with the geology and elevations, based on LiDAR last return data (December 2012), supplied by the former Malta Environment and Planning Authority, with world coastlines plotted using public domain data from www.naturalearthdata.com, and geology plotted after Lang (1960) (R. McLaughlin).

150 boreholes were made and recorded (Appendix 6), and a further 50 boreholes were made elsewhere in the island. In addition, five test pits and one excavation area were recorded and sampled at Ġgantija temple, as well as the excavation trenches at the Santa Verna and Skorba temple sites and In-Nuffara storage pit excavations (Appendix 6). Five profiles, one at Ġgantija temple, two at Skorba temple, and one each in the valley bottoms of Ramla and Marsalforn were sampled extensively for OSL profiling and dating by Dr T. Kinnaird (SUERC, University of Glasgow) with an outlier Punic-Roman site of Tal-Istabal, Qormi, on the outskirts of Valletta also sampled with one OSL determination (see Chapter 2; Appendix 2).

This geoarchaeological survey and test excavations exposed buried soil and erosion profiles especially suitable for soil micromorphological block and small bulk sampling (Table 5.1). In total, 70 soil blocks (and 44 complementary small bulk soil samples) from 12 key soil profiles from the archaeological sites and valley profiles, and a further 50 small soil blocks (and a similar number of small bulk samples) from the valley deep cores were prepared for thin section analysis (Table 5.1) (after Murphy 1986; Courty *et al.* 1989) and described using the accepted terminology of Bullock *et al.* (1985), Stoops (2003) and Stoops *et al.* (2010) (Apps. 7 & 8). In addition, a suite of basic physical parameters (pH, loss-on-ignition and magnetic susceptibility) (Table 5.3) and multi-element ICP-AES analyses (Table 5.4) were carried out a series of small bulk samples (44 from soil profiles and 50 from the deep cores) taken in conjunction with the micromorphological block samples (Avery & Bascomb 1974; Clark 1996, 99ff; French 2015; Holliday & Gartner 2007; Oonk *et al.* 2009; Tite & Mullins 1971; Wilson *et al.* 2005, 2008, 2009). pH measurements were determined using a 10 g to 25 ml ratio of <2 mm air-dried soil to distilled water with a Hanna HI8314 pH metre. Determining loss-on-ignition followed the protocol of the Department of Geography, University of Cambridge, to record the percentages of calcium and carbon in the soil (www.geog.cam.ac.uk/facilities/laboratories/techniques/psd.html). For loss-on-ignition (*ibid.*), weighed sub-samples were heated to 105° C for six hours to measure water content, then heated to 400° C for six hours to measure carbohydrate content, then to 480° C for six hours to measure total organic matter content, and finally heated to 950° C for six hours to measure CO₂ content lost from CaCO₃ within the sediment (Bengtsson & Ennell 1986). The calcium carbonate content can then be calculated by stoichiometry (Boreham *et al.* 2011). A Malvern Mastersizer was used for the particle size analysis (Table 5.3) using the same Geography facilities at Cambridge. For magnetic susceptibility measurements, a Bartington MS2B metre

was used, giving mass specific calculations of magnetic susceptibility for weighed, 10 cm³ sub-samples (English Heritage 2007, 27). Multi-element analyses using the 35-element aqua regis ICP-AES method were conducted at the ALS Global Laboratory in Seville (www.alsglobal.com), and the elements exhibiting greater than trace amounts and/or are generally considered to be enhanced by human activities (cf. Wilson *et al.* 2008; Fleisher & Sulas 2015) are tabulated in Table 5.4.

5.3. Results

5.3.1. Santa Verna and its environs

Santa Verna is situated on the southwestern side of Xagħra town and the Upper Coralline Limestone plateau overlooking a small valley running south–north, the Wied Ġnien Imrik (Fig. 5.1). The hand-auger survey on the Upper Coralline Limestone plateau around the temple (13 boreholes) revealed less than 50 cm of reddish brown, fine sandy silt loam topsoil to the north of the temple, present in small-holder arable fields (Appendix 6, Transect L). To the south, this was even thinner with increasingly extensive patches of bare rock with open scrub pasture, mainly used for bird hunting today. East of the temple and dipping into the Wied Ġnien Imrik valley, the soil profiles in the auger survey deepened quickly to as much as 100 cm with some B horizon survival consisting of a well-structured, reddish brown silt loam to silty clay loam, before thinning again eastwards to c. 10–45 cm of modern ploughsoil, where the area was all used for small-holder arable fields.

The 2015 excavations on the southern edge of the temple surprisingly discovered *in situ* buried soils beneath a series of temple floors and deposits (Fig. 5.2). New radiocarbon dates indicate that this is the earliest monument present on the Xagħra plateau where temple construction began in the early fourth millennium BC (c. 3800–3700 cal. BC; 4945±87 BP, 4905±37 BP; UBA-33706, UBA-3141), well prior to the construction of Ġgantija temple just to the east (see Chapter 2). This was particularly well exemplified in Trench E, as well as in the 2015 excavations on the southern edge of the temple where *in situ* buried soils were discovered beneath a series of temple collapse and midden deposits, and in the re-excavated sondages of Ashby and Trump (Figs. 5.3 & 5.4). The base of the Ashby 1911 Sondage revealed a well preserved, c. 45 cm thick, palaeosol which comprised of a c. 15 cm thick organic A (Ah) silt loam horizon over a reddish brown silt loam B horizon of about 30 cm in thickness. A similar occurrence was also revealed in the Trump Sondage about 3 m to the north and in the trial trench which was cut some 30 m to the northeast

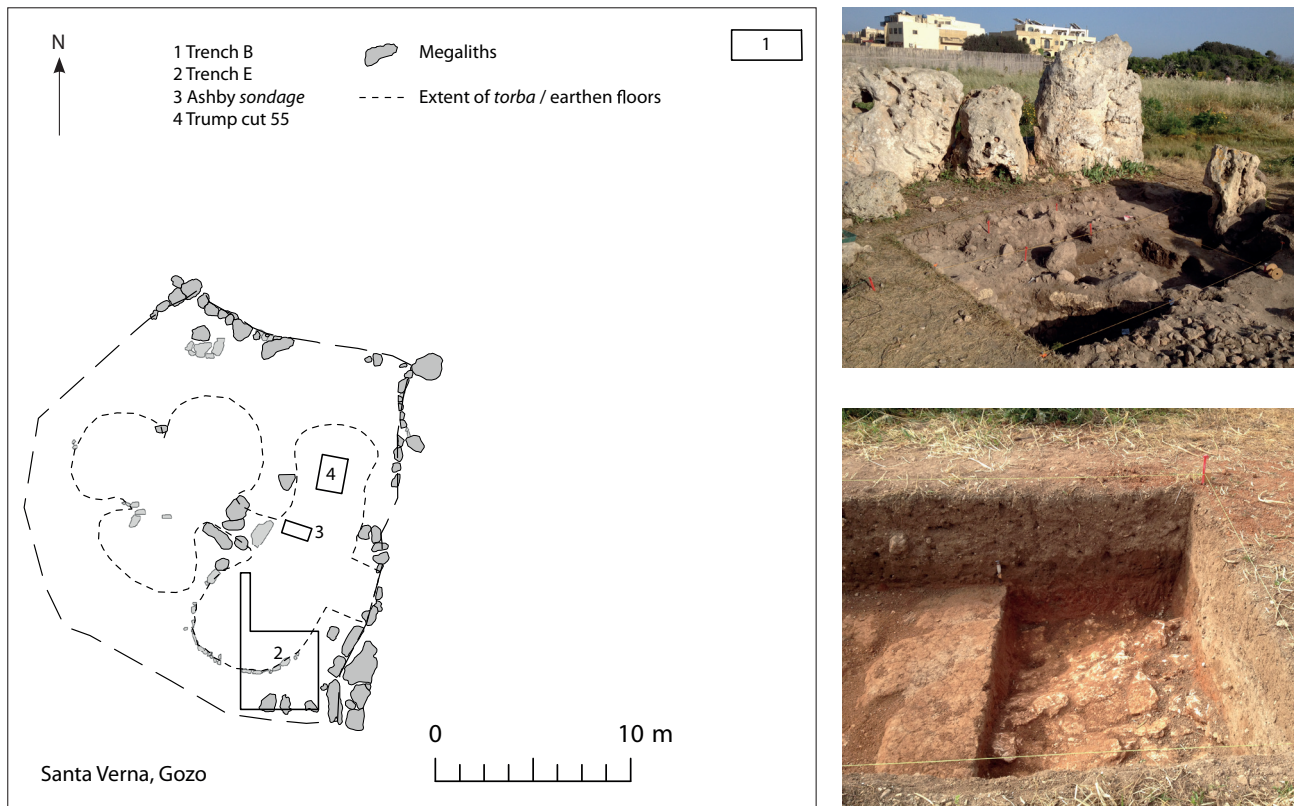


Figure 5.2. Plan of Santa Verna temple and the locations of the test trenches (R. McLaughlin) (left) with a view of upstanding temple megaliths behind Trench E (upper right) and the terra rossa soil below terrace deposits in Trench B outside the temple (lower right) (C. French).

of the temple site. All three buried soil profiles were sampled for soil micromorphological analysis and physical characterization. Thick (c. 30–100 cm) stone rubble deposits were observed directly above these intact buried soils, and these were either interrupted by thin *torba* or earthen floors (Figs. 5.2 & 5.3) (and see Volume 2, Chapter 4).

In July, 2014, the soil sequences around Santa Verna Temple were investigated, especially those to the north of the temple remains where field walking had led to the recovery of a polished stone axe and Żebbuġ, Red Skorba and Għar Dalam pottery of the Neolithic period (see Volume 2). The reason for the interest in these soils was to understand whether there is a correlation between soil properties and prehistoric settlement/activity. A reasonable thickness of soil coverage in this area meant that these fields are presently cultivated. The soils are characterized by reddish brown silt and silty clay loams, and are in places at least 1 m deep. The archaeological material together with the nature of the soils make this a potentially important part of the landscape for geoarchaeological investigation. To the south, closer to the edge of the

Upper Coralline Limestone plateau, the soils were characterized as Leptosols, i.e. they were either very thin or non-existent, often with large irregular patches of bare Coralline bedrock exposed. Thus severe rain, wind and agricultural erosion has taken place here, demonstrating the fragility of the soil system on these mesa plateau areas on Gozo.

5.3.1.1. Physical and elemental characterization

At Santa Verna, pH values from the buried soils are very alkaline (ranging from 8.5–8.92) and the magnetic susceptibility values were generally low, except for the lower fill of the pit in Trump Cut 55 (sample 3/4) (Table 5.3). This probably also reflects the amount of organic and fire-related settlement debris contained within this fill deposit (Allen & Macphail 1987; Tite & Mullins 1971). The total organic matter content is a reasonable c. 4.1–6.5 per cent in the buried soils, better than the modern topsoil at c. 3.4 per cent (Table 5.3). There is a strong calcium carbonate component throughout, ranging from c. 8–64 per cent (Table 5.3), but this is generally lower than the values observed in the Ġgantija soil sequence, especially in the base of

the buried soil. The particle size analysis results indicate that the buried soils tend to be dominated by the silt fraction (c. 46–76 per cent), a potential loessic or wind-blown component, but with a strong but variable quartz sand component (c. 10–52 per cent), with the clay fraction ranging between c. 5 and 15 per cent (Table 5.3). The higher clay component in the buried soils as compared to those at Ġgantija is reflected in the well organized clay fraction observed in thin section in the basal horizon of the buried soil (see §5.3.1.2).

In the multi-element analysis, the upper parts of the soil profiles and the *torba* floors at Santa Verna were notably all moderately to highly enhanced with phosphorus and strontium values (Table 5.4). Phosphorus values varied from 1200 to >10000 ppm, with the Trench E profile and pit fill very enhanced throughout (i.e. 4510 ppm in the pit base to 9250 ppm in the upper *torba* floor), with relatively enhanced strontium

varying between 195–406 ppm. These elements suggest that the upper horizon of the soils and the *torba* floors were receiving substantial amounts of midden-type, organic settlement-derived, waste material prior to burial (Entwistle *et al.* 1998; Wilson *et al.* 2008) (and see Volume 2). Although calcium values were often of a similar range to those at Ġgantija, the range of values in the pre-temple buried soils (Profiles 2 and 3) was much less (ranging from 1.4–8.4 per cent with higher/lower values in the upper and lower samples), a factor which is also reflected in the micromorphological results below.

5.3.1.2. Soil micromorphology

From the borehole transect and Trench B to the north-northeast of Santa Verna temple, there was a well preserved buried soil of variable thicknesses present beneath c. 40 cm of gravelly fine sandy silt

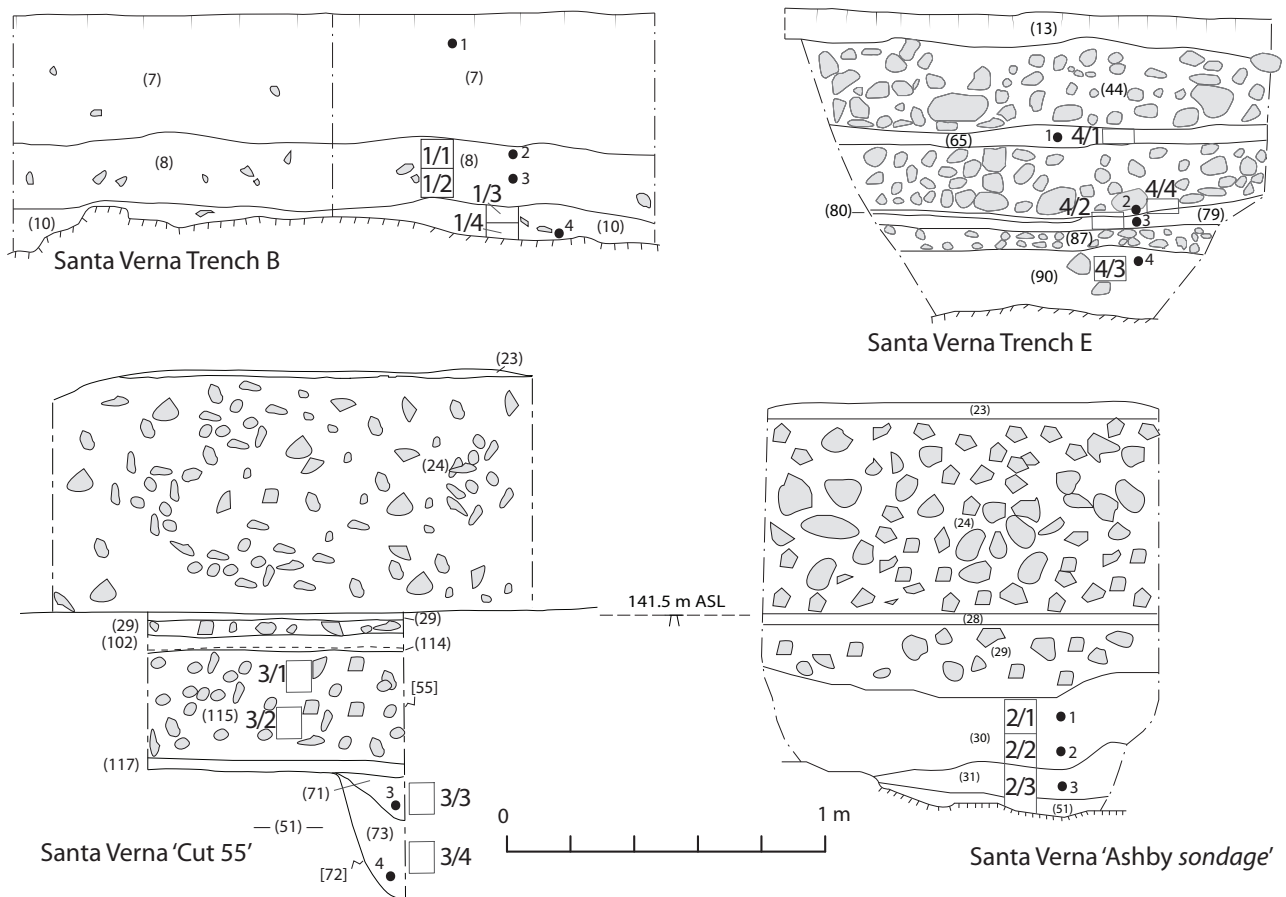


Figure 5.3. Santa Verna excavation trench profiles all with sample locations marked: upper left: the off-site Trench B buried red soil below terrace deposits; lower left: the Trump Cut 55 profile with pit fill and associated buried soil; upper right: Trench E profile showing a series of thin earthen floors with limestone rubble inbetween and buried soil below; lower right: the Ashby Sondage profile with the buried soil at its base (Note: open boxes = micromorphology block samples; back circles = small bulk samples) (R. McLaughlin).

Table 5.3. pH, magnetic susceptibility, loss-on-ignition (% organic matter) and % sand/silt/clay particle size analysis results for Ġgantija, Santa Verna, Xaghra town, Marsalforn valley and Ramla valley profiles, Gozo.

Site, sample and depths (cm)	pH	MS SI/g x10 ⁻⁸	% total organic matter	% Ca CO ₃	% sand	% silt	% clay
Ġgantija TP1:							
Modern topsoil: 16, 16–20 cm	7.79	1.77	3.42	72.1	82.24	17.62	0.14
Terrace soil: 17, 70–80 cm	7.91	1.46	5.0	49.25	8.51	82.36	9.13
Buried soil: 18, 80–90 cm	8.0	1.46	5.3	45.26	21.55	71.65	6.8
Buried soil: 19, 90–100 cm	8.06	1.52	4.82	41.42	49.47	45.09	5.44
Buried soil: 20, 100–110 cm	8.16	1.69	4.74	51.65	77.98	21.58	0.44
Buried soil: 21, 110–120 cm	8.2	1.83	4.55	54.26	30.39	60.92	8.69
Buried soil: 22, 120–130 cm	8.19	1.82	4.67	33.83	12.37	73.42	14.21
Ġgantija WC Trench:							
Arch horizons: 12, 1015	8.65	1.04	2.15	77.69	38.74	56.06	5.2
Arch horizons: 13, 1016	8.55	568.6	3.225	70.25	66.73	32.86	0.41
Arch horizons: 6, 1004	8.44	1.085	3.07	70.2	12.24	76.5	11.26
Arch horizons: 7, 1004	8.74	516.4	2.45	72.63	4.9	80.11	14.99
Transition: 11, 1004/1019	8.05	66.4	3.16	67.16	65.21	34.14	0.65
Buried soil: 10, 1019	8.48	62.3	3.5	59.68	62.06	37.44	0.5
Buried soil: 9, 1019	9.05	1.02	4.5	47.26	77.98	21.58	0.44
Buried soil: 8, 1019	9.15	1.97	5.1	41.2	82.25	17.6	0.15
Xaghra town buried soils: (no sample material left)							
Quarry: 4	7.62	2.56	-	-	-	-	-
Site 3: S16	7.59	3.22	-	-	-	-	-
Site 2: S10	7.37	1.78	-	-	-	-	-
Santa Verna buried soils:							
Tr B 1/1, 10–20 cm	8.72	3.65	5.38	51.26	47.47	47.49	5.04
Tr B 1/2, 50–58 cm	8.84	3.72	4.1	49.35	26.31	69.56	4.13
Tr B 1/3, 60–70 cm	8.7	5.68	5.44	14.58	25.4	66.6	8.0
Tr B 1/4, 80–90 cm	8.5	4.54	6.5	10.14	38.47	55.98	
Ashby 2/1, 95–105 cm	8.36	4.18	4.4	25.15	23.33	71.45	5.22
Ashby 2/2, 105–115 cm	8.5	3.97	5.52	7.68	52.32	46.64	1.04
Ashby 2/3, 115–125 cm	8.6	2.65	5.45	8.17	40.04	54.84	5.12
Trump Cut 55 3/1, 100–110 cm	8.68	2.6	4.92	25.3	32.93	60.33	6.74
Trump Cut 55 3/2, 120–130 cm	8.86	2.6	5.5	15.76	17.02	73.67	9.31
Trump Cut 55 3/3, pit fill: 110–120 cm	8.72	2.62	4.5	42.27	23.97	66.95	9.08
Trump Cut 55 3/4, pit fill: 150–160 cm	8.7	2.6	6.7	31.26	21.18	68.51	10.31
Tr E 4/1, 40–43 cm	8.92	3.01	4.53	48.71	25.09	65.01	9.9
Tr E 4/2, 69–74 cm	8.84	3.02	3.89	64.16	9.71	75.7	14.59
Tr E 4/3, 83–93 cm	8.68	2.8	4.65	36.12	24.81	66.86	8.33
Marsalforn, Pr 626:							
626/1	8.23	136.2	1.97	77.6	28.68	62.33	8.99
626/2	8.36	147.0	2.24	75.02	18.22	64.67	17.11
626/3	8.13	242.72	1.66	79.71	34.57	58.46	6.97
Ramla valley, Pr 627:							
627/1	8.16	117.08	6.3	64.16	17.92	71.28	10.8
627/2	8.07	72.71	3.15	54.95	10.52	79.17	10.31
627/3	8.0	138.21	3.18	56.0	36.4	59.97	3.63

The geoarchaeology of past landscape sequences on Gozo and Malta

Table 5.4. Selected multi-element results for Ġgantija, Santa Verna and Xagħra town buried soils, and the Marsalforn and Ramla valley profiles, Gozo.

Site, sample and depths (cm)	Ba ppm	Ca %	Cu ppm	Fe %	K %	Mg %	Mn %	Na %	P ppm	Pb ppm	Sr ppm	Zn ppm
Ġgantija TP1:												
Modern topsoil: 16–20 cm	30	17	40	2.48	0.45	0.79	0.03	0.04	4610	41	193	110
Terrace soil: 70–80 cm	30	18	36	2.32	0.43	0.74	0.03	0.04	4820	10	198	97
Buried soil: 80–90 cm	30	18.6	33	2.17	0.49	0.78	0.02	0.06	8200	5	255	126
Buried soil: 90–100 cm	30	16.8	32	2.14	0.52	0.71	0.02	0.08	>10000	5	271	148
Buried soil: 100–110 cm	20	15.5	35	2.42	0.61	0.76	0.03	0.09	>10000	6	261	157
Buried soil: 110–120 cm	30	14.8	37	2.48	0.63	0.69	0.03	0.07	9970	10	235	143
Buried soil: 120–130 cm	30	14.2	40	2.65	0.66	0.69	0.03	0.06	8570	8	219	132
Ġgantija WC Trench: ppm:												
Arch horizons: 12, 1015	40	>25	27	1.25	0.3	1.07	122	0.07	5770	3	322	71
Arch horizons: 13, 1016	40	>25	38	1.47	0.37	0.94	142	0.07	5010	3	292	75
Arch horizons: 6, 1004	40	>25	33	1.83	0.47	1.33	207	0.13	>10000	3	380	185
Arch horizons: 7, 1004	60	22.4	41	2.44	0.64	1.03	378	0.13	9600	11	355	164
Transition: 11, 1004/1019	50	>25	32	1.65	0.87	1.06	160	0.07	8830	4	293	86
Buried soil: 10, 1019	30	21.3	40	2.3	0.73	0.9	221	0.07	7520	9	281	100
Buried soil: 9, 1019	50	18.5	43	2.66	0.59	.85	243	0.08	6940	10	260	108
Buried soil: 8, 1019	30	14.7	46	3.1	0.4	0.89	309	0.08	6720	13	238	120
Xagħra town buried soils:												
Quarry S4	<10	1.66	73	4.59	0.78	0.5	350	0.03	350	25	37	75
Site 3: S16	<10	0.87	79	4.95	0.85	0.53	260	0.03	260	21	36	68
Site 2: S10	<10	1.56	72	4.54	0.74	0.48	330	0.05	330	23	34	63
Santa Verna buried soils:												
Tr B 1/1, 10–20 cm	100	17.6	40	2.61	0.5	1.1	346	0.06	7010	20	222	132
Tr B 1/2, 50–58 cm	80	18.9	26	2.43	0.61	1.18	272	0.06	5380	9	229	86
Tr B 1/3, 60–70 cm	90	1.67	21	4.46	1.16	0.96	381	0.05	480	22	58	75
Tr B 1/4, 80–90 cm	90	3.87	22	4.16	1.03	1.01	392	0.04	1200	18	76	80
Ashby 2/1, 95–105 cm	80	6.18	28	3.51	1.03	1.0	476	0.08	2800	16	122	86
Ashby 2/2, 105–115 cm	80	1.43	26	4.19	1.16	0.89	553	0.06	910	20	57	77
Ashby 2/3, 115–125 cm	80	1.54	26	4.23	1.2	0.88	450	0.06	900	20	53	78
Trump Cut 55 3/1, 100–110 cm	90	13.3	69	2.57	0.9	1.33	482	0.24	>10000	9	301	261
Trump Cut 55 3/2, 120–130 cm	90	8.4	31	3.41	1.04	1.08	464	0.11	3270	16	155	88
Trump Cut 55 3/3, pit fill: 110–120 cm	90	2.41	28	4.04	1.08	0.94	541	0.08	970	19	57	80
Trump Cut 55 3/4, pit fill: 150–160 cm	100	17.4	53	2.22	0.88	1.17	357	0.28	>10000	6	328	178
Tr E 4/1, 40–43 cm	70	18.5	40	2.43	0.75	1.41	307	0.12	9250	9	327	133
Tr E 4/2, 69–74 cm	70	20.7	42	2.03	0.7	2.81	280	0.17	8400	8	361	131
Tr E 4/3, 83–93 cm	70	14.8	34	2.98	1.05	1.24	368	0.09	6850	12	195	115
Marsalforn valley:												
626/1	40	19.4	15	2.61	0.58	0.84	198	0.08	2020	12	527	55
626/2	40	19.4	12	2.58	0.55	0.8	193	0.08	1960	11	506	53
626/3	30	19.6	13	2.61	0.54	0.71	224	0.1	1930	12	494	52
Ramla valley:												
627/1	20	>25	17	1.38	0.31	0.56	168	0.08	2240	26	693	48
627/2	30	>25	10	1.72	0.33	0.52	173	0.09	2300	14	667	41
627/3	30	23.6	11	1.84	0.41	0.6	179	0.11	1930	10	703	47

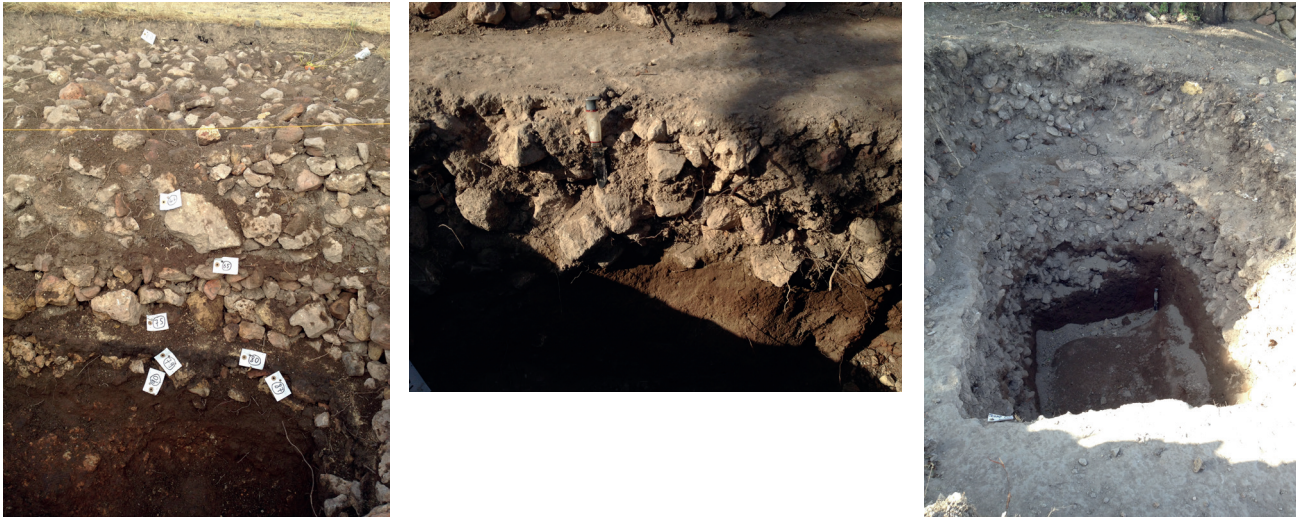


Figure 5.4. The red-brown buried soil profiles in Trench E (left), the Ashby (centre) and Trump (right) Sondages within the Santa Verna temple site (C. French).

loam ploughsoil (Figs. 5.2–5.5; Table 5.5). In all other directions surrounding the temple, the auger survey revealed that the land surface is either severely denuded with large areas of bare exposed areas of Upper Coralline Limestone bedrock present and/or supports only a single horizon, thin (<15 cm thick), turf/organic micritic, fine sandy silt loam topsoil which is often a strong reddish brown in colour.

This buried soil revealed in Trench B exhibited three horizons in thin section. The uppermost horizon (sample 1/1 and the upper c. 4 cm of sample 1/2) was a pellety to aggregated, gravelly silty clay, strongly reddened with amorphous sesquioxides (Figs. 5.5a & b). There is a dust of very fine organic matter/charcoal as well as about 10–20 per cent micro-sparite (or silt-sized calcium carbonate), and common sesquioxide nodules throughout the groundmass. The middle horizon (lower part of sample 1/2) was completely dominated by micro-sparitic calcium carbonate with c. 30 per cent as small aggregates of the same reddish brown silty clay fabric present in sample 1/1 above (Fig. 5.5c). There was a similar dust of very fine organic matter/charcoal throughout. The lowermost horizon (samples 1/3 & 1/4) was indicative of very different soil formation conditions. It is composed of a weak to moderately developed, small blocky, silty clay with very abundant, moderately birefringent, pure to dusty clay in speckles and striae throughout the groundmass (Fig. 5.5d).

This observed sequence suggests that the upper horizon of the buried soil is the lower A horizon of a very disturbed soil that has been subject to much physical mixing, oxidation and rubification processes

(Fedoroff 1997; Kooistra & Pulleman 2010), as well as considerable evapo-transpiration leading to the abundant secondary formation of micro-sparitic calcium carbonate (Durand *et al.* 2010). This importantly implies that it was an open and de-vegetated soil prior to burial. Moreover, this soil has undergone severe physical and soil faunal mixing leading to considerable aeration and oxidation with the concomitant formation of abundant secondary calcium carbonate. In particular, the middle horizon is essentially acting as a depleted, calcified and replaced, upper B or eluvial Eb horizon. The basal, organized clay-dominated lower soil horizon is indicative of a clay-enriched agric (or argillic) or the Bt horizon of a well developed Orthic Luvisol (or brown Mediterranean soil) (Bridges 1978, 69; Fedoroff 1997; WRB 2014; Yaalon 1997). It is characterized first by the weathering of the limestone substrate and then by clay illuviation down-profile creating a clay enriched lower Bt or argillic horizon. Also, there is a considerable component of aeolian dust, contributing to the ubiquitously high silt and very fine sand component of these soils, a feature that is widespread across the Mediterranean region (Muhs *et al.* 2010; Yaalon & Ganor 1973). There are also a few discontinuous linings of the voids with micro-sparite (Fig. 5.5e), indicating secondary calcification processes in this soil. The whole profile, and especially the lowermost horizon, is also becoming very reddened or rubified. This process involves iron compounds which are produced from the weathering of minerals including iron oxides and hydroxides precipitating as poorly crystalline ferrihydrites or haematite, which then coat the silt/sand grains and clays (Lindbo *et al.*

2010; Yaalon 1997). This strong reddening or rubification of the palaeosol probably occurred hand-in-hand with the process of clay illuviation (Fedoroff, 1997; Yaalon, 1997) and rapid bio-degradation of organic material, as well as increasing calcification with time. These latter processes are probably associated with the removal and disturbance of the vegetative cover and alternating periods of wetting/eluviation/leaching and long summer droughts (Bridges 1978, 33; Duchaufour 1982; Catt 1990; Clark 1996, 100; Goldberg & Macphail 2006, 70; Gvirtzman & Wieder 2001; Lelong & Souchier 1982; Lindbo *et al.* 2010; Stoops and Marcelino 2010; Yaalon 1997).

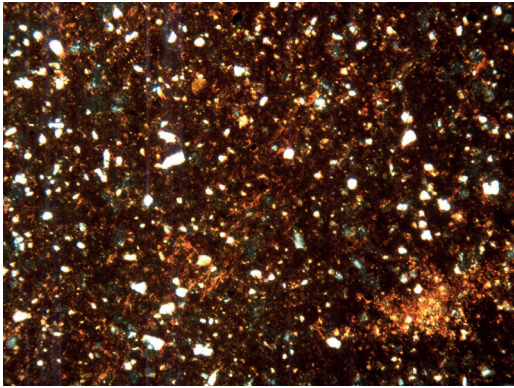
The sesquioxide nodules in the upper horizon of this soil (Fig. 5.5b) have probably formed through cheluviation as organo-metallic compounds associated with humic material from the root complex combining with strong iron staining (and aluminium, magnesium and silica) and moving down-profile through eluviation under weakly acidic and/or redoximorphic conditions (Wilson & Righi 2010). The bio-degradational processes may be caused by a number of factors such as cool and humid climatic conditions, seasonal sub-surface groundwater, acid producing vegetation, quartz-rich and base cation depleted parent materials, or a combination of two or more of these factors (Wilson & Righi 2010). Although one would not expect some of these conditions necessarily to exist here on the limestone bedrock, nonetheless the pollen analysis of

the Santa Verna (and Ġgantija) palaeosol suggests a damp, scrubby steppe habitat of pine, juniper, *Erica* and ferns, as well as the presence of aquatic organisms and particularly phytoplankton in the buried soil points to the presence of standing water bodies and an acidic flora in the immediate vicinity (see Chapter 2). These conditions may well have been conducive to creating these sesquioxide nodules in the former lower A horizon of the Santa Verna palaeosol.

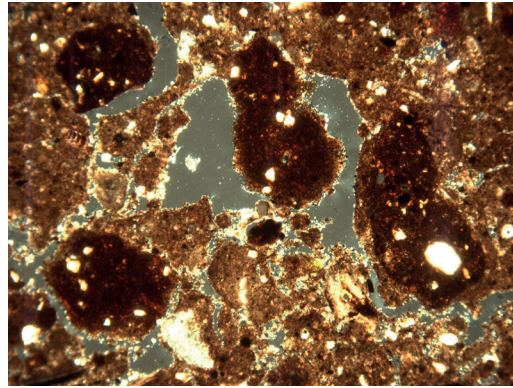
In the main excavations within the temple, a series of samples was taken from the possible *torba* floor sequences within the temple complex in Trench E (Profile 4), the Ashby Sondage (Profile 2) and Trump Cut 55 (Profile 3), all of which seal an *in situ* buried soil ranging in thickness from c. 15–60 cm (Fig. 5.4). These sequences will be more fully described in the excavation volume (Vol. 2), with the evidence from the buried soils concentrated on here.

In Trench E (Profile 4) just inside the main surviving arc of upright megaliths (Fig. 5.3), there was a series of at least two earthen/plaster ‘floors’ (samples 4/1 & 4/2) (Fig. 5.5h & i) interrupted by stone rubble deposits, all situated on a possible buried soil (sample 4/3). The buried soil (sample 4/3) beneath was composed of a pellety to small aggregated, reddish brown silty clay loam with common, birefringent, pure to dusty clay striations throughout the groundmass, as well as common very fine organic/charred punctuations and common sesquioxide nodules (Fig. 5.5f) and rare

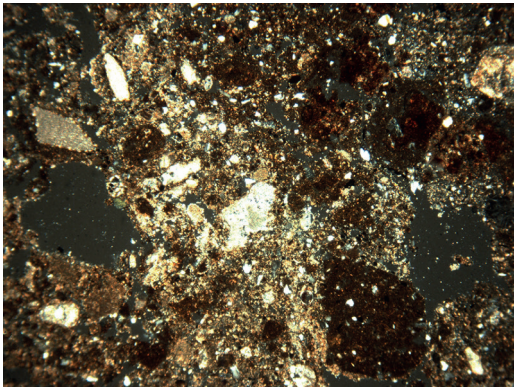
Figure 5.5 (overleaf). *Santa Verna soil photomicrographs (C. French): a) Photomicrograph of the buried reddish brown, calcitic fine sandy clay loam soil in BH115 (frame width = 4.5 mm; cross polarized light); b) Photomicrograph of pellety, micritic silty clay with sesquioxide nodules, Trench B, sample 1/1 (frame width = 4.5 mm; cross polarized light); c) Photomicrograph of mixed fabric of micritic calcium carbonate with aggregates of reddish brown silty clay fabric, Trench B, sample 1/2 (frame width = 4.5 mm; cross polarized light); d) Photomicrograph of pure clay (centre area) to fine dusty clay (to either side), Trench B, sample 1/4 (frame width = 2.25 mm; plane polarized light); e) Photomicrograph of striated clay-dusty clay groundmass with micritic calcium carbonate void linings, Trench B, sample 1/3 (frame width = 4.5 mm; cross polarized light); f) Photomicrograph of fine humic/charcoal dust with a burnt bone fragment in the basal soil, Trench E, sample 4/3 (frame width = 4.5 mm; plane polarized light); g) Photomicrograph of possible ‘floor’ composed an even mix of very fine limestone gravel and calcitic silt with abundant very fine organic punctuations and occasional bone fragments, Trench E, sample 4/4 (frame width = 4.5 mm; cross polarized light); h) Photomicrograph of a torba floor composed of a dense, brown silty clay with bone inclusions, Trench E, sample 4/1 (frame width = 2.25 mm; cross polarized light); i) Photomicrograph of a possible ‘floor’ or ‘mortar’ composed of a fine gravel size limestone, Trench E, upper part of sample 4/2 (frame width = 4.5 mm; cross polarized light); j) Photomicrograph of a mixture of silty clay with 25 per cent fine limestone gravel with a few included sub-rounded aggregates of birefringent clay and common very fine organic punctuations, torba floor context 28 (frame width = 4.5 mm; cross polarized light); k) Photomicrograph of similar mixed fabric of micritic calcium carbonate with aggregates of reddish brown silty clay fabric, Ashby Sondage, sample 2/1 (frame width = 4.5 mm; cross polarized light); l) Photomicrograph of striated silty clay fabric, Ashby Sondage, sample 2/3 (frame width = 2.25 mm; cross polarized light); m) Photomicrograph of micritic sandy silty clay with included bone and organic fragments, sample 78 torba floor (frame width = 4.5 mm; cross polarized light); n) Photomicrograph of the strongly reddened silty clay buried soil, Trump Cut 55, sample 3/2 (frame width = 4.5 mm; cross polarized light); o) Photomicrograph of finely laminar silt and organic dust in pit fill, Trump Cut 55, sample 3/3 (frame width = 4.5 mm; plane polarized light).*



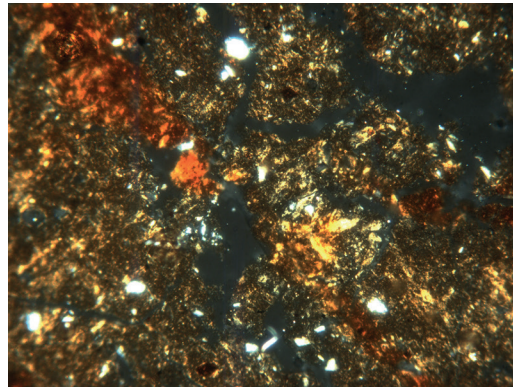
a



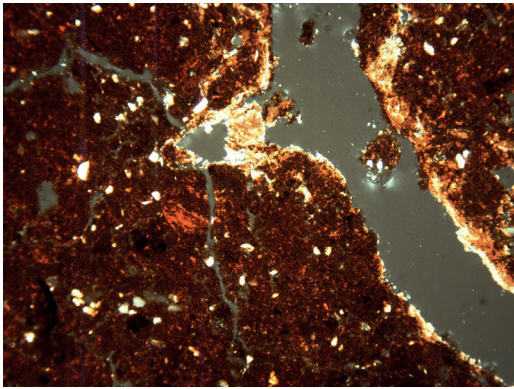
b



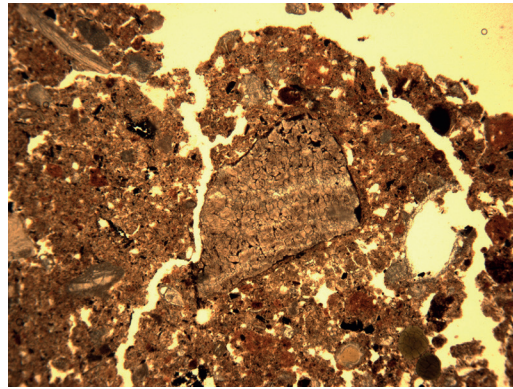
c



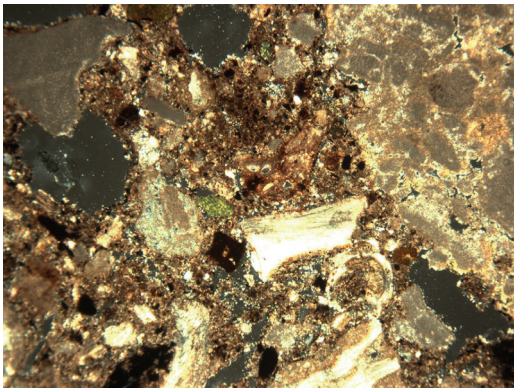
d



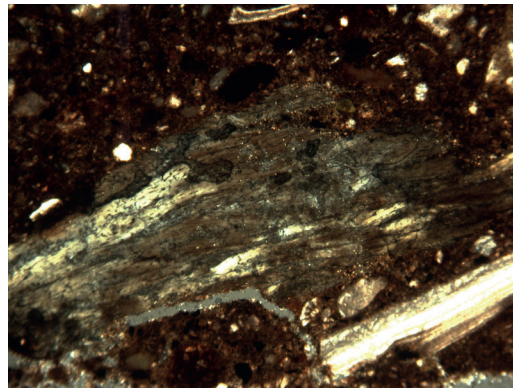
e



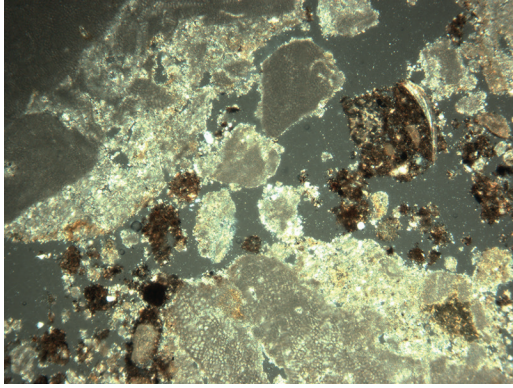
f



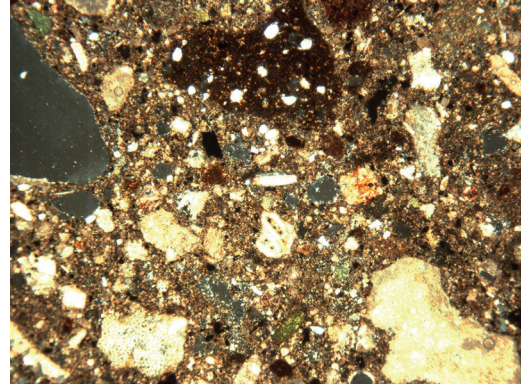
g



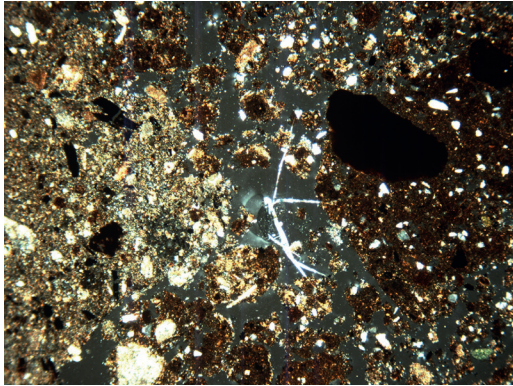
h



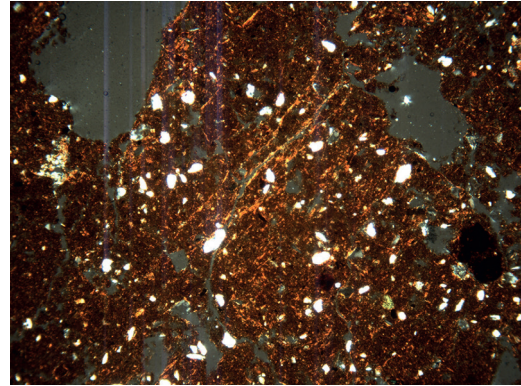
i



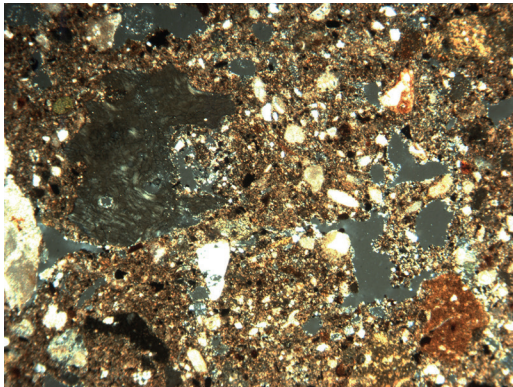
j



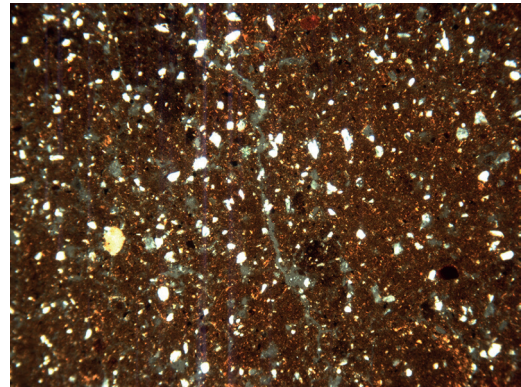
k



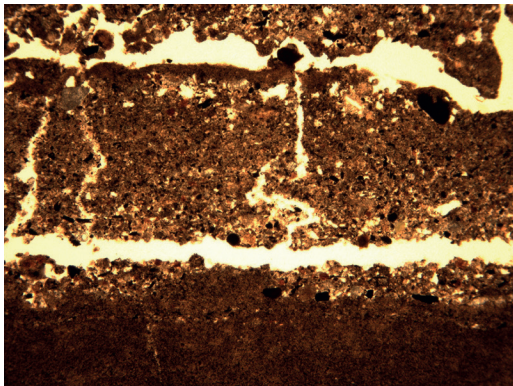
l



m



n



o

occurrences of very small burnt bone fragments. This points to a very disturbed and bioturbated, reddened and clay enriched Bt horizon soil, essentially similar in structure and fabric to that observed outside the temple in Trench B. No upper, organic Ah horizon was present, probably suggesting truncation associated with the act of temple construction.

Five metres to the north in the adjacent Ashby Sondage (Profile 2) (Fig. 5.4), also beneath a *torba* floor (contexts 27 & 28) (Figs. 5.5j & m) and limestone rubble (context 29) sequence, there was a c. 45 cm thick *in situ* buried soil. The upper c. 15 cm of this soil (sample 2/1; context 30) was a heterogeneous, pelley mixture of mainly micro-sparitic calcium carbonate with abundant fine to very fine charcoal fragments and fine aggregates of orangey brown silty clay, with an occasional pot and bone fragment present (Figs. 5.5g & k). Samples 2/2 (context 51) and 2/3 below over the next 20 cm were predominantly comprised of a striated, birefringent silty clay with strong amorphous sesquioxide reddening and only minor (<5 per cent) micro-sparitic calcium carbonate present (Figs. 5.5h & l). These samples also exhibited an irregular small blocky structure defined by fine channels, and they contained a fine organic/charcoal dust throughout. These features suggest that the buried soil represents a mixed, disturbed, lower A horizon over a relatively undisturbed clay-enriched and organized argillic B (or Bt) horizon. It has not suffered severe disruption, mixing and calcification as in the other profiles at Santa Verna.

In the adjacent Trump Cut 55 (Profile 3) (Fig. 5.3), there was a well preserved buried soil (samples 3/1 & 3/2) about 55 cm thick present beneath a hard-packed earthen floor. In contrast to the soil present in the Ashby Sondage (Profile 2), this buried soil exhibited a blocky to columnar blocky with a micro-aggregated microstructure, but exhibited a similar silty clay fabric strongly reddened with iron oxides and hydroxides with a dust of organic matter and very fine charcoal throughout (Fig. 5.5n). This soil became denser and more clay enriched with depth, exhibiting a well-developed striated to reticulate and birefringent, pure to dusty clay groundmass, just as in the base of the buried soil in Trench B (Fig. 5.5e) and in the Ashby Sondage (Fig. 5.5l). Although these reddened clays could simply be relict in origin (Davidson 1980; Fedoroff 1997) and the result of the long-term weathering of the limestone bedrock material (Catt 1990), the well organized, reticulate, gold to reddish-yellow, pure to dusty clay aspect of the groundmass is more indicative of an illuvial clay-enriched or argillic Bt horizon developed in the base of an *in situ* buried soil (Bullock & Murphy, 1979; Fedoroff 1968, 1997; Kuhn *et al.* 2010). This luvisolic

soil is the most well-developed of all the buried soil profiles observed in pre-Neolithic contexts at Santa Verna and Ġgantija.

It is clear that Profiles 2 and 3 have not suffered as severe disruption, mixing and calcification as the other buried soils encountered here and at nearby Ġgantija (see §5.3.2). Significantly, this soil is indicative of an earlier, well-developed and less disturbed soil type, more akin to a brown luvisolic Mediterranean soil associated with more moist and well vegetated conditions (Bridges 1978, 68–9; WRB 2014). Nonetheless, this soil is just beginning to be disturbed and opened-up, as shown by the minor but increasing secondary calcium carbonate formation and the fine organic and micro-charcoal dust throughout its fabric. This soil type change from a well structured and clay enriched agric brown soil (or Orthic Luvisol) to a calcitic reddish brown to red Mediterranean soil (Calcic Luvisol) (Bridges 1978, 68–9; WRB 2014) would appear to be beginning just prior to the construction of the temple at Santa Verna (from c. 3800 cal. BC), a process that was interrupted by this soil being sealed by the sequence of temple floors above.

The adjacent upper pit fill in Trump Cut 55 (sample 3) was of similar structure and composition to the buried soil in Trench E/sample 4/3, with a 6–7 cm thick horizon of alternating thick/thin, fine calcitic silt crusts (Fig. 5.5o), generally fining upwards. This suggests soil infilling of the pit, interrupted by a phase of intermittent in-washings of finely sorted soil material in an open and bare earth environment adjacent into the open pit, subject to episodic rain-splash.

5.3.2. Ġgantija temple and its environs

The upper part of the Xagħra plateau comprises three natural terrace steps in the Upper Coralline Limestone over a rising slope height of about 30 m. Ġgantija temple is located on the middle of these three terraces, adjacent to a probable former fault line with a freshwater spring (Ruffell *et al.* 2018). Nearby Santa Verna is located on the uppermost part of the same mesa plateau about a kilometre to the west (Figs. 5.1 & 5.6). Ġgantija temple is dated from about 3510–3080 cal. BC and through the Tarxien period between c. 2840 and 2380 cal. BC (see Chapter 2 & Volume 2, Chapter 5).

Augering survey around the southern fringe of the site (below the retaining viewing platform wall) mainly produced thin soils with no sign of the presence of deep agricultural terrace soils or any buried soil being present (Appendix 6). Nonetheless, in the small walled triangular field of the southwestern corner of the Ġgantija platform and in the olive grove to the northeast of the temple results from hand augering suggested the presence of a well preserved buried soil,

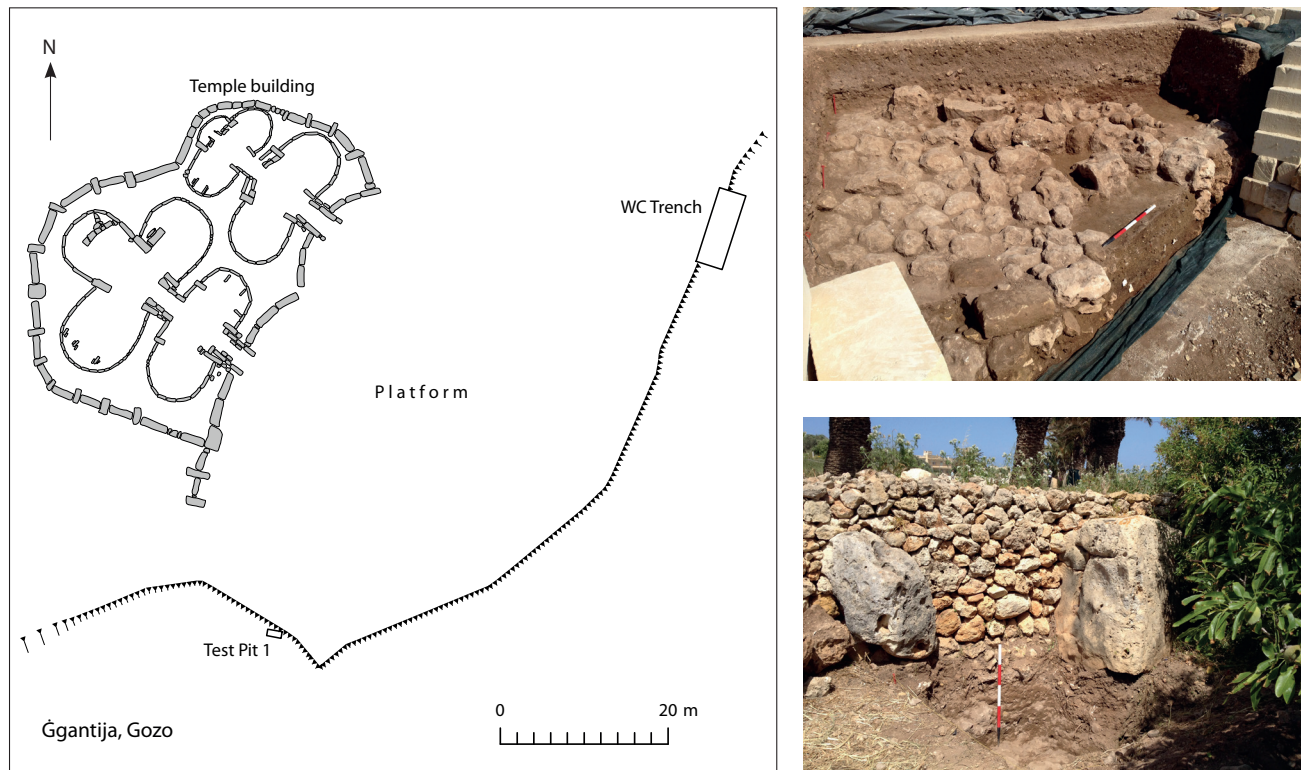


Figure 5.6. Plan of Ġgantija temple and locations of Test Pit 1 and the WC Trench excavations (R. McLaughlin) (left), with as-dug views of the WC Trench (upper right) and TP1 (lower right) (C. French).

which was consequently followed up by a resistivity survey and targeted test pitting by hand and machine (TP 1–5) (Appendix 6; see Volume 2).

Immediately to the east of Ġgantija temple there was a small olive grove, established in 1961 (resident farmer, pers. comm.). The greyish brown, silty clay loam modern soil was imported from the adjacent Ramla valley at the same time and dumped over an area of terraced fields in 1961 and again in 1982. Upon augering and test pitting, in places there was survival of a thin reddish brown silty clay loam soil, with a few artefacts within it which were suggestive of temple period Neolithic activity just to the east of Ġgantija temple, beneath about 75–155 cm of made ground. Two spot samples (35 & 41) were taken for micromorphological analysis from the surviving old land surface. The old ground surface/buried soil surviving in Test Pit 5 (sample 35) was a bioturbated, calcitic, sandy clay loam, and that in BH54 (sample 41) was a fine stoney calcitic silt. These appear to indicate a lower B horizon and weathered B/C sequence, essentially similar to that observed in the base of WC Trench 1 (see §5.3.2.2).

On the other side of the paved lane to the south of the olive grove field, four test pits (TP 2–5; c. 2.5 x 3 m) were cut by machine in advance of planting palm trees.

In each case, there was c. 75–155 cm of made ground over a variable but thin thickness (<20 cm) of reddish brown, fine sandy silt loam soil. This buried B horizon soil which had developed on the weathered surface of the Upper Coralline Limestone bedrock was similar to that found beneath the made ground in the olive grove immediately to the north, but with no sign of architecture or artefacts of any period.

In the small triangular field immediately to the west of the Ġgantija temple platform, augering revealed the presence of a buried soil about 50–70 cm in thickness beneath the modern ground surface. A small test pit (TP 1; c. 2.5 x 1.85 m) was hand-excavated immediately in front of the platform wall and two large limestone slabs which appear to be part of the temple complex, now incorporated in the platform wall (Figs. 5.6 & 5.7). First, the test pit revealed several large, sub-rectangular limestone blocks just at and below the ploughsoil surface, which may be part of temple collapse and/or modifications. Beneath, there was c. 80 cm of heavily rooted greyish brown silt loam with a mixture of limestone gravel pebbles and abundant artefacts. This horizon is indicative of an agricultural soil but which contains artefactual material contemporary with the late Neolithic use

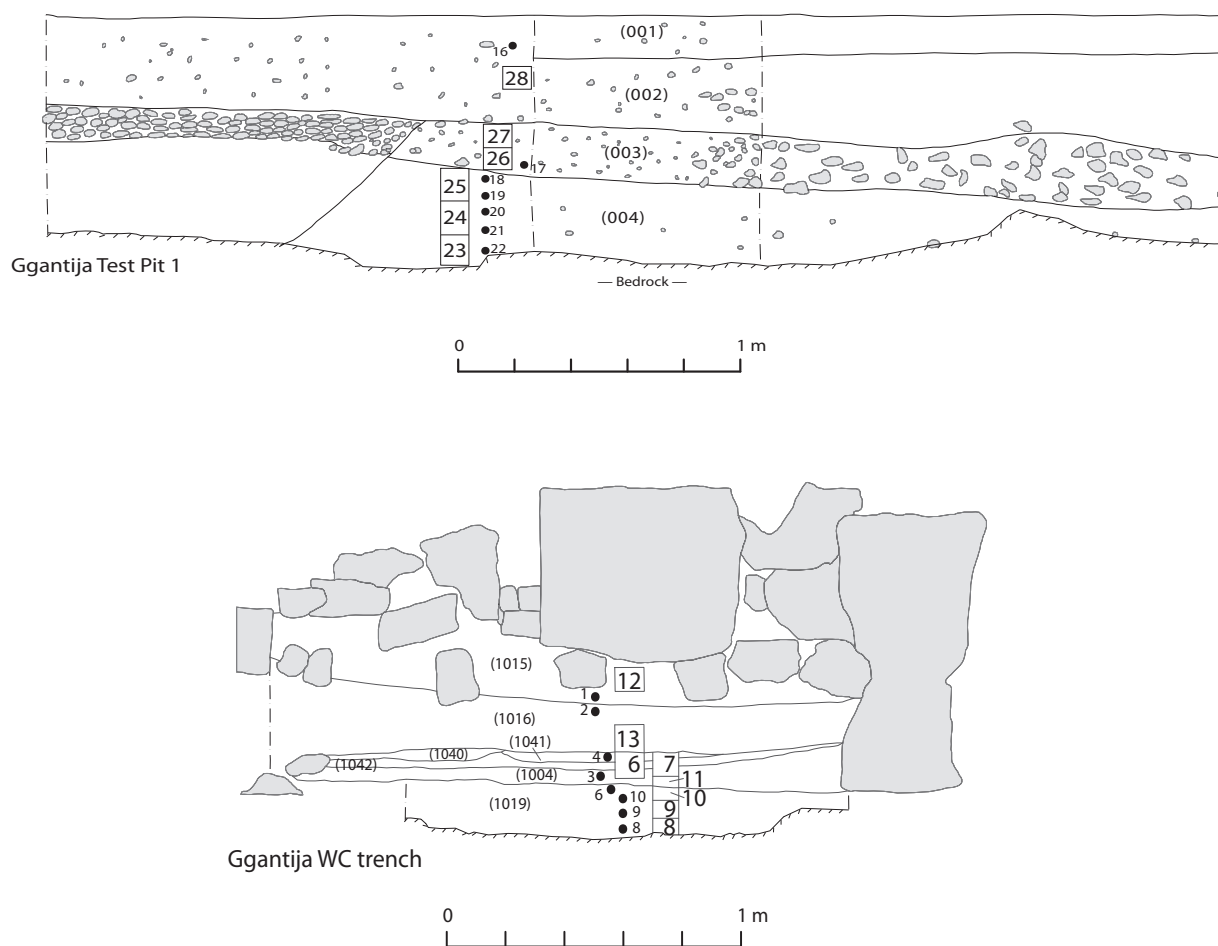


Figure 5.7. Section profiles of Ggantija Test Pit 1 on the southwest side of Ggantija temple (above), and the east–west section of the Ggantija WC Trench on the southeast side of the temple (below) (Note: open boxes = micromorphology block samples; black circles = small bulk samples) (R. McLaughlin).

of the temple (see Volume 2, Chapter 5). Then there was a distinctive contact with an *in situ* buried soil profile from c. 80–130 cm in depth. Abundant artefacts, primarily Tarxien period pottery sherds (of the later Neolithic) with some bone and lithics continued to be present down-profile to the base of this soil. Their abundance certainly suggests considerable use of this area immediately outside the temple during the Neolithic, perhaps even occupation in the vicinity.

The buried soil comprised three horizons: an upper dark brown silt loam (at 80–90 cm), a brown silt (90–120 cm), a dark reddish brown fine sandy/silt loam (120–125/130 cm), all developed on the weathered Upper Coralline Limestone bedrock (at 125/130+ cm) (Fig. 5.7). Furthermore, at the 80 cm level, there was one large rectilinear block at the horizon boundary in one corner of the test pit, and a cut feature infilled with brown silt loam soil and abundant limestone rubble in

the other corner. This suggests that there was an old land surface at 80 cm down-profile associated with a c. 45–50 cm thick buried soil. This profile was sampled for micromorphological, geochemical, phytolith and pollen analyses, as well as OSL profiling and dating.

In the WC Trench 1 (beneath the 1970s shop and WC building demolished in 2014), in a similar position to TP1 but on the eastern side of the present-day visitors viewing terrace there was a similar but more complicated sequence was located (Figs. 5.6 & 5.7). Beneath terrace soil make-up, stone-wall collapse and perhaps the construction of a stepped stone entranceway to the temple, there was a well preserved sequence of midden-like deposits overlying an intact and complete buried soil sequence. The abundant artefact recovery suggests that the material is indicative of the whole breadth of the Neolithic, not just the later Neolithic Temple Period itself (see Volume 2, Chapter 5). The

buried soil was of c. 35–45 cm in thickness and consists of a lower, brown silty clay loam B horizon with an *in situ* humic silt loam A horizon above. The mixing of the artefact assemblage throughout the profile, albeit with much lesser quantities recovered in the lower half of the profile, suggests that this area has undergone considerable soil faunal mixing and modification in the past. Above this soil there were a series of discontinuous lenses of calcitic ash, fine pea-grit gravel and humified/charcoal rich ‘soot’ over a thickness of about 10 cm (contexts 1004 & 1041) which are suggestive of a series of thin dumps or accumulations of overlying settlement-derived debris. These in turn were overlain by two major phases of silt loam soil accumulation (contexts 1016 & 1015) which contain very large quantities of later Neolithic Tarxien pottery and bone. These are also suggestive of intensive human settlement activity in the near vicinity, as well as soil surface modification. A wide area of large, collapsed and broken stone blocks then sealed this soil/midden sequence from further disturbance, which could be related to later Neolithic and subsequent modifications of the temple site. This important sequence was thoroughly sampled from a soil and palaeoenvironmental perspective.

5.3.2.1. Physical and elemental characterization

pH values from both test trenches at Ġgantija were all alkaline (ranging from 7.3 to 8.2) and most of the multi-element values were low and/or unremarkable (Tables 5.3 & 5.4). Nonetheless, phosphorus (P) was very enhanced in every horizon, especially in the buried soil in Test Pit 1, as were the calcium (Ca) and strontium values (Sr) (Table 5.4). Phosphorus values in Test Pit 1 ranged from 2200 ppm at the base of the soil to >10,000 ppm in the upper 20 cm of this soil. Strontium values were also relatively enhanced ranging from c. 172–380 ppm (Table 5.4). The enhancement of these two elements suggests large additions of organic material and household refuse to the soil (Entwistle *et al.* 1998; Holliday & Gartner 2007; Wilson *et al.* 2008), coincident with the substantial quantities of fragmentary animal bone and Tarxien-period pottery recovered during the excavation. Similarly in the WC Trench, the buried soil and especially the multiple horizons of accumulating soil and archaeological debris above gave very high P values, ranging from 5010 to >10000 ppm along with enhanced strontium values (c. 238–322 ppm) (Table 5.4). Likewise the magnetic susceptibility values were either very enhanced or low (Table 5.3), especially in the horizons dominated by archaeological material that had built-up on the buried soil. This suite of high values probably reflects the amount of organic and fire-related settlement debris contained within these deposits (Allen & Macphail 1987; Clark 1996, 109ff;

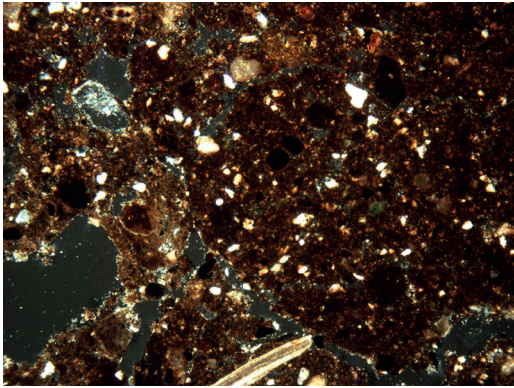
Fassbinder 2016, 502). Calcium and calcium carbonate values were also very high (Tables 5.3 & 5.4), which complements the enhanced phosphorus and strontium values to indicate the strong influence of midden-type refuse and hearth rake-out (Entwistle *et al.* 1998), but may equally reflect weathering and solution from the overlying limestone blocks of the collapsed temple structure above and the large amounts of secondary calcium carbonate observed in the micromorphological analysis of the buried soils at Ġgantija.

5.3.2.2. Soil micromorphology of Test Pit 1 at Ġgantija

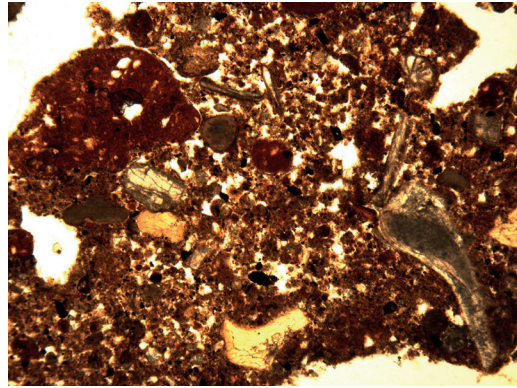
In Test Pit 1 on the southern side of Ġgantija temple, there were two soil horizons evident in the buried soil. The basal two-thirds of the buried soil (samples 23 & 24) is a calcitic, fine sandy/silty clay loam with a weakly developed blocky structure and a pellety to small aggregated micro-structure (Fig. 5.8a). Few to common, small sub-rounded aggregates of organized silty clay indicative of Bt horizon or agric material are commonly mixed with the crumb-like soil material. Fine organic matter, charcoal and shell are commonly present throughout, as are minor occurrences of bone fragments (Fig. 5.8b). There is a generally moderate impregnation with amorphous sesquioxides throughout the dusty or silty clay groundmass, as well as common aggregates of strongly amorphous sesquioxide stained clay. There are few if any illuvial clay or dusty clay coatings in the voids or of the grains and/or clay striae in the groundmass, rather dusty clay is only present as the groundmass. In addition, there are some partial to complete infills of the voids with micro-sparitic to amorphous calcium carbonate and very fine organic matter punctuations (Fig. 5.8c), which is becoming increasingly prevalent towards the upper part of the buried soil (Fig. 5.8d).

The upper one-third of the buried soil in samples 25 and 26 is becoming more dominated by micro-sparitic calcium carbonate, humic brown staining, fragments of bone, organic matter and fine charcoal, as well as fine aggregates of herbivore dung (Fig. 5.8e) and red clay soil (Fig. 5.8f). In particular, sample 26 is a very dark brown, humic and amorphous sesquioxide stained, very fine sandy clay loam soil with common interconnected vughs between an aggregated structure (Fig. 5.8g).

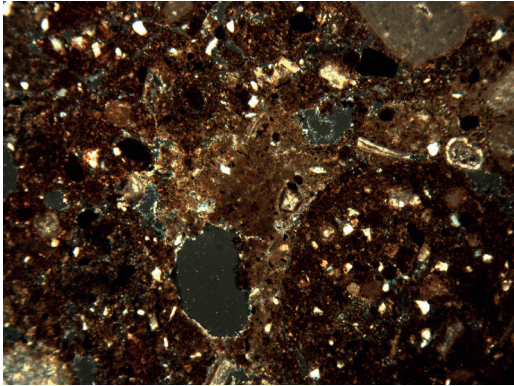
The c. 80 cm of terrace soil above (samples 27 and 28) is a pellety to aggregated sandy loam with minor micro-sparite and <20 per cent dusty clay in the groundmass, with minor amounts of fine charcoal, bone and shell fragments, and weak to moderate staining with amorphous sesquioxides. It becomes increasingly humic and dark brown stained up-profile (Fig. 5.8h).



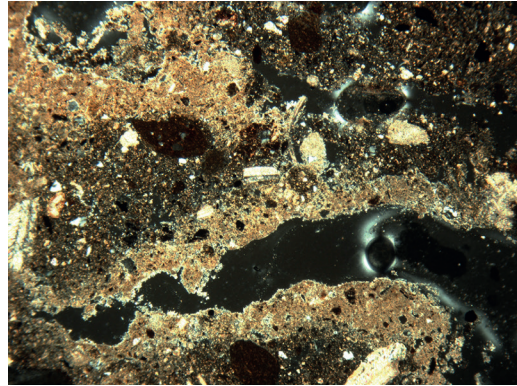
a



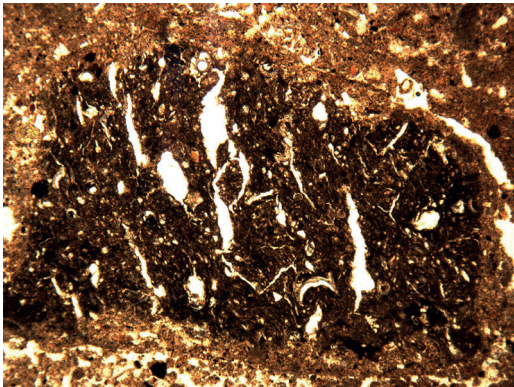
b



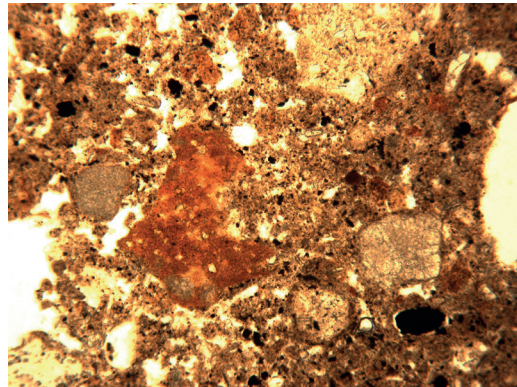
c



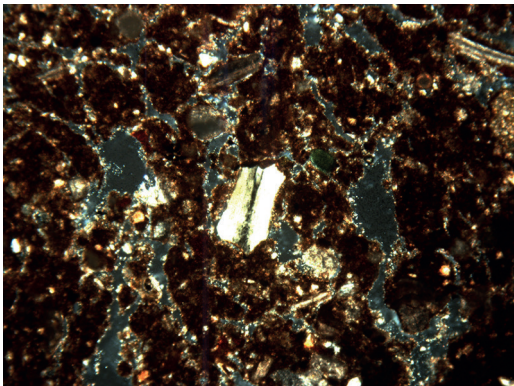
d



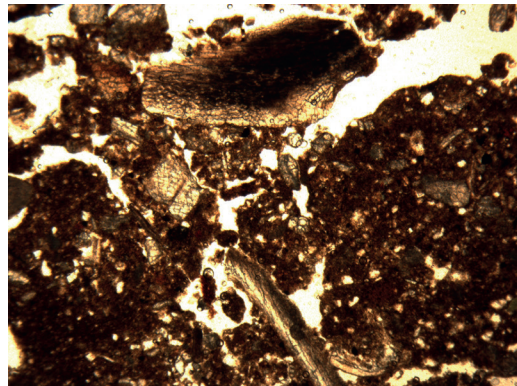
e



f



g



h

In summary, both the terrace soil and the palaeosol beneath are essentially of the same soil material. The terrace make-up is more humic and aggregated, containing few to common fine organic additions such as bone and charcoal. The buried soil beneath is essentially a variation on the same theme. It is marked by very dark brown humic aggregates in its upper organic Ah horizon, and then the B horizon below is more of a mixture of this humic fine sandy clay loam with the addition of much secondary calcium carbonate throughout the groundmass, and especially lining and filling in the voids as a secondary process. There is a slight increase in dusty or silty clay content with depth, and an associated better small blocky ped structure. Thus, it appears that there is a complete Ah/B horizon of a brown earth or cambisol type of palaeosol present (after Bridges 1978, 58), although it is not well developed. It has undergone some pedogenesis, but little in the way of silt and clay illuviation, and then has become disturbed and opened up with the associated secondary formation of calcium carbonate and iron oxides and hydroxides, as well as the incorporation through soil mixing processes by the soil fauna of fine anthropogenic debris (mainly fine charcoal and bone fragments). Significantly soil aggregates indicative of both organic A and argillic Bt horizon material

are intimately mixed in the B horizon. This suggests that allochthonous agric or Bt horizon material was contributing to the soil profile, most probably from the erosion of disturbed and truncated soils upslope on the Upper Coralline Limestone plateau. There is also some definite evidence for sedimentation in the form of horizontally orientated planar voids, defining a stacked sequence of micro-facies. This process must have proceeded relatively quickly, which is even more surprising as the soil was biologically active.

Thus this soil has changed from being a relatively stable and structured soil to one that is opened up, disturbed and receiving both eroded soil and midden-derived materials such that its development was interrupted. Consequently, there was up-building and over-thickening of the soil profile, and at the same time it became increasingly affected by drying out and evapo-transpiration. The ubiquitous fine to coarse artefact inclusions are indicative of considerable soil mixing processes at work, that suggest that the anthropogenic inputs to this soil were deliberate, adding organic status and friability to this soil, effectively creating an 'amended soil' suitable for agricultural use (Simpson 1998; Simpson *et al.* 2006).

The terrace soil material above is essentially similar to the organic A horizon of the buried soil below, but more organic-rich and also contains abundant Neolithic artefactual material of the temple period (see Volume 2, Chapter 5) and limestone rubble. This could just be a rubbish heap just outside the temple, but it may well suggest the deliberate inclusion of midden derived settlement waste to create an 'enhanced' and thickened soil, in effect creating the first recognizable agricultural soil adjacent to the southwestern part of Ġgantija temple.

Figure 5.8 (opposite). Ġgantija TP 1 photomicrographs (C. French): a) Photomicrograph of the calcitic, fine sandy clay loam with a weakly developed blocky structure and a pellety to small aggregated micro-structure, sample 23 (frame width = 4.5 mm; cross polarized light); b) Photomicrograph of the fine bone fragments, sample 28 (frame width = 4.5 mm; plane polarized light); c) Photomicrograph of the partial to complete infills of the voids with micritic to amorphous calcium carbonate and very fine organic matter punctuations, sample 23 (frame width = 4.5 mm; cross polarized light); d) Photomicrograph of the partial to complete infills/linings of the voids with micritic calcium carbonate, sample 25 (frame width = 4.5 mm; cross polarized light); e) Photomicrograph of an aggregate of herbivore dung, sample 25 (frame width = 4.5 mm; plane polarized light); f) Photomicrograph of a fine aggregate of red clay soil in the sandy clay loam with frequent organic punctuations, sample 25 (frame width = 4.5 mm; plane polarized light); g) Photomicrograph of the aggregated, very dark brown, humic and amorphous sesquioxide stained very fine sandy clay loam soil with common interconnected vughs, sample 26 (frame width = 4.5 mm; cross polarized light); h) Photomicrograph of the aggregated, humic sandy clay loam, sample 28 (frame width = 4.5 mm; plane polarized light).

5.3.2.3. Soil micromorphology of the Ġgantija WC Trench 1

The buried soil (samples 3/3, 3/6, 3/7 & 3/8) at the base of the WC Trench 1 profile (Fig. 5.7) is a pellety to finely aggregated, calcitic, fine sandy loam (Figs. 5.9a & b) with an even mix of fine gravel-sized limestone pebbles (<1.5 cm). The groundmass is dominated by interconnected vughs and non-birefringent dusty clay, with moderate staining with amorphous sesquioxides. There is also a common presence of very fine organic/charcoal punctuations throughout. It is suggested that this is a very bioturbated, formerly quite organic but poorly developed B horizon. Moving up-profile, this soil becomes more organic with increasing amounts of very fine anthropogenic debris (Fig. 5.9c), with the upper surface in sample 3/6 indicative of an organic Ah horizon (Fig. 5.9d). Immediately above the apparent upper contact of the buried soil there

was a c. 4 cm thick horizon of calcitic fine sand, then c. 6 cm of a calcitic sandy loam soil, with c. 4.5 cm of calcitic fine sand above (Fig. 5.7), then a fine limestone gravelly horizon c. 4 cm thick. All of these horizons

contained abundant later Neolithic Tarxien pottery sherds and animal bone fragments. This alternating soil/fine gravel repeated sequence is suggestive of a cumulative stop/start soil build-up interrupted by

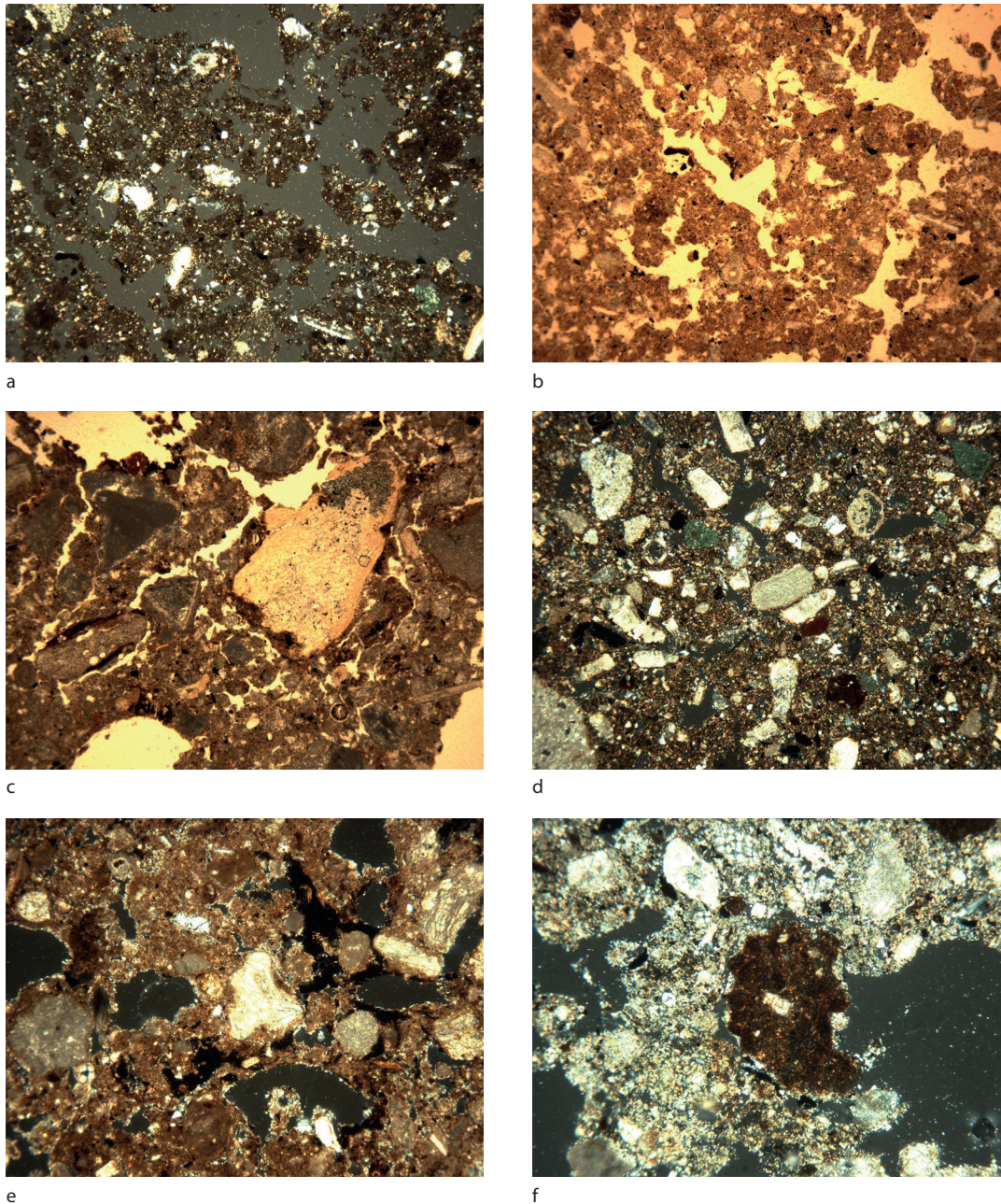


Figure 5.9. Ġgantija WC Trench 1 photomicrographs (C. French): a) Photomicrograph of the aggregated calcitic sandy loam soil, sample 3/8 (frame width = 4.5 mm; cross polarized light); b) Photomicrograph of the aggregated, humic calcitic sandy loam soil, sample 3/8 (frame width = 4.5 mm; plane polarized light); c) Photomicrograph of fine anthropogenic debris, sample 3/3 (frame width = 4.5 mm; plane polarized light); d) Photomicrograph of the humic calcitic sandy loam Ah horizon, sample 3/6 (frame width = 4.5 mm; cross polarized light); e) Photomicrograph of soil/midden calcitic sandy loam, sample 3/10 (frame width = 4.5 mm; cross polarized light); f) Photomicrograph of reddish brown silty clay soil aggregates in fine calcitic plaster, sample 3/1/2 (frame width = 4.5 mm; cross polarized light).

The geoarchaeology of past landscape sequences on Gozo and Malta

Table 5.5. Summary of the main soil micromorphological observations for the Santa Verna, Ġgantija and Xaghra town buried soil profile

Site and context	Micromorphology	Interpretation
Santa Verna:		
Buried palaeosol inside temple	<p>c. 30–60 cm thick buried soil below earthen temple floor; pre-3800 cal. BC;</p> <p>Small sub-angular blocky, reddish brown silty clay with pellety micro-structure; common dusty clay striae in groundmass; minor very fine charcoal/organic dust and few sesquioxide nodules;</p> <p>Over sub-angular blocky, reddish brown silty clay, with pellety micro-structure; very abundant, moderately birefringent, pure to dusty clay in speckles and striae throughout the groundmass;</p> <p>Developed on Upper Coralline Limestone</p>	<p>Truncated earlier Neolithic palaeosol;</p> <p>Well structured clay-enriched Bw horizon;</p> <p>Well structured, clay-enriched, argillic Bwt soil horizon of brown Mediterranean soil (orthic luvisol);</p> <p>Weathered bedrock C</p>
Buried palaeosol outside temple	<p>c. 40 cm thick buried soil below c. 60 cm thick terrace soil; undated;</p> <p>Pellety to aggregated, reddish brown, silty clay with fine limestone gravel; very strongly reddened with amorphous sesquioxides; common sesquioxide nodules; common very fine organic dust/micro-charcoal and micrite;</p> <p>Over heterogeneous mix of 30% aggregates of above silty clay fabric with 70% micro-sparitic calcium carbonate;</p> <p>Over moderately to well developed small blocky, orangey brown silty clay; with very abundant, moderately birefringent, pure to dusty clay in speckles and striae throughout the groundmass; few discontinuous linings of voids with micrite;</p> <p>Developed on Upper Coralline Limestone</p>	<p>Undated pre-terrace palaeosol;</p> <p>Lower A horizon of a red Mediterranean (chromic luvisol or <i>terra rossa</i>) buried soil, with strong rubification and common micritic calcium carbonate formation throughout, all completely mixed by the soil fauna;</p> <p>Disturbed mix of lower A/eluvial and micritic Eb horizon material, with severe secondary calcification and physical/soil faunal mixing throughout;</p> <p>Argillic Bt horizon of transitional brown to red Mediterranean soil, with slight indications of drying out and secondary calcification in the voids;</p> <p>Weathered bedrock C</p>
Ġgantija:		
Terrace soil over buried palaeosol in Test Pit 1	<p>60–70 cm thick terrace soil over a buried soil; from c. 8770±680 to 1140±250 cal. BC; with abundant Tarxien period pottery in the buried and terrace soils</p> <p>Vughy, pellety, dark brown to reddish brown, humic fine sandy clay loam with common fine limestone fragments; weak calcium carbonate and amorphous sesquioxide formation, minor shell, bone and charcoal fragments; abundant Tarxien pottery sherds;</p> <p>Over aggregated, vughy, dark brown, very humic, fine sandy clay loam; moderate amorphous sesquioxide formation, minor micrite, minor shell, bone and charcoal fragments, and abundant Tarxien pottery sherds;</p> <p>Over finely aggregated, golden brown, calcitic, fine sandy clay loam; few to common anthropogenic components of shell, bone, dung and charcoal;</p> <p>Over weakly blocky structured, golden brown, calcitic, fine sandy clay loam; common partial void infills with amorphous to micritic calcium carbonate, and few to common anthropogenic components of shell, bone and charcoal;</p> <p>Developed on Upper Coralline Limestone</p>	<p>Holocene palaeosol buried by post-late second millennium BC terrace soil;</p> <p>Bioturbated, humic soil with minor included fine anthropogenic components and late Neolithic pottery comprising terrace soil;</p> <p>Organic Ah horizon of buried soil with included fine anthropogenic components and late Neolithic pottery;</p> <p>Bioturbated, calcitic Bca horizon with included fine anthropogenic components;</p> <p>Weakly structured, calcitic and clay-enriched Bcaw horizon with increasing secondary calcitic infills and included fine anthropogenic components;</p> <p>Weathered bedrock C</p>

Table 5.5 (cont.).

Site and context	Micromorphology	Interpretation
Archaeological strata over buried palaeosol in WC Trench 1	<p>Coralline Limestone blocks of broken stone temple structure;</p> <p>Over at least 5 superimposed horizons (c. 65–70 cm thick) of pellety to fine aggregated, calcitic, coarse to fine sand; with up to 40% fine limestone gravel; few fine bone, charcoal and humified organic matter fragments; abundant Tarxien pottery sherds;</p> <p>Over c. 40 cm thick palaeosol; pre-c. 2400 cal. BC; small to columnar blocky, calcitic fine to coarse sand; up to 20% moderate staining with humic matter and amorphous sesquioxides; rare fine bone fragments and rare silty clay soil aggregate;</p> <p>Over fine stoney, pellety, reddish brown organic sand; common fine charcoal, shell and organic punctuations, and minor bone fragments; moderate amorphous sesquioxide impregnation throughout;</p> <p>Over fine stoney, pellety, vughy, sandy/silty clay loam; minor micrite; 10–15% micro-charcoal and organic punctuations; moderate amorphous sesquioxide impregnation throughout; rare silty clay soil aggregate;</p> <p>Developed on Upper Coralline Limestone</p>	<p>Collapsed former structure of Neolithic temple period;</p> <p>Midden-like soil accumulations with abundant late Neolithic pottery;</p> <p>Late Neolithic, weathered former lower A horizon of palaeosol, but missing the organic upper Ah, with some included fine anthropogenic debris;</p> <p>Bioturbated lower A horizon with some rubefaction and fine anthropogenic debris included;</p> <p>Bioturbated, organic, poorly developed Bw horizon with moderate rubefaction;</p> <p>Weathered bedrock C</p>
Xaghra town:		
Buried palaeosol, House site 2 and quarry	<p>20–35 cm thick; undated, sealed below nineteenth century house basement and street level;</p> <p>Well developed sub-angular blocky reddish brown fine sandy clay loam; with common, moderately birefringent, pure to dusty clay in speckles and striae throughout the groundmass;</p> <p>Over undulating Upper Coralline Limestone</p>	<p>Buried, well structured argillic Bt of chromic luvisol (or <i>terra rossa</i>) palaeosol;</p> <p>Weathered bedrock C</p>
Buried palaeosol, House site 3	<p>50–80 cm thick; undated, sealed below nineteenth century house basement;</p> <p>Sub-angular blocky, dark brown fine sandy clay loam with even mix of limestone fragments; with very abundant, moderately birefringent, pure to dusty clay in speckles and striae throughout the groundmass;</p> <p>Over sub-angular blocky, dark reddish brown, calcitic, fine sandy clay loam with minor charcoal and bone fragments;</p> <p>Developed on undulating Upper Coralline Limestone</p>	<p>Buried, well developed, argillic Bt horizon of chromic luvisol (or <i>terra rossa</i>) palaeosol;</p> <p>A well developed clay/micrite enriched Bcat horizon of chromic luvisol;</p> <p>Weathered bedrock C</p>

thin, coarse, weathered surfaces. It is suggestive of an open, accumulating soil surface associated with the large upright Coralline stones immediately to the east of this sample sequence. This could in fact be an early terrace construction built in front of the temple.

The two thick overlying contexts, 1016 and 1015 (Fig. 5.7), also beneath the fallen Coralline stones, are both calcitic sandy loams with a weakly developed small blocky structure and up to 20 per cent fine limestone gravel, 10–20 per cent organic punctuations

and minor anthropogenic inclusions of bone and charcoal (Fig. 5.9e). There is the occasional silty clay soil aggregate present (Fig. 5.9f). These contexts contained abundant artefactual remains, mainly pottery and bone of the later temple period (see Volume 2) and the occasional ‘plaster’ fragment. This ‘plaster’ is an homogeneous, silt-sized calcium carbonate material with minor vughs and fine channels present (Fig. 5.9f).

Thus the buried soil in the WC Trench is a very bioturbated, organic Ah over a poorly developed

weathered, moderately rubified B (or Bw) horizon, and is very similar to that observed in Test Pit 1 at Ġgantija. The ubiquitous silt and very fine quartz sand components suggest that these horizons contain a considerable wind-blown component (Muhs *et al.* 2010; Yaalon & Ganor 1973), probably from fine, dry unconsolidated soil surfaces in the vicinity. Both soil horizons been much affected by soil mixing processes, additions of fine humic and settlement-derived waste material as corroborated by the palynofacies analysis (see Chapter 3), and the formation of secondary calcium carbonate throughout. This is primarily a result of bioturbation by the soil fauna, and the exposure/drying and weathering of the fine limestone gravel content in this soil. Much of this limestone content could be related to the weathering of the adjacent large uprights of the monument adjacent, as well foot traffic/trample on the entrance route into the temple itself.

Subsequently the buried Ah horizon has been deliberately built up in several episodes of deposition through the addition of a similar soil material

containing abundant pottery, bone and organic matter. As was evident in the TP1 sequence, the multiple overlying horizons present above the buried soil in the WC Trench could be indicative of a rubbish dump, but equally could suggest the deliberate thickening and enhancement of the underlying soil with settlement-related refuse. This could be seen as an early form of soil amendment and perhaps even an early form of terracing. All indications are that this occurred within the later Neolithic period of the mid- to later third millennium BC, and not just here but also at the Santa Verna and Skorba temple sites (see §5.3.1.2 and §5.3.3.2).

5.3.3. Skorba and its immediate environs

The test excavations in April 2016 exposed buried soil profiles suitable for soil micromorphological block and small bulk sampling, as well as OSL profiling and tube sampling (Figs. 5.1 & 5.10; Tables 5.6 & 5.7; see Chapter 2). New radiocarbon dating places the construction of the temple in the early fourth millennium BC (see Volume 2, Chapter 7) and thus the soil profiles sampled



Figure 5.10. Section profiles of Trench A at Skorba showing the locations of the micromorphological and OSL samples: a) section 1, profile A–B; b) section 2, profile D–E (Note: open boxes = micromorphology block samples; white circles = small bulk samples) (D. Redhouse).

Table 5.6. pH, magnetic susceptibility and selected multi-element results for the palaeosols in section 1, Trench A, Skorba.

Sample	pH	MS SI/g x10 ⁻⁸	Ba ppm	Ca %	Cu ppm	Fe %	K %	Mg %	Mn ppm	Na %	P ppm	Pb ppm	Sr ppm	Zn ppm
Trench A:														
11	8.15	1.99	50	<2	51	1.55	0.5	0.67	335	0.35	7570	8	319	146
20	8.36	1.78	30	<2	47	1.78	0.59	0.6	371	0.34	6960	11	288	136
24	8.32	1.91	40	2	47	1.93	0.64	0.57	387	0.33	6820	11	267	131
28	8.27	2.27	40	<2	40	2.05	0.67	0.57	400	0.34	6750	9	243	127
75	8.44	1.7	50	<2	57	1.75	0.6	0.74	419	0.37	8370	7	323	172
78	8.63	1.59	30	<2	39	1.64	0.53	0.58	344	0.31	6680	10	270	125

Table 5.7. Loss-on-ignition organic/carbon/calcium carbonate frequencies and particle size analysis results for the palaeosols in section 1, Trench A, Skorba.

Sample	% organic	% carbon	% CaCO ₃	% clay	% silt	% sand
Trench A:						
11	4.88	1.14	48.14	0.34	30.9	68.76
20	4.99	1.23	42.71	0.42	32.32	67.26
24	5.05	1.34	39.19	0.31	26.63	73.06
28	5.76	1.35	35.84	0.33	29.24	70.43
75	4.34	0.92	47.54	0.31	34.07	65.62
78	3.92	0.76	55.55	0.3	30.48	69.22

are indicative of the early to mid-Holocene period. In addition, a hand-augered transect from the site down-slope into the valley to the south revealed a consistently present reddish brown silty clay loam with common limestone pebbles of *c.* 40–55 cm in thickness on wide shallow, natural terraces on the Upper Coralline Limestone.

Section 1 (A–D) in Trench A (Fig. 5.10) was characterized by an upper 80 cm of pale greyish brown calcareous fine sandy/silt loam with varying admixtures of limestone rubble. This overlies *c.* 20 cm (at 80–100 cm) of a dark greyish brown fine sandy/silt loam, which in turn overlies a further *c.* 50 cm of dark brown fine sandy loam, a probable *in situ* buried soil. The whole profile was cut through by two superimposed limestone walls.

Section 2 (D–E), also in Trench A (Fig. 5.10), was characterized by an upper 80 cm of rubbly sandy silt loam (contexts 10, 12 and 23), and as in Section 1 was probably disturbed and/or re-deposited. Beneath this was a *c.* 3–6 cm thick (at *c.* 75–78/82 cm), *in situ* floor horizon (context 26) composed of a pale brown, calcitic loamy sand material with occasional lenses of pale grey calcitic plaster visible in it. This context overlies three horizons of brown, fine sandy loam (at *c.* 78/82–122 cm), with the lowermost horizon (*c.* 10–12 cm thick) being

an undisturbed buried soil with a slightly greater clay content and the two horizons above probably being disturbed buried soil material.

5.3.3.1. Physical and multi-element analyses

The deposit sequence in Trench A is all highly alkaline with relatively low magnetic susceptibility values (Table 5.6). The phosphorus (P) values are all very enhanced, especially in the plaster spot sample, the floor level sample/context 26, and the horizon context/sample 75 below. Each of these contains high amounts of wood ash and humified organic matter as seen in the micromorphological analyses; unusually the presence of ash is not also corroborated by high barium (Ba) values in these cases. Nonetheless, these features indicate the high amounts of organic waste which has been incorporated in the soil, presumably from the deposition and incorporation of settlement-derived midden material (Entwistle *et al.* 1998; Wilson *et al.* 2008). The relatively enhanced strontium (Sr) values also corroborate this. The remainder of the soil profiles are also very enhanced with phosphorus, and the high amounts of humified organic matter, very fine charcoal and fine anthropogenic debris as seen to be included in the thin sections of these contexts (see below) appears to corroborate these high values. The loss-on-ignition

values for total organic and carbon are quite consistent around 5 per cent and just over 1 per cent, respectively, throughout the whole profile (Table 5.7).

The particle size analysis is characterized by the near absence of clay, considerable silt (26–34 per cent) and a predominance of sand (65–73 per cent) (Table 5.7), the majority of which is very fine to fine sand in size range. These results are corroborated to some extent by the soil micromorphological analysis (below), but consistently under-represents the amount of clay actually present, and mistakes much of the silt component as micritic (or silt-sized) calcium carbonate.

5.3.3.2. Soil micromorphology

The basal horizon of Section 1 (A–D; sample 28) has a micritic fine sandy loam fabric with variable amounts of fine to coarse limestone pebble inclusions (Fig.

5.11a). It is quite well organized with a humic brown, fine fabric of micro-sparitic dusty clay well mixed with c. 10 per cent very fine quartz sand. There were few to occasional very fine charcoal and bone fragments, and a minor fabric of a calcitic fine sandy clay loam included as small aggregates. The fabric of the horizon (context 24) above was similar, but it exhibited a pellety to small aggregated microstructure throughout (Fig. 5.11b). In horizon context 20 above, the fabric was a massive, dense, brown, micro-sparitic, very fine sandy clay loam with common included micro-charcoal (Fig. 5.11c). Immediately above in the base of horizon 11, a similar soil exhibited a well, developed small sub-angular blocky ped structure with a pellety micro-structure and strong humic staining (Fig. 5.11d).

In the field, this sequence was thought to be an aggrading soil on an *in situ* soil, all beneath disturbed/

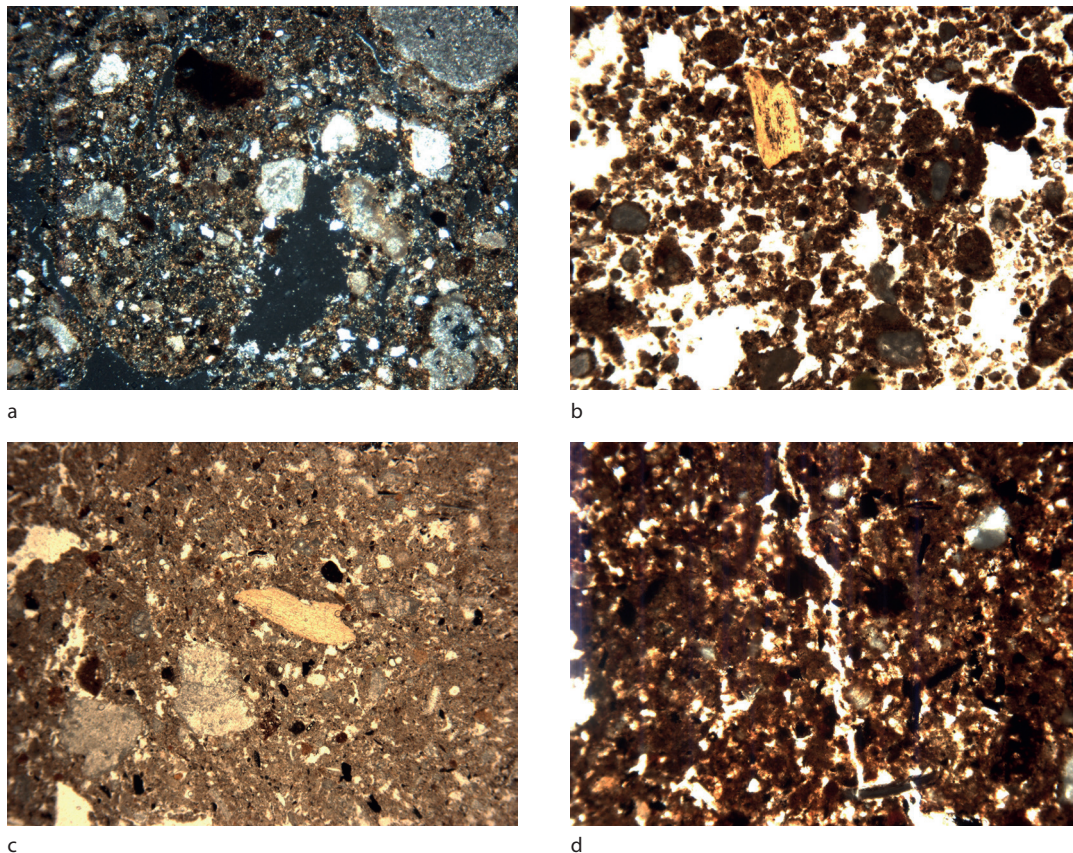


Figure 5.11. Skorba Trench A, section 1, photomicrographs (C. French): a) Photomicrograph of the loosely aggregated, micritic, fine sandy clay loam fabric, sample 28, section D–E, Trench A (frame width = 4.5 mm; cross polarized light); b) Photomicrograph of the pellety, humic, fine sandy clay loam fabric, sample 24, section D–E, Trench A (frame width = 4.5 mm; plane polarized light); c) Photomicrograph of the massive, micritic fine sandy clay loam fabric with common included micro-charcoal, sample 20, section 1, Trench A (frame width = 4.5 mm; plane polarized light); d) Photomicrograph of the humic, aggregated, fine sandy clay loam fabric within larger peds defined by fine channels, sample 20, section 1, Trench A (frame width = 4.5 mm; plane polarized light).

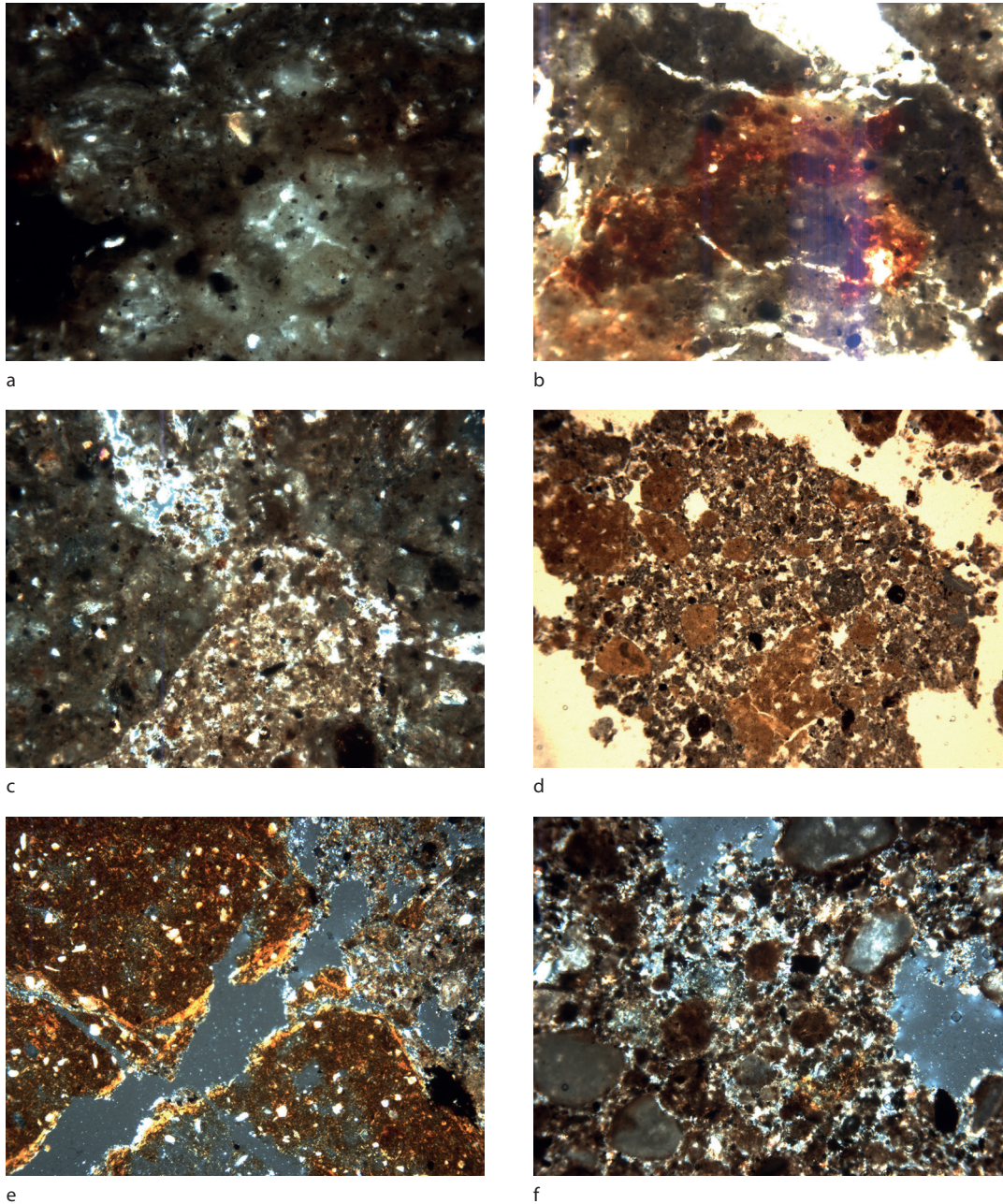


Figure 5.12. Skorba Trench A, section 2, photomicrographs (C. French): a) Photomicrograph of the calcareous 'slurry' of ash and silty clay soil material with abundant micro-charcoal, sample 26, section 2, Trench A (frame width = 4.5 mm; plane polarized light); b) Photomicrograph of the burnt zones in/on the ash, sample 26, section 2, Trench A (frame width = 4.5 mm; cross polarized light); c) Photomicrograph of calcitic, charcoal-rich, 'slurry', sample 75, section 2, Trench A (frame width = 4.5 mm; plane polarized light); d) Photomicrograph of the pellety, micritic fine sandy/silty clay loam fabric, sample 78, section 2, Trench A (frame width = 4.5 mm; cross polarized light); e) Photomicrograph of the birefringent coatings on the silty clay aggregates, sample 75, section 2, Trench A (frame width = 4.5 mm; cross polarized light); f) Photomicrograph of the micritic plaster and soil aggregates in a plaster fragment, plaster spot sample 1, Trench A (frame width = 4.5 mm; cross polarized light).

dumped archaeological material. In thin section, the whole sequence from *c.* 80–150 cm has been transformed by a number of processes. Each horizon has undergone varying degrees of soil faunal mixing, and the humification and removal of most of its organic content. This has led to variable porosities and openness of the fabric, and intensive comminution of the organic components and bioturbation of the whole fabric. In conjunction with this and the drying out of the profile, there had been the considerable formation of secondary calcium carbonate as silt-sized micro-sparite throughout the whole profile. At the transition from the lower to upper half of the sequence at *c.* 70–80 cm, the same soil material exhibited a small blocky ped structure. This was unexpected, but it could suggest that this represented a period of stability as an undisturbed soil surface during the life of the immediately adjacent Neolithic site, protected by later soil and stone rubble fall.

Section 2 (D–E) was characterized by a similar accumulation of rubbly soil material on an *in situ* surface (Fig. 5.10). This surface (context 26) is composed of a dense ‘slurry’ of amorphous calcium carbonate with common micro-charcoal punctuations (Fig. 5.12a), irregular zones of humified organic matter and wood ash aggregates, and a few burnt zones (Fig. 5.12b). The spot sample of a ‘plaster’ fragment from the same context location was essentially a similar dense ‘slurry’ of calcium carbonate with fine gravel-size/coarse sand-sized limestone and very fine charcoal inclusions (Fig. 5.12c). Sample 75 below is composed of three different fabrics, present either as aggregates and/or as a ‘slurry’ – a micro-sparitic fine quartz sand (*c.* 40–60 per cent), a golden brown dusty clay (*c.* 20–30 per cent) and 10–20 per cent calcitic ash aggregates, with up to 20 per cent interconnected vughy pore space and common micro-charcoal throughout (Fig. 5.12d). The dusty/silty clay aggregates generally exhibit weak birefringence, but occasionally have birefringent surface coatings (Fig. 5.12e). Sample 78 below is a pelley, calcitic, fine sandy clay loam as seen in the base of section 1/sample 28 (Fig. 5.12f), but which exhibits a weakly to moderately well developed columnar blocky ped structure. The channels defining the peds often exhibit discontinuous soil infills of the same fabric.

Context 26 is an *in situ* calcareous floor deposit. The predominantly dense, amorphous calcium carbonate material was spread on the underlying soil surface wet, and quickly dried. In addition, the horizon below (in sample 75) appears to comprise broken-up fine aggregates of calcitic flooring material evenly mixed with humic silty clay soil aggregates and wood ash. This could result from weathering and collapse of adjacent wall and floor surfaces, or could perhaps

be from the dumping of floor sweepings. These two horizons are found above a thick, calcitic soil horizon, essentially similar to that observed in section 1 (see above), but exhibiting some ped structure.

5.3.3.3. Interpretative discussion

The buried soil profiles in Trench A at Skorba comprise a *c.* 40–50 cm thick A horizon over a *c.* 15–30 cm thick *in situ* B horizon (Table 5.8). The soil fabrics are generally aggregated to small blocky structured, calcitic fine sandy clay loams, with the A horizon typified by humified organic matter, calcitic ash and very high phosphorus values. There are few to common fine anthropogenic debris throughout the profile, including very fine charcoal, humified organic matter, calcitic ash, pottery and bone fragments. The whole profile appears to have been disturbed in the past, and once much more organic as indicated by the vughy/interconnected vegetal voids present. The bulk of the silt component was comprised of micro-sparitic calcium carbonate throughout, indicative of severe seasonal drying out of the profile (Durand *et al.* 2010). The B horizon is also calcitic, but it exhibits abundant illuvial silty clay striae which are suggestive of a once more well developed and clay enriched argillic B horizon (Kuhn *et al.* 2010), as also observed in the pre-temple buried soil at Santa Verna. There is little sign of the secondary formation of amorphous sesquioxides leading to soil reddening.

In the field, this sequence was thought to be an aggrading soil over an *in situ* soil, all beneath disturbed/dumped archaeological material. The soil micromorphological analysis has confirmed this. Also, the high phosphorus values and common fine anthropogenic debris components suggest that this is an amended soil, with the A horizon built up through the addition of settlement derived midden-type debris as a cumulative soil, perhaps even a form of early managed terrace soil formation.

In many respects, this soil profile is a better developed version of what has already been observed in the WC Trench 1 on the southeast side of Ġgantija temple on Gozo where there were at least two horizons of soil with abundant included midden debris. The soil profile has been a well developed clay enriched soil but it was already open and becoming desiccated with very strong calcification and secondary formation of micro-sparitic calcium carbonate prior to the period of temple collapse above. The OSL and radiocarbon chronology would suggest that this process has already occurred by the early fourth millennium BC, and similarly implies major human impact on the surrounding landscape during the middle-later Neolithic period leading to similar associated soil changes and degradation effects as

Table 5.8. Summary of the main soil micromorphological observations of the buried soils in sections 1 and 2, Trench A, Skorba.

Sample	Main features	Additional features	Interpretation
Profile A-D: Section 1			
11	Well developed small sub-angular blocky, micritic fine sandy clay loam	5% limestone pebbles; common fine charcoal; rare shell, bone & plant fragments	Pre-temple stable, lower A1 soil horizon, once more organic sandy clay loam, with fine anthropogenic inclusions; affected by evapo-transpiration and secondary formation of calcium carbonate
20	Massive, micritic, humic, fine sandy clay loam fabric	10% limestone pebbles; common charcoal fragments & organic punctuations, and few shell, bone & plant fragments; moderate humic & amorphous sesquioxide staining	Affected by evapo-transpiration and secondary formation of calcium carbonate; possible aggrading/amended soil (A2) with well mixed, fine anthropogenic inclusions
24	Pelley, micritic, fine sandy clay loam fabric	10% limestone pebbles; few charcoal, shell, bone & plant fragments; some birefringence in dusty clay	Once more organic sandy clay loam, bioturbated, affected by evapo-transpiration and secondary formation of calcium carbonate; possible aggrading/amended soil (A3) with well mixed, fine anthropogenic inclusions
28	Loosely aggregated, micritic, fine sandy clay loam fabric	10% limestone pebbles; few charcoal fragments & organic punctuations; rare dusty clay aggregate	Disturbed <i>in situ</i> micritic B3ca soil horizon; once more organic sandy clay loam, bioturbated, affected by evapo-transpiration and secondary formation of calcium carbonate
Profile D-E: Section 2			
75	Even mix of aggregates of micritic fine sand, silty clay and ash	20% open vughy; common micro-charcoal; few birefringent surface coatings of the silty clay aggregates	Dumped, mixed deposit of an heterogeneous mix of micritic soil, silty clay soil and ash; amended A soil horizon
78	Micritic, pelley to loosely aggregated, fine sandy/silty clay loam fabric	Discontinuous channel fills with fine fabric; few charcoal fragments	<i>In situ</i> micritic Bca soil horizon; affected by evapo-transpiration and secondary formation of calcium carbonate

have also been observed at Santa Verna and Ġgantija over a similar time span.

5.3.4. Tač-Ċawla settlement site

The main micromorphological study was carried out by McAdams (2015) and is reported on in detail in *FRAGSUS* Volume 2, Chapter 3. This work and the investigation of settlement-related deposit sequences in the Horton Trench at Tač-Ċawla (samples 47, 48, 52–54, 151 and 159) are not included here, but the present report instead concentrates on the description and micromorphological study of several possible buried soil contexts encountered (Tables 5.1 & 5.9). It should be pointed out that none of these buried soil contexts exhibited anything like the thicknesses observed at the Santa Verna, Skorba and Ġgantija temple sites. Samples 9, 14, 139 and 261 in the Horton Trench, and 301 in the deep karstic feature were examined in thin section, some or all of which may be the very base of the surviving buried soil beneath this Neolithic settlement site.

Sample 9 is very fine sandy clay loam with strong reddening with amorphous sesquioxides. The dusty clay component varies from stipple speckled to short striae with moderate to strong birefringence, and the

groundmass contains minor fine charcoal fragments (Fig. 5.13c). Sample 14 exhibits a similar fabric, but also has a weakly developed sub-angular blocky ped structure. Both of these samples are indicative of clay enriched lower B (or Bt) horizon material with strong secondary impregnation with amorphous sesquioxides, making it a Bst horizon.

In contrast, sample 301 is a much more poorly preserved and thin soil. It is a reddish brown, humic silty clay about 5 cm thick over limestone pebbles with common organic/charcoal punctuations and strong reddening with amorphous sesquioxides (Fig. 5.13b). The soil in sample 261 was even more poorly preserved. It exhibited a largely micro-sparitic calcium carbonate dominated secondary fabric with minor very fine quartz and dusty clay, but which contained common charcoal fragments and a few sub-rounded aggregates of herbivore dung (Fig. 5.13a).

Sample 139 is a calcitic, fine sandy clay loam with invasive micro-sparitic calcium carbonate in the voids (Fig. 5.13d). It does not appear to be an *in situ* soil, but its similarity to the buried soils on site may suggest that it is either re-deposited local soil material and/or represents some soil development subsequent to the Neolithic occupation.

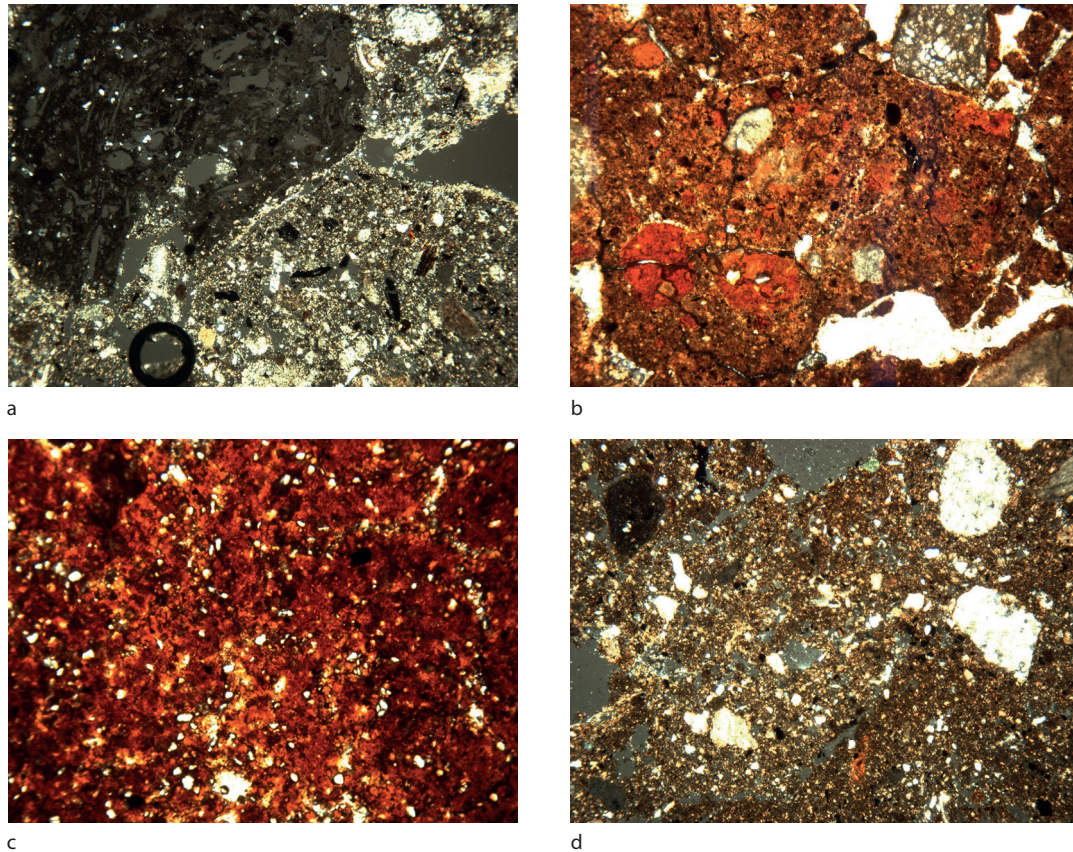


Figure 5.13. Tač-Ċawla soil photomicrographs (C. French): a) Photomicrograph of micritic calcium carbonate secondary fabric with common charcoal fragments and an aggregate of herbivore dung, sample 261 (frame width = 4.5 mm; cross polarized light); b) Photomicrograph of the 'dirty' silty clay fabric with included clay aggregates, sample 301 (frame width = 4.5 mm; plane polarized light); c) Photomicrograph of the stipple speckled to short striae dusty clay fabric, sample 9 (frame width = 4.5 mm; plane polarized light); d) Photomicrograph of the 'dirty' micritic silty clay fabric with very fine charcoal included (frame width = 4.5 mm; cross polarized light).

Table 5.9. Summary of the main soil micromorphological observations of the possible buried soils at Tač-Ċawla.

Context	Sample number	Main fabric	Features & inclusions	Interpretation
? buried soil	9	Reddish brown, very fine sandy clay loam	Dusty clays are stipple speckled to short striae; strong reddening with amorphous sesquioxides	Basal clay and iron enriched Bst horizon of an <i>in situ</i> buried soil on Coralline limestone
? buried soil	14	As above, with blocky ped structure	As above	As above
dark soil deposit below 58, with 137-8	139	Fine stoney, aggregated, micritic fine sandy clay loam	Frequent partial infills & linings of voids with calcium carbonate, & minor charcoal fragments	Brown sandy clay loam with abundant secondary calcium carbonate associated with strong evapo-transpiration; redeposited soil or post-occupation soil development?
? buried soil	261/1	Predominantly micritic dusty clay	Few dung aggregates; few to common fine charcoal fragments	Weathered calcitic Bc horizon with incorporated fine charcoal & dung
? buried soil	301	Reddish brown, humic silty clay over limestone pebbles	Organic dust and micro-charcoal in groundmass	Thin Ah horizon over weathered B/C of limestone

5.3.5. Xaghra town

As many houses were under construction in Xaghra town and deep basement areas were being excavated into the top of the Upper Coralline Limestone plateau (or mesa), there was the opportunistic chance of observing some relatively well preserved buried soil profiles in the town. In three instances, there were thick (c. 50–80 cm), strongly reddened and structurally well-developed soils observed, all developed on the limestone bedrock and also in vertical weathering fissures into this bedrock (Fig. 5.14; Table 5.10).

These palaeosols exhibited two distinct horizons, both in the field and in thin section: a lower, deep purplish red, silty clay loam, and an upper orangey red, fine calcitic, silty clay loam. In the lower horizon, strongly amorphous sesquioxide impregnated dusty clay predominates, with only about 15 per cent very fine quartz sand present in addition. The clay component is speckled to striated, weakly reticulate striated in places, with moderate to strong birefringence (Figs. 5.15a–c) and has a considerable very fine organic/charcoal component present throughout, well worked into the groundmass. The upper horizon is more vughy, contains a greater

very fine to fine quartz sand component and minor micro-spartic content, and exhibits some very fine organic/charcoal punctuations (Fig. 5.15d).

These strongly reddened soils are characterized by a well-developed blocky ped structure, organized illuvial clays and silty clays with depth, a great degree of reddening with secondary iron oxides and hydroxides (rubification), and lesser amounts of included limestone pebbles and fragments with depth. Although these soils were becoming slightly more organic and vughy up-profile, no *in situ* organic Ah horizons were observed in any location; these have probably been truncated and removed by house building in the last century and more recently. Nonetheless, there is a very fine to fine included organic component throughout these soils, which is suggestive of the long-term incorporation of organic material, especially carbonized and fine humified organic material.

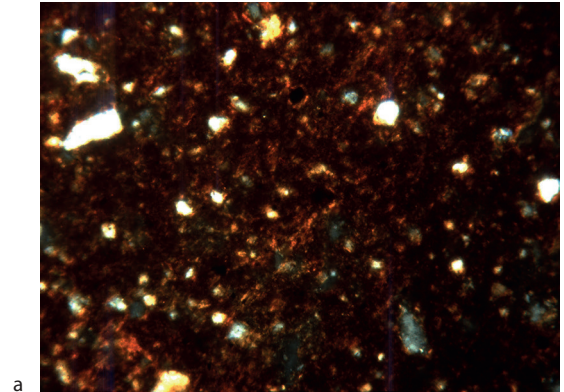
Although these palaeosols are undated, they have been sealed by buildings above for at least a century. They appear to be characteristic red Mediterranean soils (*terra rossa* or Chromic Luvisols) (Bridges 1978, 68; WRB 2014). They feature an A/B1/B2/C set of horizons,

Table 5.10. Field descriptions and micromorphological observations for the quarry and construction site profiles in Xaghra town.

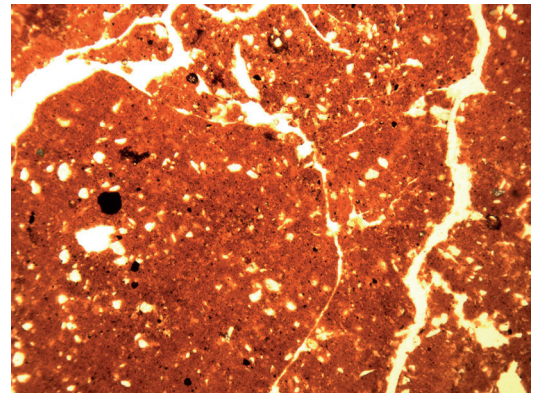
Context	Sample no.	Field descriptions and depths	Micromorphology	Interpretation
Stone quarry	5		Well developed sub-angular blocky, reddish orange fine sandy clay loam; very strong amorphous sesquioxide impregnation of all groundmass	Well developed Bst horizon of a buried soil
House 1 (N 36 03.058/E 014 16.601)	None	0–15 cm: brown silt loam with tree rooting 15–25 cm: red silt loam 25–80 cm: pale reddish brown calcareous silt loam with common limestone pebbles; terrace soil 80–85 cm: pockets of reddish brown silt loam; buried Bw of palaeosol 85+ cm: undulating Upper Coralline Limestone bedrock		0–15 cm: modern topsoil 15–25 cm: redeposited soil ? 25–80 cm: buried Bwt of <i>terra rossa</i> palaeosol
House 2 (N 36 03.004/E 014 16.549)	9	0–15 cm: modern concrete yard surface 15–25 cm: reddish brown silt loam	As below	As below
House 2	11	25–35 cm: reddish brown silt loam 35+ cm: undulating Upper Coralline Limestone bedrock	Compact/dense, dark red, fine sandy clay loam	Well developed clay-enriched Bt horizon of a buried soil
House 3 (N 36 03.004/ E 014 16.549)	12 upper	0–50/80 cm: dark brown silt loam with even mix of limestone fragments (<3 cm)	50–60 cm: fine stoney, small sub-angular blocky, reddish brown fine sandy clay loam	Well developed clay-enriched Bt horizon of a buried soil
House 3	12 lower	Red silt loam	60–70 cm: dark reddish brown, calcitic, fine sandy clay loam; minor charcoal and bone fragments	Well developed clay/micrite enriched Bct horizon of a buried soil
House 3	14	As above 100+ cm: undulating Upper Coralline Limestone bedrock	As above	As above



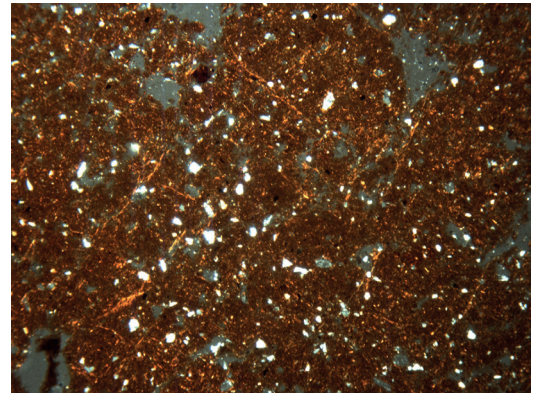
Figure 5.14 (above). A typical terra rossa soil sequence in Xaghra town at construction site 2 (C. French).



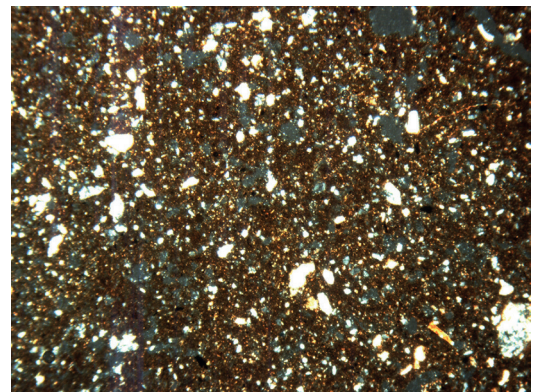
a



b



c



d

Figure 5.15 (right). Xaghra soil photomicrographs (C. French):
 a) Photomicrograph of the reticulate striated clay in the lower horizon, sample 5, abandoned quarry (frame width = 4.5 mm; cross polarized light);
 b) Photomicrograph of the blocky silty clay groundmass with very fine included organic matter punctuations in the lower horizon, sample 5, abandoned quarry (frame width = 4.5 mm; cross polarized light);
 c) Photomicrograph of the striated fine sandy clay loam in the upper horizon, sample 12, construction site 3 (frame width = 4.5 mm; cross polarized light);
 d) Photomicrograph of the organic, striated silty clay loam in the upper horizon, sample 11, construction site 2 (frame width = 4.5 mm; cross polarized light).

with strong weathering, clay eluviation and illuviation, and abundant secondary iron oxide/hydroxide formation, probably predominantly haematite (Fe_2O_3) (Duchaufour 1982; Lelong & Souchier 1982), much of which could be related to the long-term weathering of the limestone bedrock beneath (Catt 1990). There is also the illuvial deposition of pure clay and/or sometimes calcium carbonate in the lower agric horizon (B2 or Bt). Although these soils may be of much greater antiquity than the Holocene (Catt 1990; Kemp 1986; Yaalon 1997), the environmental factors which are thought to be important for the development of this soil type include strong seasonal variation with rainfall during the winter and spring months (<650 mm) and xeric conditions during the summers (Bridges 1978, 68; Yaalon 1997), conditions which still prevail today in the Maltese Islands.

5.3.6. Ta' Marżiena

Transect H comprised nine hand-augered boreholes in a north–south aligned transect from Ta' Marżiena temple across the shallow valley between the towns of Sannat and Munxar. Both within and immediately around the temple, there is only very shallow soil cover of <10 cm. Once off the low Upper Coralline Limestone promontory on which the temple site is located, the soil profile thickens southwards to c. 75–80 cm and becomes a grey silty clay throughout. This thick silty clay ploughsoil may well have colluvial additions to it. About 20 m north of the main road in the valley bottom in borehole 73, there was a reddish to strong brown silty clay loam buried soil present that was up to 40 cm thick. Although no soil samples were taken for analysis, this is probably indicative of *in situ* buried Bt horizon material, which points to soil formation and landscape stability here earlier in the Holocene, as is also evident in the palaeosols present at Santa Verna and Ġgantija.

5.3.7. In-Nuffara

Test excavations of two later Bronze Age (c. 1000 cal. BC) storage pits cut into the Upper Coralline Limestone bedrock on the In-Nuffara plateau revealed a number of primary/lower secondary fills composed of what appeared to be soil-like material (Table 5.11). Given

the otherwise severe denudation of the topsoil over this plateau, this was the only opportunity to investigate the soil material that had been associated with the construction of these pits in the later Bronze Age, and they were accordingly sampled for micromorphological analysis. Four soil blocks (samples 17, 40, 503, 509) from four pits were prepared for thin section analysis (Appendix 7).

5.3.7.1. Thin section descriptions

Samples 17 and 40 were essentially similar to each other, as were samples 503 and 509. Samples 17 and 40 were both calcitic, fine limestone-rubble rich, silty clay primary deposits (Fig. 5.16a). Sample 17 exhibited at least four horizons of the same material, suggesting pulses of fine erosion into the pit cavity. These pit fills were all finely aggregated, and they contained only minor small fragments of anthropogenic material such as pottery, bone, fired clay and very fine charcoal (Fig. 5.16b). These deposits were also stained brown, suggesting a strong humic content, and occasionally exhibited zones of finely sorted micro-laminar silt crusts (Fig. 5.16c) as a result of fine soil material washing into the pit cavities.

In contrast samples 503 and 509 were fine sandy clay loam material which exhibited a weakly developed blocky ped structure and weakly birefringent dusty clay predominant throughout the groundmass. Again, fine anthropogenic inclusions of pottery, bone, fired clay and charcoal are present, but on a very low scale.

5.3.7.2. Interpretative discussion

The deposits in samples 503/509 are likely to have been soil material that had fallen into the pit, and thus could be representative of the mid-Holocene soil cover of the In-Nuffara plateau. This is suggested by its well structured aspect and the predominance of silty clay illuvial material integral to the fine groundmass. These features may well suggest a period when the plateau was still well vegetated and not yet disrupted by significant human activities (Aguliar *et al.* 1983; Bullock & Murphy 1979; Kuhn *et al.* 2010) from the Bronze Age onwards (see Volume 2, Chapter 8). This is also corroborated by the fact that there is little or no micritic calcium carbonate present in this soil material.

Table 5.11. Sample contexts and micromorphological observations for two silo fills at In-Nuffara.

Sample number	Silo	Context	Micromorphology
17	1, context 22	Lower secondary fill	Four horizons of porous, finely aggregated, micritic, brown humic silty clay primary deposits with a common fine limestone-rubble component, and a minor, fine anthropogenic content of pottery, bone, fired clay and very fine charcoal fragments
40	2, contexts 41/42	Upper primary fill	Pellety to finely aggregated, brown humic silty clay with occasional zones of finely sorted micro-laminar silt crusts

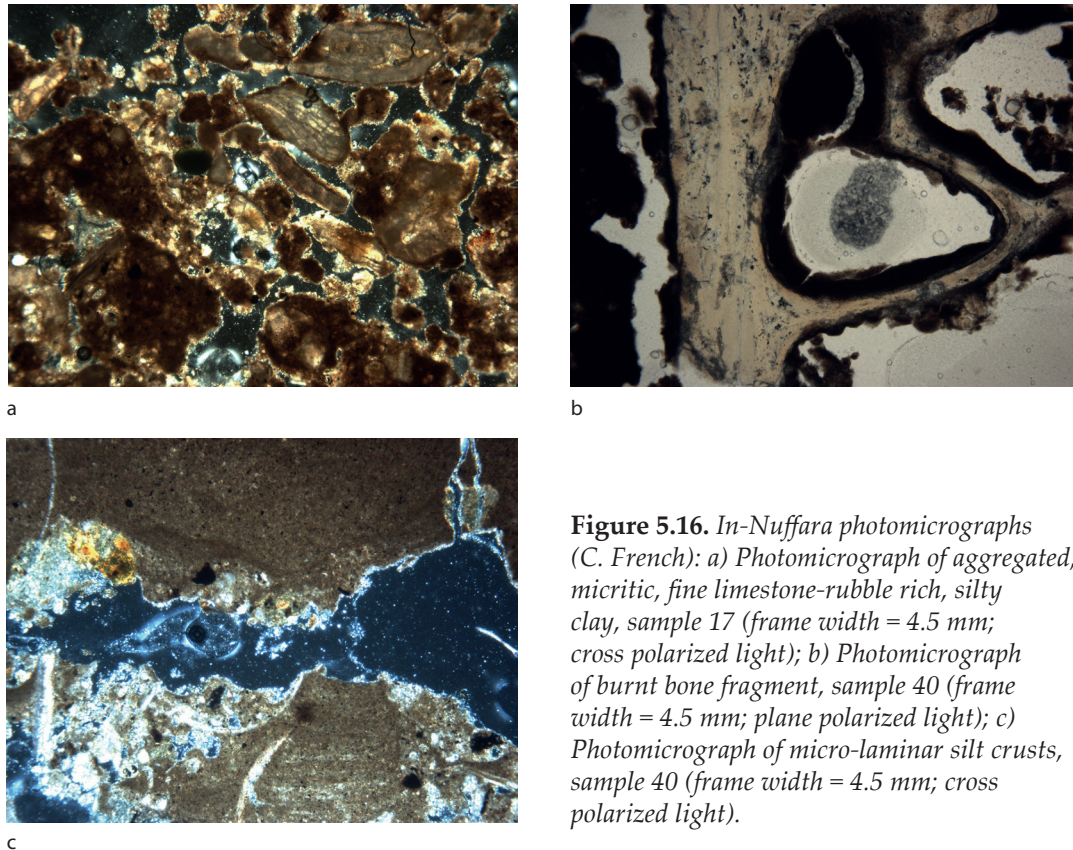


Figure 5.16. *In-Nuffara photomicrographs (C. French): a) Photomicrograph of aggregated, micritic, fine limestone-rubble rich, silty clay, sample 17 (frame width = 4.5 mm; cross polarized light); b) Photomicrograph of burnt bone fragment, sample 40 (frame width = 4.5 mm; plane polarized light); c) Photomicrograph of micro-laminar silt crusts, sample 40 (frame width = 4.5 mm; cross polarized light).*

By contrast the humic silty clay in samples 17 and 40 exhibits the ubiquitous secondary formation of secondary micro-sparitic calcium carbonate, a feature most probably related to the opening-up of the landscape, soil drying and evapotranspiration (Durand *et al.* 2010). In many respects this secondary soil material is more similar to the later Neolithic calcitic buried soils observed across the Ramla valley at the Ġgantija temple site (see §5.3.2.2).

5.3.8. The Ramla valley

The upper part and mid/lower slopes of the Ramla valley are dominated by grey silty clay loam soils developed on the Blue Clay geology. These are essentially single horizon ploughsoils, often in part saturated and gleyed below a depth of c. 50–60 cm. As the valley opens out and shallows towards the sea to the north, flat lower plateau tongues of land emerge of Globigerina Limestone. These have a very characteristic calcitic, fine sandy/silt loam soil developed on them, almost like a loessic silt loam soil, generally <50–60 cm in thickness.

In the central area of the valley towards the sea, a modern drainage canal cut revealed up to c. 3 m of hillwash and alluvial deposits that had aggraded across the valley bottom. This cut profile is typified by a series

of alternating thin horizons of calcitic silt loam and coarse sand/pebble horizons, with the whole profile generally fining upwards, over a depth of c. 1.4 m (i.e. BH66/Pr 627, c. 200 m inland from Ramla Bay) (Figs. 5.1 & 5.17). The profile was developed on the weathered Globigerina Limestone bedrock, and the upper 1 m of the profile above was disturbed by recent agricultural activities and water pipes.

A series of 11 small bulk samples were taken from the finer silt loam horizons and three tubes taken for OSL dating at 15, 62 and 103 cm down-profile (see Chapter 2 & Appendix 2). The latter sample loci were also sampled for micromorphological analysis. Initial field impressions indicated aggradation over time with at least two clear breaks, suggesting palaeo-surfaces of some kind at c. 46 cm and 115 cm, potentially indicative of changes in erosion processes from alternating fast/slow to a much slower aggradational dynamic (Fig. 5.17). The profiles indicate the parts of the sedimentary sequence which are likely to have been re-deposited without the luminescence signals being re-set at deposition; note, the step-like shifts in signal intensities at 46 cm and 115 cm are to be noted. The most promising targets for dating were the horizons immediately beneath these units. Moreover, the ratio of net signal intensities between the upper (those not affected by

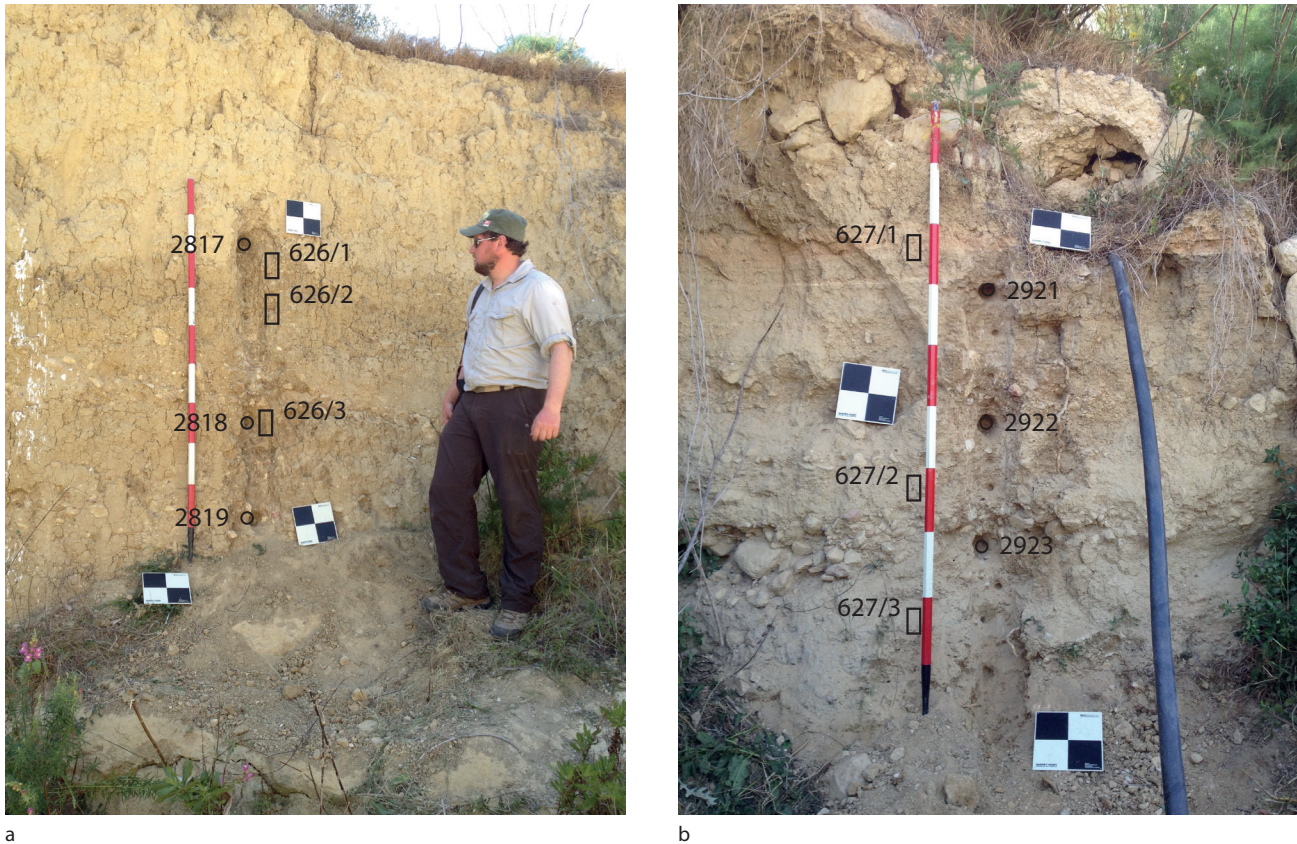


Figure 5.17. The Marsalform (Pr 626) (a) and Ramla (Pr 627) (b) valley fill sequences, with the micromorphology samples and OSL profiling/dating loci marked (scale = 2 m) (C. French).

recent soil turnover) and lower units, implies that the temporal range represented by these units was relatively short. In fact, the OSL dates obtained indicate that this variable flow valley deposition took place in the mid-nineteenth to early twentieth centuries AD.

The multi-element results of the three spot samples taken from the alluvial fills in the Ramla valley profile reveal a similar story of elemental enhancement to that described for the Marsalform valley (Table 5.4). The fill deposits were all alkaline but with quite low magnetic susceptibility enhancement (Table 5.4), high calcium carbonate (c. 55–64 per cent) and silt component (c. 60–79 per cent) (Table 5.4), and moderately enhanced phosphorus values (Table 5.4). This may reflect activities in the immediate catchment, but it is harder to ascribe to *in situ* rather than derived evidence of human activity.

The soil micromorphological analysis of three levels in the Ramla sequence revealed at least four pale grey, calcareous ‘soil’ horizons alternating with fine to coarse pebbly horizons (Table 5.12). The physical and soil micromorphological analyses of these grey ‘soil’ horizons (at 4–13, 13–15, 26–28 & 60–90 cm) indicated

that they are composed of relatively organic, very calcitic, fine sandy/silty clay loam soil (Table 5.12) with greater/lesser amounts of included very fine limestone gravel (Fig. 5.18a). They exhibit evident bioturbation and some weak secondary ped formation. There were minor amounts of silt and clay, very fine charcoal and organic matter fragments present, and the occasional silt or silty clay crust (Fig. 5.18c). There was also the very occasional void infill or aggregate of a very fine sandy clay loam with a reticulate striated dusty (or silty) clay component reminiscent of argillic (or Bt) horizon material (Fig. 5.18d), incorporated in this profile. The lowermost horizon (627/3; 100–140 cm) is a dense but aggregated, calcitic, shelly sand with indications of fine laminations (Fig. 5.18b) is situated directly on the Globigerina Limestone bedrock. The laminar aspect of this profile suggests the stop/start aspect of its accumulation, with the coarse limestone rubble units (at least three) indicative of episodic phases of alluvial fan type of deposition, and the finer units inbetween indicative of fine soil erosion from the catchment and overbank deposition in the valley bottom (Goldberg & Macphail 2006, 77ff).

5.3.9. The Marsalforn valley

An erosion cut in a lane in the central area of the Marsalforn valley near Ta'Mena (BH110/Pr 626) in Wied ir-Riggu exhibited a c. 3.7 m thick colluvial sequence of deposits of grey, calcitic, fine sandy/silt loam (Figs. 5.1 & 5.17). This hillwash-dominated sequence was interrupted by two phases of incipient soil formation, more weakly developed at c. 2.70–2.85 m and better developed at c. 1.75–2.10 m down-profile. Between these two soils and below the lower soil, the hillwash was of a more gravelly in character, with the whole sequence developed on the Globigerina Limestone bedrock.

This profile was cut back and sampled for OSL profiling and dating (see Chapter 2 & Appendix 2). A series of 10 small bulk samples were taken for OSL profiling from 1.75–3.25 m, and three OSL tube samples at 1.75, 2.65 and 3.2 m down-profile. Initial field

impressions were that there was an age-related gradual accumulation of hillwash-type sediment throughout the profile (Fig. 17). This is corroborated by the OSL dates obtained which indicate deposition from the earlier to mid-second millennium BC and well into the earlier first millennium BC (Table 2.2).

The three samples taken from the upper (1.75–2.10 m) and lower (2.70–3.10 m) incipient soils within the colluvial profile at the Marsalforn valley profile 626 (Fig. 5.17) were all very alkaline with a low total organic content (c. 1.6–2.2 per cent) and very high calcium component (Table 5.4) as well as relatively enhanced phosphorus and strontium values (Table 5.4). The high calcium content is corroborated by the silt-sized micro-sparitic calcium carbonate so dominant in the thin sections of the same contexts, and the moderately enhanced phosphorus and strontium components would indicate the receipt of midden-type refuse

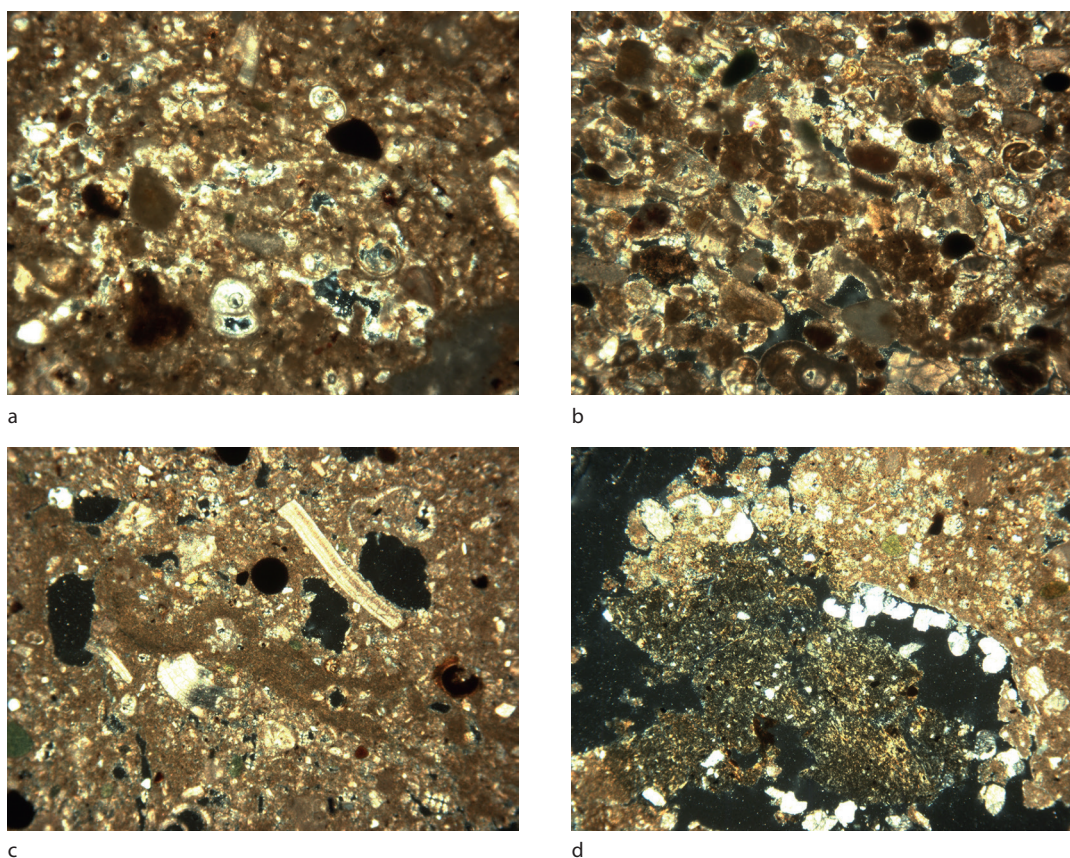


Figure 5.18. Ramla and Marsalforn valley profiles soil photomicrographs (C. French): a) Photomicrograph of dense calcitic, shelly sand with included fine charcoal, Marsalforn Pr 627, sample 1 (frame width = 4.5 mm; cross polarized light); b) Photomicrograph of dense but aggregated, calcitic, shelly sand with indications of fine laminations, Marsalforn Pr 627, sample 3 (frame width = 4.5 mm; cross polarized light); c) Photomicrograph of calcitic, shelly sand with fine silt crust, Ramla Pr 626, sample 3 (frame width = 4.5 mm; cross polarized light); d) Photomicrograph of silty clay aggregate in the calcitic, shelly sand, Ramla Pr 626, sample 1 (frame width = 4.5 mm; cross polarized light).

Table 5.12. Summary of the main micromorphological observations from the Ramla and Marsalforn valley fill profiles.

Profile and sample number	Micromorphology	Features and inclusions	Interpretation
Marsalforn Pr 626:			
626/1	Calcitic fine sandy loam with weakly developed sub-angular blocky ped structure	Common fine limestone gravel and shell fragments; rare silty clay soil aggregate	Weathered and hillwash eroded micritic soil and fine limestone gravel derived from Coralline Limestone bedrock up-valley/ upslope; with secondary ped formation; similar calcitic fabric to late Neolithic altered soil at Ġgantija
626/2	Calcitic fine sandy loam with well developed sub-angular blocky to columnar ped structure	Occasional fine limestone gravel and shell fragments	As above
626/3	Calcitic fine sandy loam with weakly developed sub-angular blocky to columnar ped structure	Few fine limestone gravel and shell fragments; occasional silt or silty clay crust or lens	Weathered and eroded micritic soil derived from Coralline bedrock up-valley/upslope; occasional surface exposure and rapid wetting/ drying events; with secondary ped formation
Ramla Pr 627:			
627/1	Calcitic fine sandy loam with well developed sub-angular blocky ped structure	Common fine limestone gravel and shell fragments; rare bone and plant fragments	Weathered/eroded micritic soil with secondary ped formation; stabilized alluvial valley fill
627/2	Calcitic fine sandy loam with well developed sub-angular blocky ped structure	Up to 50% fine limestone gravel, occasionally oriented horizontal; abundant shell fragments and rare bone fragment	Weathered/eroded micritic soil material with bioturbation and some weak secondary ped formation; stabilized alluvial valley fill
627/3	Aggregated micritic sandy loam with fine limestone gravel over dense, shelly, micritic fine sandy loam	Occasional laminar aspect; few fine limestone gravel in upper half, and shell fragments throughout	Weathered/eroded micritic soil material with/without bioturbation; episodic alluvial valley fill

and hearth rake-out material (Entwistle *et al.* 1998), as does the moderately enhanced magnetic susceptibility values, especially in the basal colluvial soil horizon. These features could be seen as an attempt to increase the fertility of these soil surfaces in the past, which is also reflected in the fine included anthropogenic debris visible in thin section.

Soil micromorphological analysis of three samples taken from the upper (1.75–2.10 m) and lower (2.70–3.10 m) incipient soils within this colluvial profile revealed highly calcitic, shell-rich, fine sandy loams with the sand-size component being almost entirely composed of fine, sub-rounded Coralline Limestone material (Table 5.12; Fig. 5.18c). There were minor amounts of silt and clay, very fine charcoal and organic matter fragments present, the occasional silt or silty clay crust (Fig. 5.18c), and the very occasional void infill or aggregate of a very fine sandy clay loam with a reticulate striated dusty clay component reminiscent of argillic (or Bt) horizon material (Fig. 5.18d), most probably eroded and incorporated in this colluvial profile. Nonetheless, each of these incipient soil levels exhibited a sub-angular to columnar blocky ped structure of greater and lesser expression, respectively,

which implies some longer-term stability of these horizons in the profile. There is a general absence of anthropogenic inclusions, even very fine charcoal.

5.3.10. Micromorphological analyses of possible soil materials in the Xemxija 1, Wied Żembaq 1, Marsaxlokk and Salina Deep (SDC) cores

Recording and sampling of the intact sediment cores from Malta were undertaken in the laboratory in Queen's University Belfast by the authors, not in the field. Cores from Xemxija 1, Wied Żembaq 1, Marsaxlokk and the base of Salina Deep Core (21B) on Malta (Fig. 3.1) were selected from the larger assemblage of available cores as they appeared to contain possible buried soils and/or sequences of alluvial/colluvial sediments derived from eroded soils which could relate to prehistoric land-use and erosion in each associated valley catchment. In combination with the radiocarbon chronology, pollen and molluscan evidence from the same cores (see Chapters 2–4), these datasets should provide reliable data on the nature of landscape exploitation and land-use practices in each valley. In turn, these sequences should be comparable to the detailed molluscan and palynological studies from

several places on the islands and the geoarchaeological investigations carried out in the Ramla and Marsalforn valleys of Gozo (see §5.3.8 & 5.3.9).

Small 2 x 2 cm size cubes of sediment were taken judgements from the cores for micromorphological analysis (after Bullock *et al.* 1985; Courty *et al.* 1989; Goldberg & Macphail 2006; Murphy 1986; Stoops 2003; Stoops *et al.* 2010) (Tables 5.13–5.17; Appendix 8). Twenty-five small blocks from Xemxija 1, thirteen blocks from Wied Żembaq 1, nine blocks from Marsaxlokk and three spot samples from the base of the Salina Deep Core (21B) were selected for micromorphological analysis.

5.3.10.1. The Xemxija 1 core

This core appears to be primarily composed of an upper *c.* 4.5 m of fine eroded soil as overbank alluvial deposition over *c.* 2 m of highly organic (black) silt mud, over overbank alluvial deposition in the form of *c.* 3.4 m of silt loam soil material, all developed on a *c.* 1.1 m thickness of aggrading eroded soil material at its base (Appendix 8; Table 5.13). The micromorphology of the core deposits is described in more detail below, as are the interpretative implications, from the base to the top.

Samples 25 to 18 in the basal *c.* 1 m of this 9.9 m Xemxija 1 core profile can be grouped together as they broadly share similar properties. This soil/sediment is a silty clay loam with some structure and organic component (Figs. 5.20a & b) which began to accumulate from at least 8780–8452 cal. BC (9353 BP; UBA-25001). Sample 25 (9.75–9.77 m) is characterized by humified plant tissue, very fine channels, and fine horizontally orientated bedding planes, but without pedogenic indicators of soil maturity with the exception of evidence for gleying. Sample 24 (9.65–9.67 m) is slightly more porous with slightly increased gleyic properties and associated humified plant tissue and hypo-coatings. Sparitic and micro-sparitic calcium carbonate and iron hydroxide pedofeatures suggest that oxidation and reduction phases had intensified. This trend increases in sample 23 (9.45–9.47 m) and the sediment/soil becomes more biologically active with abundant soil faunal excrements associated with root tissues. Sample 22 (9.25–9.27 m) shows similarities but is more intensely gleyed with horizontally bedded planes and abundant channels from about 6010–5840 cal. BC (7045 BP; UBA-31704). Sample 21 (9.13–9.15 m) is less gleyed with an increase in chambers and channels,

Table 5.13. Main characteristics of the Upper and Lower Coralline Limestone, Globigerina Limestone, Blue Clay and Greensand (after Bianco 1993; Pedley *et al.* 1976, 2002).

Geological source	Geological characteristics (youngest to oldest)	Mineral inclusions
Upper Coralline Limestone	Shallow marine limestone with abundant coral-algal mounds and reefs, commonly altered to micrite and sparite; hard but porous, crystalline, brittle and pale grey limestone; resistant to erosion but freshwater slowly dissolves the limestone and forms fissures; easily worked; the lower division is characterized by micrites and bio-sparites, with diverse included fauna and flora; the upper division is coarser, bio-clastic and oolitic limestones, rich in coralline algae	Carbonate clasts, silt-sized calcite, feldspar, dolomite, glauconite, apatite and haematite
Greensand	Bioclastic, friable, glauconitic argillaceous sandstone, deposited under shallow marine conditions; moderate permeability; poorly cemented; with iron oxides from weathering	Fine quartz sand and sand-size glauconite; cemented by silica, lime, clay and iron oxides
Blue Clay	Massive to bedded grey/blue shallow marine/offshore calcareous claystones with occasional to abundant marine fossils and planktonic calcium carbonate detritus; very soft; impermeable to water flow	Mainly fine grained carbonates and clay minerals; rich in alumina and very fine quartz silt and lime-rich fossil fragments; upper parts have increased glauconite and brown phosphatic sand grains
Globigerina Limestone	Shallow marine, calcareous mudrocks with abundant fossils, poor permeability, divided into three beds with two thin, harder phosphatic conglomerate beds characterized by francolite; the lower and middle Globigerina is pale yellow to pale grey, fine-grained limestone, bedded, and with globigerinid biomicrites; phosphorite pebbles in upper main conglomerate bed above; high percentage of planktonic foraminifera above indicative of deposition in shallow water in Upper Globigerina	Yellow to pale grey biomicrites, phosphatic pebbles and foraminifera; chert outcrops intercalate with Middle Globigerina Limestone
Lower Coralline Limestone	Shallow marine limestones with spheroidal algal structures and abundant echinoid fossils; well-cemented and permeable; hard and resistant; forms sea cliffs; yellow biomicrites rich in benthonic foraminifera with bedded, pale grey, Coralline Limestone above	Yellow bio-micrites; foraminifera

and sample 20 (8.68–8.7 m) returns to being more gleyed. Samples 19 (8.33–8.35 m) and 18 (8.23–8.26 m) are characterized by a significant increase in organic matter with large pseudomorphs and channels infilled with fine calcitic material and gypsum crystals. Sample 18 becomes more organic with much of the plant tissues horizontally bedded, but with iron-hydroxide hypo-coatings.

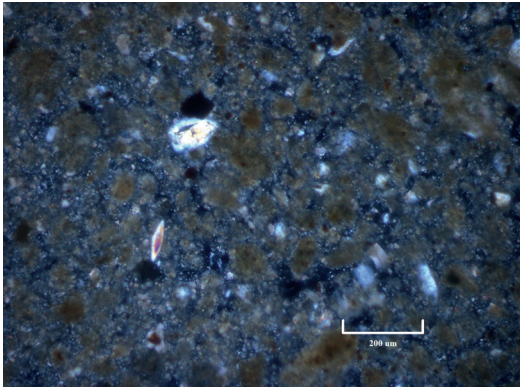
The humic components and several phases with hints of some soil structure and micro-lamination in samples 25–18 suggest that there have been repeated episodes of surface vegetation and stabilization, with greater/lesser effects of gleying. On balance, this appears to be slowly accumulating eroded soil material that has been affected by calcium carbonate rich groundwater and strong seasonal drying.

Importantly, samples 25–18 appear to have a parent material that is very similar to the Blue Clay/Greensand geological substrates regularly found beneath the Upper Coralline Limestone in valley exposures across the Maltese Islands (Table 5.13; Figs. 5.19a & b). The assemblage of fine calcitic material is similar to that found in undisturbed deposits of Blue Clay from mid-upper-valley locations (Fig. 5.19a). The fine fossiliferous limestone material and gypsum could also be derived from the Globigerina Limestone outcrops in the base of many valleys, but there is an absence of foraminifera which would be more indicative of this substrate (Figs. 5.19d–f). In particular in sample 20 (8.68–8.70 m), there is the first occurrence of the mineral glauconite and very fine quartz sand (Fig. 5.19g) which suggests that soil material was being derived from the intersection of the Blue Clay and the Greensand through erosion. Considered together, this evidence strongly suggests that this material is coming from soils developed on several different lithologies and therefore spatially different loci within the Xemxija valley landscape. On the Globigerina Limestone today, the soils today are fertile, very fine sand, silt, alumina and calcium carbonate dominated or Leptic Calcisols (or xero-rendzinas) (*cf.* Lang 1960), but in the past may have been more of a Luvic Calcisol (or calcitic argillic soils). On the Blue Clay in the past, the soils would almost certainly have been classified as a Humic Lep-tosol (or rendzina soil type) (*cf.* Lang 1960). The soils on the Greensand zones up-slope would have had a lighter and well drained texture because of their higher sand content and consequently would have been easier to cultivate, and may also have been in response to the negative consequences of soil change and erosion of the soils which had developed on the Globigerina Limestone and Blue Clay. Secondly, glauconite is a source of potassium (Loveland & Findlay 1982), as is the Globigerina Limestone (Rehfeld & Janssen 1995),

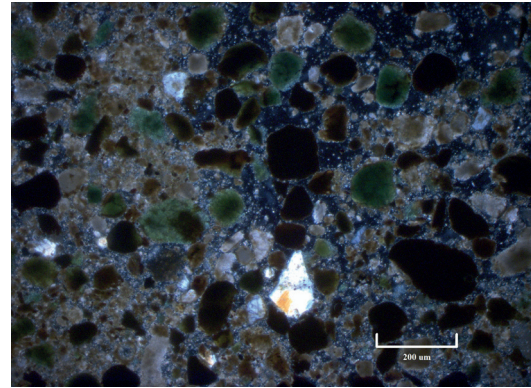
an important soil nutrient which would have resulted in increased yields when compared with the initial interaction of earlier Neolithic people with a variety of ‘fragile’ soils.

Above this first zone of eroded soil accumulation, there is a further *c.* 3.2 m accumulation of a fine, calcitic silt soil material (Fig. 5.20c) which contains occasional to frequent limestone fragments and pebbles, which is also indicative of overbank alluvial accumulation coincident with greater erosion and exposed limestone substrate surfaces in the immediate catchment. Interrupting this fine/coarse aggradation are at least three phases of a slowing in the aggradational dynamic with some organic accumulation and weak pedogenesis suggestive of incipient organic A horizon formation at 8.15–8.32, 6.7–6.85 and 6.0–6.3 m (Fig. 5.20d). These latter deposits essentially indicate a period of relative stabilization of the floodplain surface.

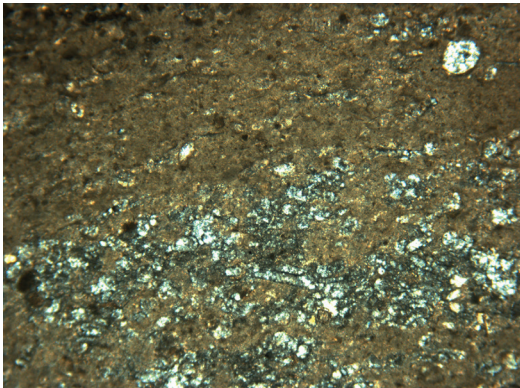
Figure 5.19 (*opposite*). *Photomicrographs of the Blue Clay and Greensand geological substrates from the Ramla valley (S. Taylor and C. French): a) Photomicrograph of the fine carbonate material impregnated with sesquioxides, well sorted very fine quartz and a few gypsum crystals in the Blue Clay, Ramla valley background sample (frame width = 1.25 mm; cross polarized light); b) Photomicrograph of the glauconite and carbonates in the Upper Coralline Limestone, Ramla Bay background sample (frame width = 4.5 mm; cross polarized light); c) Photomicrograph of the fine quartz sand, fine carbonate material and glauconite aggregates as opaque rounded sand, some of which are stained with iron oxides, in the Greensand, Ramla valley background sample (frame width = 1.25 mm; cross polarized light); d) Photomicrograph of the fossils and fine calcitic material of the Globigerina Limestone, background sample from Fungus Rock, Gozo (frame width = 4.5 mm; cross polarized light); e) Photomicrograph of the fine fossiliferous limestone material, Xemxija sample 23 (9.45–9.47 m) (frame width = 2.25 mm; cross polarized light); f) Photomicrograph of lenticular gypsum, Xemxija sample 23 (9.45–9.47 m) (frame width = 2.25 mm; cross polarized light); g) Photomicrograph of well sorted, very fine quartz and glauconite within a highly calcitic, massive structured groundmass, Xemxija sample 20 (8.68–8.7 m) (frame width = 1.25 mm; plane polarized light); h) Photomicrograph of mixed organic topsoil aggregates, silty clay aggregates, calcite, fine quartz, limestone clasts and glauconite, Xemxija sample 5 (3.02–3.04 m) (frame width = 4.5 mm; cross polarized light).*



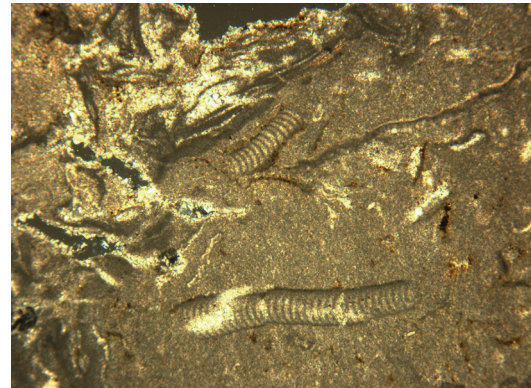
a



b



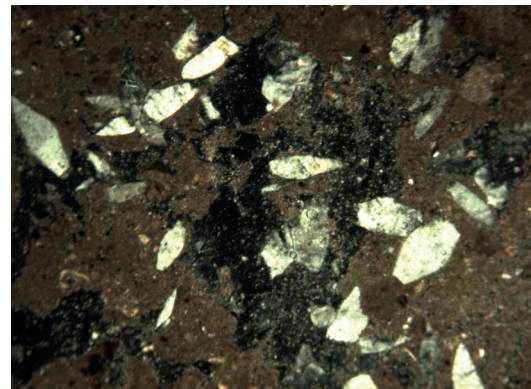
c



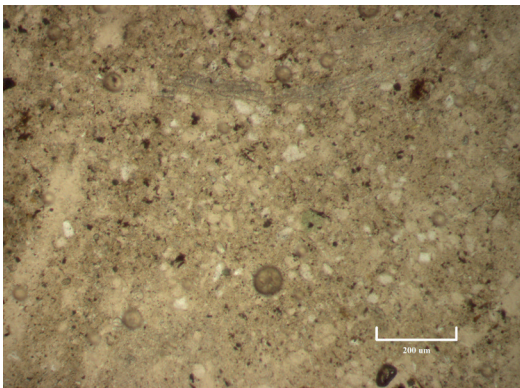
d



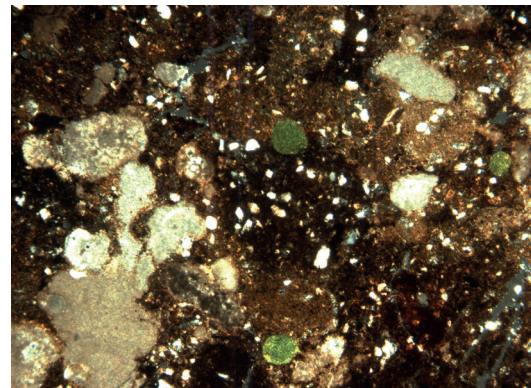
e



f



g



h

Table 5.14. *The summary micromorphological descriptions and suggested interpretations for the Xemxija 1 core.*

Sample number	Depth (cm)	C-14 dates cal. bc (2 σ)	Micromorphology	Interpretation
1	199–201		Fine gravelly, micritic sandy clay loam, with few to common very fine organic/charcoal punctuations	Eroded soil material?; very similar to the Ġgantija buried soil fabric; affected by evapotranspiration and secondary micrite formation
2	220–223		Sub-angular blocky, fine gravelly, micritic sandy clay loam	As above, but slightly coarser substrate material included; highly alkaline; subject to wetting and drying
3	250–253		Mix of fine gravel, sand-size limestone and crumb structured minor micritic silty clay	As above, but coarser substrate material included
4	273–275		Very fine sandy clay loam with 10% very fine limestone gravel	Hillwash type material probably derived from the soils of the Upper Coralline Limestone plateau
5	302–304		Mix of very fine sandy clay loam and 25–50% very fine limestone gravel	Hillwash type material probably derived from the soils of the Upper Coralline Limestone plateau
	318	1290–450 BC		
6	335–339		Finely aggregated very fine sandy clay loam with up to 50% amorphous sesquioxide staining	Possible eroded topsoil, bioturbated and humified, derived from the soils of the Upper Coralline Limestone plateau
7	403–405		Micro-laminar very fine quartz and silt, strongly reddened with amorphous sesquioxides	Episodically aggrading fine alluvial sediments
	460	2198–1985 BC		
	460–543		Black organic silt mud to highly humified peat	Shallow, freshwater marsh
8	495–497		Horizontally bedded very fine quartz sand and silt with greater/lesser zones of amorphous sesquioxides and strong humic staining, but with <10% of striated clay soil fabric similar to sample 1; few limestone clasts and minor glauconite	Brief period of mixed, disturbed, eroded soil, probably derived from the Upper Coralline Limestone plateau, deposited in a moist marshy environment
	508	3709–3541 BC		
9	515–517		Very dark brown humic fine sandy/silty clay loam; striated b-fabric with rare to few dusty clay coatings with strong birefringence; 60% amorphous sesquioxide staining	Eroded soil derived from Luvisols of Upper Coralline Limestone plateau, deposited in a moist marshy environment
10	545–547		Very fine sandy/silt with strong sesquioxide staining of clay and calcitic groundmass; very fine organics and impregnated with calcite; strong sesquioxide staining; very fine quartz silt and glauconite from the Blue Clay, carbonate clasts may have come from the plateau areas	Fine organic and calcitic alluvial sediments, strongly humified; material derived from both the Blue Clay and Upper Coralline Limestone
11	578–580		Very fine sandy/silt with strong sesquioxide staining of clay and calcitic groundmass; very fine organics and impregnated with calcite; moderate sesquioxide staining; very fine quartz silt and glaucophane from the Blue Clay, carbonate clasts may have come from the plateau areas	Fine, organic and calcitic alluvial sediments, moderately humified; material derived from both the Blue Clay and Upper Coralline Limestone
12	610–612		Heterogeneous mix of shelly micritic very fine sand/silt and 10% charred plant matter	Fine alluvial sediments with shells and included fine charred matter
13	645–647	4050–3940 BC	Very fine sandy/silt loam with >50% strong sesquioxide staining and 10–15% charred plant remains and few gypsum crystals	Alternating wet/dry fine alluvial sediments with fine charred matter incorporated, and very strong humifying conditions

Table 5.14 (cont.).

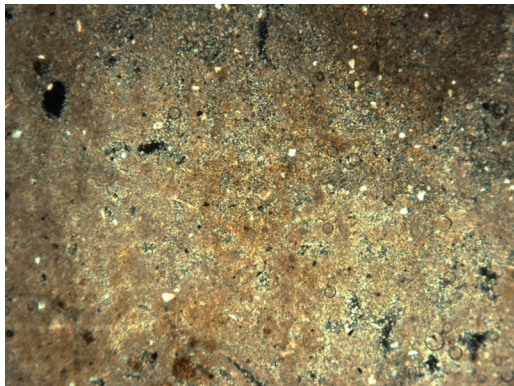
Sample number	Depth (cm)	C-14 dates cal. BC (2σ)	Micromorphology	Interpretation
	670	4326–4053 BC		
14	685–687		Micritic very fine sandy/silt loam with >50% strongly amorphous sesquioxide staining	Alternating wet/dry fine alluvial sediments with fine charred matter incorporated, and strong wet/dry humifying conditions
	718	6401–6102 BC		
15	725–727		Micritic very fine to fine sandy clay loam with abundant organic matter and root tissues; c. 50% strong amorphous sesquioxide staining; gypsum crystals and calcium carbonate nodules	Fine alluvial sediments with fine charred matter incorporated, and strong wet/dry humifying conditions, possibly marshy; with sediment derived from Blue Clay/Greensand transition
16	772–774		Very humic, shelly, micritic silt with very strong amorphous sesquioxide staining	Lithological discontinuity; fine alluvial sediments with humic and fine charred matter incorporated; and strong wet/dry humifying conditions; first freshwater shells
17	785–787		Dark reddish brown, micritic, very fine sandy silt with strong amorphous sesquioxide staining throughout; presence of fine quartz silt, silt, glauconite and gypsum	Fine alluvial sediments with strong wet/dry humifying conditions; probably derived from upper Blue Clay/Greensand zone of valley
18	823–826	6417–6244 BC	Yellowish brown, micritic, very fine sandy silt with common strong amorphous sesquioxide replaced organic matter fragments; horizontally bedded plant tissues; large pseudomorphs; infilled channels; fine calcitic material and gypsum iron-hydroxide hypo-coatings	Rooted and bedded, fine alluvial sediments with strong wet/dry humifying conditions
19	833–835		Pale yellowish brown, micritic, very fine sandy silt; common organic matter with large pseudomorphs and infilled channels; fine calcitic material and gypsum	Fine alluvial sediments, with strong humifying and drying conditions
20	868–870		Yellowish brown/grey, micritic, very fine sandy silt with small, very weakly developed sub-angular blocky peds (<1 cm) with 10% organic punctuations; strong amorphous sesquioxide staining of groundmass; first appearance of glauconite and fine quartz sand of Greensand origin	Stabilized fine alluvial sediments with some pedogenesis and strong gleying; probably derived from upper Blue Clay/Greensand zone of valley
21	913–915		A more porous and less gleyed version of sample 20	Stabilized fine alluvial sediments with some pedogenesis with some gleying
22	925–927		Weak sub-angular blocky, pale brown, micritic silty clay, with abundant channels and bedding planes; strong amorphous sesquioxide staining of groundmass	Cumulative, stabilized fine alluvial soil with some pedogenesis and strong gleying
	933	7524–7197 BC		
23	945–947		As below with minor charcoal and amorphous sesquioxide replaced organic matter, root tissues and excrements	As below
24	965–967		As below	As below
25	975–977		Dense, homogeneous, pale golden brown, micritic silty clay with vertical fine channels and horizontal bedding planes, minor organic punctuations, humified plant tissue, and sesquioxide nodules and 20% amorphous sesquioxide staining of groundmass; quartz silt and fine calcite of Blue Clay origin	Alluvial silty clay soil; probably derived from upper Blue Clay zone of valley; with evidence of alternating groundwater and secondary calcification
	990			Base of valley fill

Sample 17 (7.85–7.87 m) is significantly different from the previous samples although there is some continuity in processes. There is a continued input of fine quartz silt, glauconite and gypsum, but there is a significant increase in concentration of silt and there is abundant fine humified organic matter. This suggests that the soil environment was becoming saturated but also aerobic, with a mineral assemblage derived from the Greensand/Blue Clay boundary as below.

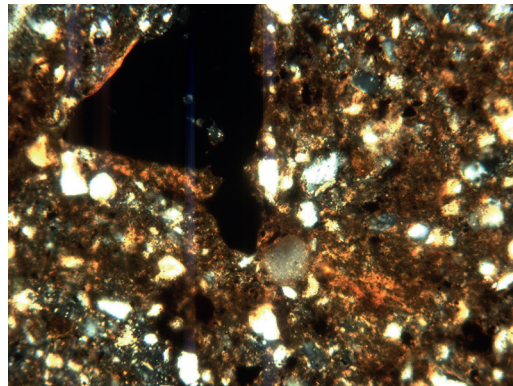
A major change in the system followed as shown by the accumulation of a thick zone of black humic mud between 5.65 and 4.05 m, after about 4326–4053 cal. bc

(5357 BP; UBA-29041) and up to at least 2198–1985 cal. bc (3704 BP; UBA-28265). Sample 16 (7.72–7.74 m) marks a lithological discontinuity with the previous samples. It is entirely organic without the quartz silts and other mineral assemblage that is typical of all the samples encountered in the lower stratigraphy of the core. The groundmass is composed almost completely of humified organic matter giving the horizon its strong brown pigmentation, with a high component of molluscan shells.

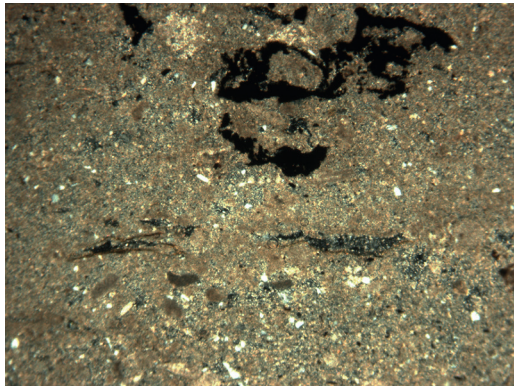
Sample 16 (7.72–7.74 m) marks a major change in the environment with shallow freshwater conditions



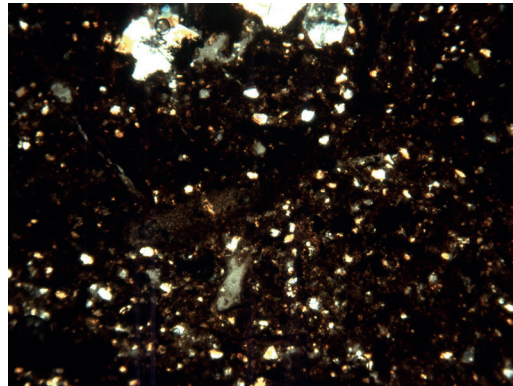
a



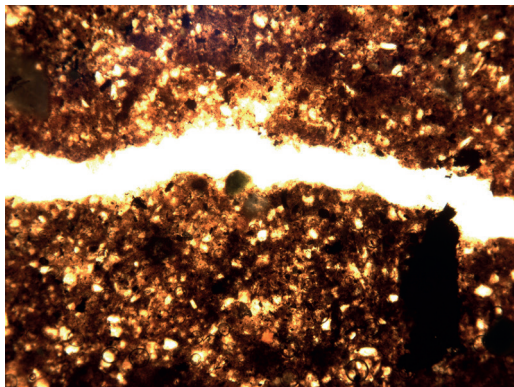
b



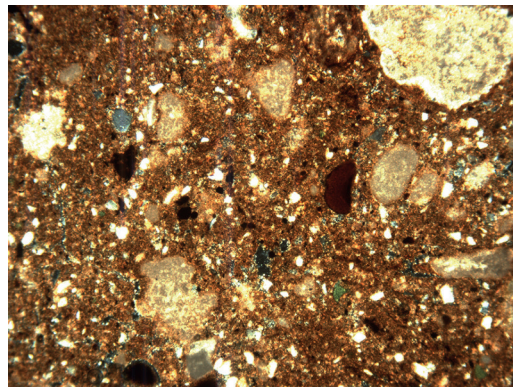
c



d



e



f

established with very little material coming into the system from soils within the valley catena. Perhaps this marks the initiation of a shallow freshwater marsh or lagoonal environment caused by sediment deposition along-shore, or perhaps an oxbow cut-off channel. This is corroborated by the molluscan data which suggest a continuing freshwater availability throughout the Neolithic, and then a major change towards the end of the Neolithic with a major erosion event (see Chapter 4). The cause of this change is unclear, but the environment was becoming significantly moister. If this were associated with increased precipitation, one would have expected greater sediment run-off, but this was not the case. Instead, there appears to have been greater stabilization of soils in the system and a greater availability of freshwater, perhaps from springs emanating from the geology (see Chapters 1 & 2) (Ruffell *et al.* 2018). Significantly this change appears to have coincided with the beginning of the Temple Period in the early fourth millennium BC. People were perhaps, for some unknown reason, interacting with soils differently for some unknown reason and this seems to correlate with the more patchy cereal cultivation observed in the pollen record at this time (see Chapter 3).

Subsequently, there was a return to fine alluvial silt accumulation, often subject to alternating wetting and drying conditions and the secondary formation of amorphous sesquioxides throughout the fabric (Fig. 5.20e). This phase of aggradation is interrupted by a period of relative stabilization at 3.19–3.35 m, a major coarser erosion phase (at 2.5–2.65 m) from c. 1300–450 cal. BC (3124 BP; UBA-31708), and then the uppermost c. 1.2 m accumulation of a calcitic silty clay as overbank alluvium (Fig. 5.20f).

Figure 5.20 (opposite). *Xemxija 1 deep valley core photomicrographs* (C. French): a) Photomicrograph of the micritic silty clay at the base of the profile, *Xemxija 1 core*, 9.75 m (4.5 mm frame width; cross polarized light); b) Photomicrograph of the illuvial dusty (silty) clays in the voids and groundmass, *Xemxija 1 core*, 9.75 m (2.25 mm frame width; cross polarized light); c) Photomicrograph of micritic very fine sand/silt, *Xemxija 1 core*, 9.45 m (4.5 mm frame width; cross polarized light); d) Photomicrograph of humic fine sand/silt, *Xemxija 1 core*, 7.85 m (4.5 mm frame width; cross polarized light); e) Photomicrograph of amorphous sesquioxide reddened, fine sandy/silty clay alluvial fabric, *Xemxija 1 core*, 5.15 m (4.5 mm frame width; plane polarized light); f) Photomicrograph of the micritic, coarse to very fine sandy silty clay alluvium, *Xemxija 1 core*, 1.99 m (4.5 mm frame width; cross polarized light).

Samples 15–12 can be grouped together. Sample 15 (7.25–7.27 m) contains abundant organic matter and root tissues within a highly calcitic sediment with large crystals of gypsum. The latter may have probably formed *in situ* through rapid drying although some of this will have come from the Blue Clay. There are large nodules of calcium carbonate that were pedogenically formed indicating not only the calcareous nature of this soil, but that sufficient drying was taking place during the year. The sediment has a relatively high porosity with inter-connecting chambers, dense clusters of faunal excrements, excremental infillings, organic punctuations and fragments of molluscs that all indicate severe bioturbation. Samples 14–12 (6.85–6.87, 6.45–6.47 & 6.10–6.12 m) are very similar with the addition of horizontally bedded organic plant tissue.

The molluscan assemblage at the same level in the core (see Chapter 4) indicates moist environmental conditions. Nonetheless it is still a dynamic environment with the presence of silt-sized quartz suggesting a re-establishment of sedimentation derived from the Blue Clay geology upslope. Radiocarbon dating of 4050–3940 cal. BC from sample 13 (5179 BP; UBA-31705) and a date of 4326–4053 cal. BC (5357 BP; UBA-29041) between samples 13 and 14 at 6.7 m suggest that this occurred just before the start of the Temple Period.

Samples 11–8 can be broadly grouped together. Samples 11 (5.78–5.8 m) and 10 (5.45–5.47 m) are a fine sandy/silt that is dominated by very fine organics and impregnated with calcite. The micromass of a brown speckled Fe-impregnated clay and calcitic crystallitic b-fabric suggest that the major component was topsoil material, although highly transformed through the process of transport and deposition. The planar microstructure and horizontal orientation of voids shows that this had been emplaced relatively rapidly, although plant tissue fragments associated with excremental fabrics within many of the voids indicate a biologically active cumulic soil. Significantly, the mineral composition of these samples suggests that there were several potential sources of the eroded soils and a significant transformation in terms of the sediment source. For the first time in the core relatively large and heterogeneous rounded carbonate rock fragments can be observed within the groundmass. The very fine quartz silt and glauconite (Fig. 5.19g) indicate a sediment source of the Blue Clay/Greensand transition, and the carbonate clasts may have come from the Upper Coralline Limestone bedrock (Fig. 5.19b) just above which is forming the plateau areas. Considered together, this evidence suggests that there was greater activity across more extensive parts of the landscape.

Sample 9 (5.15–5.17 m) is very dark in colour and is composed predominantly of fine organic material

with a high proportion of silt and sands. The groundmass is heterogeneous with a diverse fabric including aggregates of topsoil and subsoil material, and abundant fine amorphous fines exhibiting very strongly striated b-fabrics have been preserved in the weakly crystallitic b-fabric of the groundmass. These must be remnant aggregates of former topsoils and argic horizons that have been transported as sediment down-valley. These features suggest that these eroded soils had once developed on the Upper Coralline Limestone bedrock plateau under moister conditions were Luvisols, as was also concluded for the Santa Verna and Ġgantija palaeosols described above (see §5.3.2.2 & 5.3.3.3). Superimposed on this fabric are moderately impregnated, orthic, dendritic, iron-hydroxide nodules, also indicating a moist environment during their deposition. This remarkable evidence suggests that the evolution of the soil system on Malta occurred just before 3709–3541 cal. BC (4873 BP; UBA-29349) during the beginning of the Temple Period.

Sample 8 (4.95–4.97 m) is characterized by horizontally bedded very well sorted quartz silt in an organic amorphous groundmass with a high proportion of pedogenic clay in the form of striated b-fabrics, a high organic component, a small amount of glauconite, and very few carbonate clasts, larger limestone rock fragments and subsoil aggregates. The organic nature of these indicates that the soils had been forming in a relatively moist environment and elements of the whole soil profile were being eroded and deposited in the valley. Significantly the glauconite and silt components could also have been derived from the Upper Coralline Limestone plateau as could the wind sorted silt loess.

The micromorphological analysis indicates that a relatively organic rich topsoil had formed. Perhaps there had been an improvement of the soils of the plateau and this section of the core shows that people were exploiting them for arable agriculture. This was occurring just before approximately 2198–1985 cal. BC (3704 BP; UBA-28265) towards the beginning of the Bronze Age. Therefore, this is interpreted as the first stage of erosion of the rejuvenated soils of the Upper Coralline Limestone, and the interpretation is corroborated by the enriched A horizons observed in several late Temple–early Bronze Age contexts (see §5.3.2.2 & 5.3.3.3) causing the down-slope movement of organic-rich topsoil which accumulated at the base of the valley. Subsequent erosion led to the deposition of much coarser material as revealed higher in the core.

Samples 7–4 can be grouped together. Sample 7 (4.03–4.05 m) is a micro-laminar very fine quartz sand and silt, strongly reddened with amorphous sesquioxides. Sample 6 (3.35–3.37 m) is a finely aggregated, very

fine sandy clay loam with up to 50 per cent amorphous sesquioxide staining. The fine organic amorphous organic component of the micromass contains abundant silicate clay mixed in with small aggregates of humic topsoil and subsoil (Fig. 5.19h). There is little evidence for fine laminations although there are some horizontal planes suggesting sedimentation. Sample 5 (3.02–3.04 m) has a mineral component that is heterogeneous with a significant increase in carbonate clasts and clay-rich subsoil aggregates derived from the Luvisols on the plateau, and dark topsoil aggregates. The mineral assemblage is all typical of the Upper Coralline Limestone so we can be very confident as to the provenance of this sediment. Sample 4 (2.73–2.75 m) is very like sample 6 with generally fine material and the same silt component, small subsoil aggregates and the presence of silicate clay.

These features indicate that the rate of erosion had greatly increased. Soils have lost part of their upper profile as well as striated b-fabrics of the B horizon and subsoil material, all of which had developed on the Upper Coralline Limestone. These plateau soils were now being seriously eroded, probably as a result of arable agriculture. The amount of regolith and the heterogeneous nature of the fabric suggest that ploughing had been responsible for the initial dislodgement of the soil before its subsequent erosion. The one radiocarbon date from this approximate depth in the core of 1290–450 cal. BC (3124 BP; UBA-31708) suggests that this period of greater disruption in the landscape occurred in later prehistoric times, a feature which is seen repeatedly in many of the valley deep cores (see Chapter 2).

In sample 3 (2.5–2.53 m) there is a significant change with a much greater component of abraded rock clasts of up to 1 cm and subsoil aggregates containing illuvial clay and an increase in silt-sized calcium carbonate and fine charcoal fragments. These features indicate that drier calcitic soils had developed, as observed at several Temple Period sites (see §5.3.2.2 & 5.3.3.3), probably associated with a change in the soil water balance through cultivation, generally greater anthropogenic disturbance, and relatively higher energies to move this material. It is clear that the plateau soils are becoming extensively degraded, most probably through tillage.

Sample 2 (2.2–2.23 m) is similar to sample 3 with the primary difference that the mineral assemblage is slightly coarser. It exhibits a massive microstructure with associated low porosity of void planes, and all the rock fragments, whether it be glauconite or limestone, are very well rounded and moderately sorted. This is colluvial sediment, either derived from the greater erosion of the regolith and higher energy bringing

material into the valley or from erosion of the immediate upland down to the bedrock (Alberts *et al.* 1980; Mucher *et al.* 1972, 2010).

Significantly there is abundant silt-sized angular quartz present in sample 2. It is probably derived either from the weathering of the Coralline Limestone bedrock or drawn from a significant aeolian component of the soils which were emplaced upon these rocks (Hunt 1997). However, a proportion of this material could also derive from the Greensand as there is also a large quantity of glauconite, although this too also can be derived from the weathered limestone (Felix 1973). Haematite has been inherited from the subsoils of the plateau where it had formed *in situ* as a result of soil forming processes (Lindbo *et al.* 2010; Yaalon 1997). There are several other pedofeatures which indicate soil processes which had been in operation. For example, the amorphous iron-impregnative nodules indicate wetting and drying caused by a fluctuating groundwater table (Lindbo *et al.* 2010). The system is highly alkaline with dissolution and re-precipitation of calcium carbonate (Durand *et al.* 2010). As a consequence, the entire groundmass is calcitic. The stipple speckled fabric indicates clay, derived from the former soils of the plateau, although not to the same degree, perhaps indicating that some fine particles have been removed from the system altogether.

Sample 1 (1.99–2.10 m) is a fine gravelly, calcitic sandy clay loam with a low porosity, rich in clay, some silt, a few rounded grains of glauconite, and occasional limpid clay adhering to the gravel fraction (Fig. 5.20f). Redox features indicate the effects of a fluctuating groundwater table (Lindbo *et al.* 2010). It is clear that this deposit is derived from soil material that had formed on the Upper Coralline Limestone plateau (Lang 1960) as well as from the Greensand geological strata immediately above the Blue Clay (Pedley 1976), with an almost certain aeolian material which was incorporated into the soils and then subsequently moved down the valley as colluvial fill.

5.3.10.2. Wied Żembaq

The Wied Żembaq 1 core profile (samples 26–38) is dominated by the aggradation of *c.* 5.6 m of coarse to fine alluvial material from about 3331–2920 cal. BC (4428 BP; UBA-28263; at 4.95 m) until some time after 913–806 cal. BC (2707 BP; UBA-29042; at 2.15 m), associated with pollen evidence of cereal crops, disturbance and grazing land (see Chapter 3; Appendix 8; Fig. 5.21a). This alluvial material is developed on what looks like cumulative eroded soil material. In at least two phases (at 3.8–4.2 and 4.8–5.6 m), this alluvial dynamic changes to one of shallow standing water and the accumulation of organic remains, with minimal

alluvial input (Fig. 5.21b). At 3.5–3.62 m, there is a phase of severe hillwash erosion leading to the accumulation of bedrock derived fine gravel-size limestone material in the core. In the other fine alluvial phases, which constitute the bulk of the stratigraphic record here, there are often indications of fine episodic variations in the aggradation of fine material and intermittent drying out of the deposits accompanied by the formation of secondary amorphous sesquioxides (Fig. 5.21c). There are also strong hints of interruptions in the erosive sequence with incipient soil formation at depths of *c.* 3.0, 3.65, 4.33 and 5.28 m, with some sub-angular blocky ped formation, illuvial silty clays (Fig. 5.21d) and moderate to strong reddening with amorphous sesquioxides, all suggestive of some relatively short-lived phases of gleying and pedogenesis. These ‘quieter’ episodes may equate with periods when pastoralism became more predominant within the associated valley catchment (see Chapter 3).

At the base of the core in sample 38 (5.28–5.3 m), there is a reddish brown, calcitic, coarse-very fine sandy/silty clay with a great amount of quartz silt, minor very fine charcoal and a heterogeneous assemblage of mainly rounded carbonate rocks that have been rolled and abraded. There is evidence for excrements, crumbs and granules which are characteristic of topsoil or Ah aggregates as well as chambers and channels, often containing highly humified organic matter. This had been a relatively moist environment because there is a good preservation of tissue and other organics although highly humified as well as minor fine charcoal. The entire fine fabric is impregnated with calcite indicating the precipitation of carbonate rich soil water. The presence of iron nodules also suggests a fluctuating groundwater table. This sample/horizon is indicative of an aggrading, cumelic topsoil with characteristic biological activity formed on limestone parent material. The size and shape of this soil material represents loessic material that had been incorporated into the soils on the valley slopes, but was easily erodible. The included glauconite and carbonate clasts indicate that the parent material derived from the Upper Coralline Limestone geology.

Sample 37 (4.96–4.98 m) is very similar to sample 38 below, although there are some differences. It is more porous with a higher prevalence of better preserved plant tissues but these are still highly humified. There is a high proportion of silt and smaller carbonate clasts, with the mineral component fining-upwards. There are iron-hydroxide nodules suggesting a fluctuating water table. It almost certainly represents an aggrading, organic and biologically active topsoil but with slightly lower energies for the erosional processes up-profile.

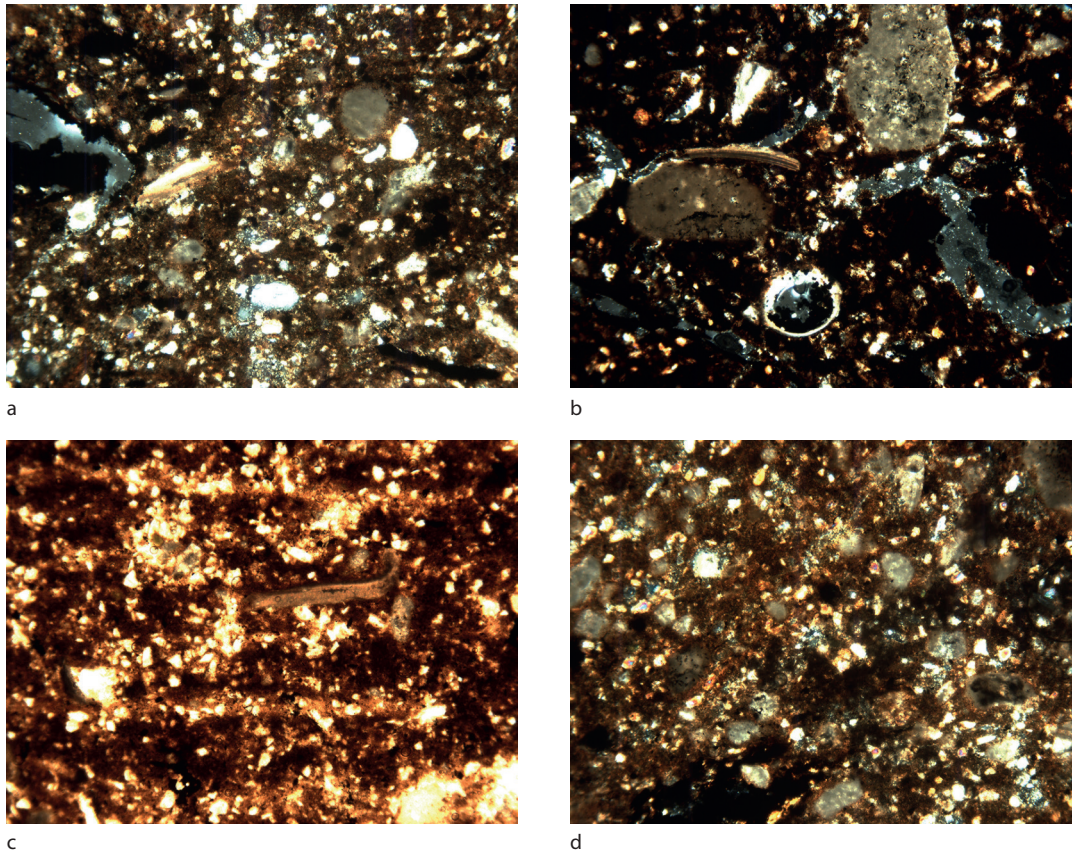


Figure 5.21. Wied Žembaq 1 deep valley core photomicrographs (C. French): a) Photomicrograph of coarse to fine sandy clay loam at the base of the profile, Wied Žembaq 1 core, 4.96 m (4.5 mm frame width; cross polarized light); b) Photomicrograph of organic accumulation, Wied Žembaq 1 core, 4.6 m (4.5 mm frame width; plane polarized light); c) Photomicrograph of episodic, micro-laminar, fine/very fine alluvial deposition, Wied Žembaq 1 core, 3.0 m (4.5 mm frame width; cross polarized light); d) Photomicrograph of illuvial dusty clay, sesquioxide formation and humic accumulation in incipient soil horizons within the alluvium, Wied Žembaq 1 core, 4.33 m (4.5 mm frame width; cross polarized light).

Sample 36 (4.6–4.61 m) is also a highly organic soil with a slightly reduced input of carbonate rock clasts and quartz silt, but there is great humification of organics and excrements associated with a very biologically active soil, and the first formation of neo-formed gypsum. There is also common calcium carbonate in the calcitic fabrics of the groundmass and in the precipitated calcite crystals in many of the voids. This is probably an incipient histic soil horizon where there is the growth and humification of organics and a high groundwater table. The gypsum is formed through a chemical reaction between calcium carbonate and sulphur compounds in the organic component (Poch *et al.* 2010), which suggests a very moist environment combined with high rates of evaporation.

The upper surface of this cumulative soil profile appears to have developed just before 3631–3373 cal. BC (4707 BP; UBA-28262; at 4.58 m). Significantly this evidence strongly suggests that soils developed

on the Upper Coralline Limestone are being eroded during this period in a manner that is consistent with evidence from the Xemxija core, all during the Neolithic Temple period.

Sample 35 (4.33–4.35 m) is similar to the previous samples of this core. It is composed of a golden/reddish brown, coarse-very fine sandy/silty clay with a large input of now humified organic material, with horizontally orientated bedding planes and a small blocky ped structure. There is a strong quartz silt component, again indicative of a loessic component. Re-precipitated calcium carbonate is common, and there are many included carbonate clasts. The presence of gypsum indicates not only a moist environment but also evaporation of soil water and the reaction of sulphides with calcium carbonate (Poch *et al.* 2010).

Sample 34 (4.1–4.12 m) is almost exclusively organic with some very fine quartz silt and a small component of carbonate rock clasts. This sample represents

Table 5.15. *The summary micromorphological descriptions and suggested interpretations for the Wied Żembaq 1 core.*

Sample number	Depth (cm)	C-14 dates cal. BC (2σ)	Micromorphology	Interpretation
26	7–9		Excremental to aggregated, porous, brown/humic, highly micritic, coarse-very fine sandy/silty clay with minor very fine charcoal	Modern alluvial topsoil, subject to strong humification and drying
27	45–7		As above	As above
28	80–2		Golden brown, micritic, coarse-very fine sandy/silty clay with illuvial silty clay infills, carbonate clasts and limestone gravel, iron hydroxide coatings and nodules, fine charcoal and bone fragments	Base of modern alluvium (as above) with periods of standing/drying water conditions
29	215–7	913–806 BC	Fine gravelly, reddish brown, micritic, coarse-very fine sandy/silty clay with minor very fine charcoal	As above, but greater energy/erosive input of coarse to fine material; possibly greater input from Upper Coralline Limestone plateau
30	253–5		Fine gravelly, golden/reddish brown, micritic, coarse-very fine sandy/silty clay with illuvial silty clay in voids, humified organic matter, gleyic features and carbonate nodules	Eroded soil material of slightly higher energy with high evapotranspiration
31	300–302		Small blocky to aggregated, golden/reddish brown, micritic, very fine sandy/silty clay, with illuvial silty clay infills and weakly laminar micro-structure	Fine, episodic stop/start eroded mix of topsoil and subsoil material; derived from the Upper Coralline Limestone plateau
32	365–7		As below with some horizontal bedding and gleying	As below; biologically active cumulic soil
33	396–8		Golden brown, micritic, coarse-very fine sandy/silty clay with illuvial silty clay infills, glauconite and carbonate clasts, plant tissues and excremental fabric	Sandy/silty clay aggrading alluvium with periods of standing/drying water conditions; derived from the Upper Coralline Limestone plateau
34	410–2		Humified and amorphous sesquioxide replaced organic matter with minor very fine quartz silt and carbonate clasts	Shallow standing water and organic, humified peat-like accumulation
35	433–5		Small blocky and finely bedded golden/reddish brown, coarse-very fine sandy/silty clay with common humified organics and very fine quartz silt	Coarse-fine alluvial aggradation with loessic additions, subject to some pedogenesis and becoming an alluvial soil
	458	3631–3373 BC		
36	460–1		Porous, very humified and amorphous sesquioxide replaced organic matter with coarse-fine limestone/quartz, micrite and gypsum	Histic organic horizon at the top of the cumulic soil with high groundwater and evapotranspiration
37	496–8		As below with greater humic matter, plant tissues and carbonate clasts	Aggrading alluvium forming a cumulic A horizon soil with periods of standing/drying water conditions, but greater energy/erosive input of coarse to fine material
38	528–30		Reddish brown, micritic, coarse-very fine sandy/silty clay with rounded carbonate gravel and glauconite, humified plant tissue and minor very fine charcoal	Aggrading coarse to fine alluvium forming a cumulic A horizon soil subject to a fluctuating groundwater table; derived from the Upper Coralline Limestone plateau

a very wet, calcareous environment where there is the growth of peat, which is amorphous because of frequent oxidation and seasonal hydrological variation.

Sample 33 (3.96–3.98 m) is quite different to the previous samples. It is quite porous with less organic pigmentation than the other samples below, but it is biologically active as seen in the amount of plant tissue

and excremental fabrics within the voids. There is abundant micro-sparite calcium carbonate, plus quartz silt, glauconite and carbonate clasts, indicative of an origin from the Upper Coralline Limestone.

Sample 32 (3.65–3.67 m) is similar to sample 33 in terms of the aggregates and crumbs, silt and carbonate clasts component, but it is exhibiting some

horizontal orientation and gleying. This soil material is a biologically active, cumulic topsoil with some evidence for sedimentation and slightly gleyic properties suggesting that there was a fluctuating groundwater table in the valley hydrology.

Sample 31 (3.0–3.02 m) it is very similar to sample 32. It is composed of topsoil aggregates, crumbs and granules with humified root tissues and organic punctuations, and strong amorphous iron-humic compounds because of recycling of organic matter. There are rounded clasts, although less than the previous samples, micro-sparitic calcium carbonate, and the same quartz silt component which suggests that this material is derived from the Upper Coralline Limestone exposures up-valley. The main difference between this and the previous two samples is the presence of a significant component of illuvial silicate clay within the soil aggregates which have formed from luvisolic subsoil parent material. Perhaps this is indicative of subsoil material being eroded and transforming into topsoil aggregates with superimposed humic compounds.

Sample 30 (2.53–2.55 m) is somewhat different from the previous samples as it is significantly more calcareous with heterogeneous rock clasts. There are abundant shell and plant tissue fragments with chambers and channels, calcium carbonate nodules throughout the groundmass, illuvial silty clay void infills, and gleyic pedofeatures. Thus this biologically active material has high evapo-transpiration despite a fluctuating groundwater table, all deposited in a slightly higher energy sedimentary environment.

Sample 29 (2.15–2.17 m) exhibits much coarser carbonate rock clasts and limestone gravel in a heterogeneous mix with a calcitic sandy/silty clay and minor included fine charcoal and bone fragments. Again, there are iron-hydroxide coatings and nodules indicating a fluctuating groundwater table. Perhaps this heterogeneous horizon indicates that regolic subsoils developed on the Coralline Limestone geology were coming into the sedimentary system through the intensification of human interaction with soils on the limestone plateau up-valley, as observed in the Xemxija core during the latter part of the Bronze Age. A radiocarbon date of 913–806 cal. BC (2707 BP; UBA-29042) for this level lends corroboration to this suggestion.

Samples 28–26 (80–82, 45–47 & 7–9 cm) can be grouped together because of their similar properties. These samples all exhibit a slightly different structure to the previous samples with a porous crumb and excremental structure with channels containing humified tissues. The brown fine material indicates humification and brunification of organic matter. The

entire system is highly calcareous and shows that calcification is a dominant soil process through the evaporation of calcium rich soil water. These features suggest that this is well developed topsoil horizon with surface vegetation formed in relatively stable conditions.

5.3.10.3. Marsaxlokk

A series of 29 small blocks were taken from this core for thin section analysis to characterize its deposits and examine the stratigraphy for evidence of eroded soil material (Appendix 8).

The basal sample 47 (3.65–3.67 m) is a very pale yellow calcitic silty clay with slight indications of gleying (Fig. 5.22c). It is 100 per cent carbonate material with no porosity and a massive microstructure. It probably represents an *in situ* weathered geological formation of the Blue Clay.

Sample 46 (3.2–3.22 m) contrasts with the previous sample. This is a dark reddish brown fine sandy/silty clay with a well developed angular blocky microstructure and a high proportion of silicate clay (Fig. 5.22a). Micro-sparitic calcium carbonate pervades the fine fabric and coats channels, and there is strong staining with amorphous sesquioxides consequent on a high and fluctuating groundwater table. This fabric represents a luvisolic (or *terra rossa*) soil which has taken time to develop in a stable environment, coincident with clay illuviation which has moved down the soil profile. It has developed through the chemical weathering of minerals, either already present in the parent material or as an aeolian component. There are some carbonate fragments showing that there is material coming from a limestone environment and very fine quartz silt. It forms a lithological and pedogenic discontinuity with the previous sample.

Sample 45 (2.96–2.99 m) is very similar to sample 46 below. It has a very well developed angular blocky microstructure with a high porosity with very large planes separating the peds. It has a silt component, abundant micro-sparitic calcium carbonate throughout, and some small carbonate clasts. The defining feature of this one is the evidence for intense calcium carbonate presence in the peds and in smaller aggregates. Fragments of the ped clasts can be seen within carbonate nodules. This shows that the entire system was moving from a de-carbonated soil environment to one dominated by calcium carbonate. There are dense infillings of sparitic and micro-sparitic calcium carbonate and hypo-coatings. All of the peds are decalcified and exhibit illuvial silty clay. These soils formed in relatively humid environments. There is repeated transpiration and re-calcification in this soil either because of changes in climate and/or vegetation complex.

Sample 44 (2.55–2.57 m) is very similar to sample 45. The main difference is that peds are larger and more well developed, and there is a greater abundance of larger carbonate rock fragments indicating an input of eroded soil material from a limestone area. It is slightly browner suggesting some organic pigmentation through humification. Although this sample is still highly calcareous, there are striated b-fabrics indicative of luvisolic properties. Sample 43 (2.15–2.17 m) is similar to sample 44, except that there is little quartz silt, perhaps indicating that the availability of loessic deposits on the valley sides in the catchment is declining. There are impregnative redox gleyic features suggesting a perched groundwater table (Lindbo *et al.* 2010).

Sample 42 (1.70–1.72 m) is very different to the previous samples and represents a lithological and pedogenic discontinuity. This is a highly calcitic and organic sediment with the organic material displaying horizontal bedding (Fig. 5.22d).

Sample 41 (1.10–1.12 m) exhibits a massive microstructure, calcareous very fine quartz silt and gleyic

properties with iron-stained fines. It contains very few minerals except the characteristic very fine quartz typical of the Blue Clay geology, as does sample 42 below. This thin section shows little soil development and probably reflects a very unstable sedimentary environment.

Sample 40 (62–66 cm) is formed from a heterogeneous mixture of different parent materials, namely from carbonate rock clasts and subsoil aggregates (Fig. 5.22b). These show strongly striated fabrics indicating illuvial clay with calcitic infillings. There are channels with remains of plant tissues, and it has been a biologically active. Iron nodules are present suggesting that there has been a fluctuating groundwater table. This material probably represents hillwash erosion from diverse and spatially extensive parts of the landscape.

Sample 39 (5–6 cm) is a brown pigmented, porous soil with a crumb and granular microstructure and plant tissue fragments and excrements in the voids which suggests that it was a biologically active topsoil. The entire fine fabric is highly calcitic and there are also redox pedofeatures suggesting a fluctuating

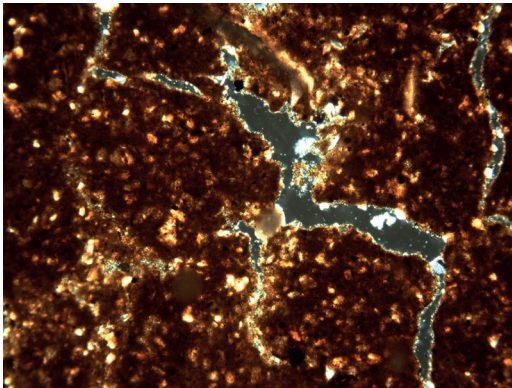
Table 5.16. The summary micromorphological descriptions and suggested interpretations for the Marsaxlokk 1 core.

Sample number	Depth (cm)	C-14 dates cal. AD (2σ)	Micromorphology	Interpretation
39	5–6		Finely aggregated, vughy, brown calcitic silt with limestone clasts	Eroded, bioturbated, xeric, calcitic silt topsoil and subsoil derived from the Upper Coralline Limestone
40	62–6		Mix of dense, pale grey weathered limestone and calcium carbonate with illuvial silty clay, iron nodules and plant tissues	Hillwash derived material from a variety of sources in the catchment
	86	AD 419–556		
41	110–2		Massive, pale grey weathered limestone and calcitic silt with minor gleying	Eroded, weathered calcitic material associated with bare surfaces upslope
	155–165		Lens of fine gravel and coarse sand	High energy erosive event
42	165–172		Micro-laminar humified and amorphous sesquioxide replaced plant remains	Repeated fine accumulations of humified plant remains under alternating wet-dry, marshy conditions
	186–192		Lens of fine gravel and coarse sand	High energy erosive event
43	215–7		Well developed sub-angular blocky structured, reddish brown, coarse to very fine sandy/silty clay loam	Aggrading alluvial soil, derived from erosion of luvisols/ <i>terra rossa</i> soils of the Upper Coralline Limestone area in catchment
44	255–7		Well developed sub-angular blocky structured, reddish brown, calcitic, coarse to very fine sandy/silty clay loam	As above
	286	AD 435–670		
45	296–9		Well developed sub-angular blocky structured, reddish brown, coarse to very fine sandy/silty clay loam with carbonate clasts and fine limestone gravel; at 286–292 cm lens of fine gravel/coarse sand	As above; with high energy erosive event interrupting soil formation at 286–292 cm
46	320–2		As above	As above
47	365–7		Dense amorphous calcium carbonate	Weathered B/C horizon of Blue Clay

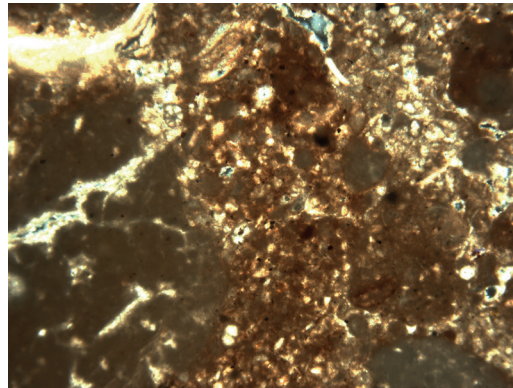
groundwater table. There are poorly sorted fossils and limestone clasts which suggests that the parent material is carbonate rock of the Upper Coralline Limestone.

Thus, this core has a different character than the Xemxija and Wied Żembaq cores. It also aggraded much later in historic times, from at least cal. AD 435–670 (at 2.86 m; 1444 BP; UBA-29351). In this case, there is a well developed, *c.* 40 cm thick, reddish brown, sandy/silty clay loam, *terra rossa*-like soil at its base. It exhibits a well developed small, sub-angular blocky structure, and its groundmass is dominated by a weakly calcitic, silty clay with moderate to strong

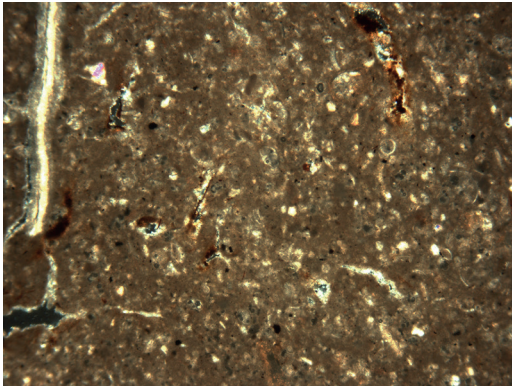
amorphous sesquioxide reddening. Above this soil, there was an episode of fine gravel and coarse sand deposition at 2.86–2.92 m, and again at 1.55–1.65 m. These latter deposits are both suggestive of relatively high energy erosive events, associated with bare rock surfaces in the catchment. There is a brief paludal, organic silt mud phase at 1.65–1.7 m, followed by the accumulation of massive calcitic fine quartz silt, possibly derived from the Blue Clay mid-slopes, and then a mixed material of calcitic silt, humic matter and illuvial clay suggestive of a variety of erosional influences from different parts of the valley hinterland.



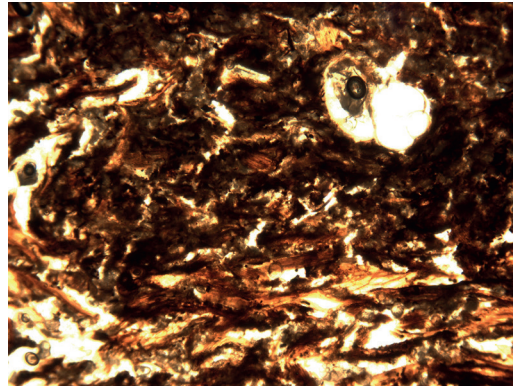
a



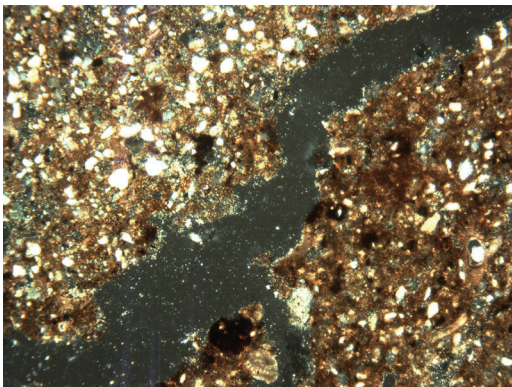
b



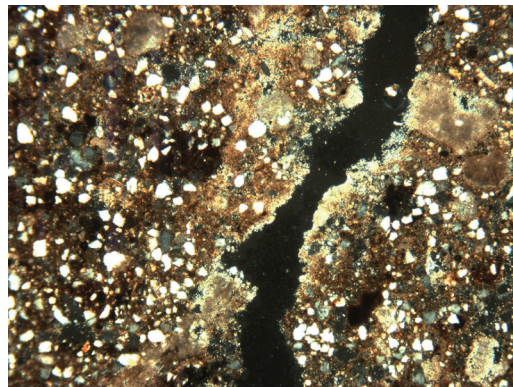
c



d



e



f

Table 5.17. The summary micromorphological descriptions and suggested interpretations for the basal zone of the Salina Deep Core.

Sample number	Depth (m)	Micromorphology	Interpretation
1	27.83–27.88	Well developed, small, sub-angular blocky, calcitic fine sandy clay loam over basal lens of fine limestone gravel	Eroded soil that has been stable for a period of time over eroded hillwash material
2	27.91–27.96	Massive, calcitic fine sandy clay loam with all voids filled with micro-sparite/amorphous calcium carbonate and 30% amorphous humic/sesquioxide staining	As below with considerable secondary influence of calcareous groundwater and wetting/drying
3	28.04–28.12	Massive, calcitic fine sandy clay loam with micritic/amorphous calcium carbonate linings of channels and iron hypo-coatings of channels, with glauconite and small limestone rock fragments	Eroded calcitic soil and subsoil, derived from the Upper Coralline Limestone

5.3.10.4. The base of Salina Deep Core

Although the Salina Deep Core (SDC) was not examined by the authors in person, it was recorded and sampled by C.O. Hunt who provided three sub-samples of the possible soil material contained in the base of core (21B) at a depth of 28.04–27.95 m (Appendix 8). Above this basal zone of soil there was a continual accumulation of eroded material from c. 6000 cal. BC to the present with the first signs of cereal cultivation occurring from about 5500–5000 cal. BC (UBA-30087/30088) (see Chapter 2).

The basal sample is a massive very fine sandy clay loam fabric (Fig. 5.22e) which exhibits sedimentation in the form of very large planes. There is a calcitic fine component of amorphous pigmented sesquioxide surrounding very well sorted quartz silt. Channels, which are almost all filled with micro-sparitic/amorphous calcium carbonate suggest that there is some residual vegetation growing on a land surface with

which this soil is associated. Redox has been intense as there are many iron hypo-coatings of channels and there is evidence for the re-precipitation of calcium carbonate indicating a calcareous soil environment. There is glauconite and small carbonate rock fragments suggesting that this material is being eroded from the Upper Coralline Limestone bedrock upslope in the valley.

The sample above is very similar although slightly more alkaline. There is some clay in the system with weakly striations superimposed on a calcitic b-fabric. This suggests that there is considerable drying and the formation of secondary calcium carbonate (Fig. 5.22f), with illuvial clay either formed *in situ* or eroded from soils in the catchment which had formed argic horizons.

The upper sample is also very similar with calcareous fine material and very fine quartz silt exhibiting a well developed sub-angular blocky microstructure comprising at least 50 per cent of the thin section with a heterogeneous mix of a wide size range of rounded to sub-angular rock clasts. The quartz shows some sedimentary properties in terms of horizontal orientation. It is suggested that this material was also derived from the Upper Coralline Limestone geology, in addition to contributions from aeolian silt, fine calcareous material and rock clasts. Subsequent soil formation developed the ped structure and gleyic soil properties through a fluctuating groundwater table.

5.3.10.5. Interpretative discussion

In three of the four cores there were good indications that buried soils and/or eroded buried soil material were present at the base of the valley core profiles. In particular at Xemxija, Wied Żembaq and Marsaxlokk, there are thick accumulations of eroded soils from their valley catchments, incrementally aggrading at different times but from as early as the seventh millennium BC at Xemxija, the mid-fourth millennium BC at Wied Żembaq and the mid-first millennium AD

Figure 5.22 (opposite). Marsaxlokk and Salina Deep Core photomicrographs (C. French): a) Photomicrograph of the sub-angular blocky, reddish brown, micritic, fine sandy clay loam, Marsaxlokk core, 2.96 m (4.5 mm frame width; cross polarized light); b) Photomicrograph of mixed fine limestone gravel and calcitic very fine sandy/silt, Marsaxlokk core, 2.15 m (4.5 mm frame width; cross polarized light); c) Photomicrograph of dense, calcitic very fine sandy/silt, Marsaxlokk core, 1.1 m (4.5 mm frame width; cross polarized light); d) Photomicrograph of laminar amorphous sesquioxide replaced and humified organic remains, Marsaxlokk core, 1.70 m (4.5 mm frame width; plane polarized light); e) Photomicrograph of calcitic fine sandy clay loam, Salina Deep Core 21B, 27.83–27.88 m (4.5 mm frame width; cross polarized light); f) Photomicrograph of calcitic channel linings, Salina Deep Core 21B, 28.08–28.12 m (4.5 mm frame width; cross polarized light).

at Marsaxlokk. These deposits also exhibit gleying features, indicative of alternating and variable more moist/dry conditions of deposition (Lindbo *et al.* 2010). Significantly at Xemxija, this early Holocene eroded soil material is aggrading through repeated alluvial additions of the same material, which is probably initially derived from the Blue Clay and Greensand geologies exposed up-slope in the valley.

Over this same period, the seventh to early fourth millennia BC, particularly at Xemxija but also at Salina and Wied Żembaq, there are a number of indications of repeated tree pollen minima at the interpolated dates of c. 6600, 6150, 5900, 5850, 5450, 4750, 4800, 4550 and 3900 cal. BC (see Chapters 3 & 11). Perhaps significantly, these are coincident with the occurrence of gypsum at Xemxija in the mid-seventh millennium BC (Table 5.14) and with two early Holocene aridification events, including the wider mid-seventh millennium BC event across the western Mediterranean and the 8.2 ka BP event (Weninger *et al.* 2006; Bini *et al.* 2018), and again at 4050–3940 cal. BC, just prior to the beginning of temple construction. This may possibly reflect periods of enhanced seasonality in a fairly dry environment, rather than overall drought, and after these two early events, increased land-use pressure at the very least.

Subsequently from about the later fifth millennium BC, eroded soil material and limestone clasts derived from the Upper Coralline Limestone plateau in the associated Pwales valley become the main source of soil material on the move in the erosion complex. This, combined with the changes in the nature of the buried soils associated with the Neolithic temple sites (see §5.3.2.2 & 5.3.3.3), points to sustained disruption of the soils in the valleys from early prehistoric times. At Xemxija during the earlier Neolithic period in the fifth millennium BC, there are inputs into the valley that indicate several landscape zones from the upper slopes of the catchment being utilized and becoming prone to erosion. At Wied Żembaq in the mid-fourth millennium BC, there is clearly the erosion of soil from the clay-rich red soils developed on the Upper Coralline Limestone plateau, also corroborating the buried soil story of disruption and change associated with the temple sites examined in this study. A remnant of these same transformed xeric *terra rossa* soils (or Luvisols) occurs in the valley base at the Marsaxlokk core site much later at about the mid-first millennium AD. All of these soil derived deposits are showing signs of strong evapo-transpiration and the secondary formation of silt-sized calcium carbonate, testifying to both the effects of aridification, poor vegetative cover and agricultural activities (Duarand *et al.* 2010; Jongerius 1993; Kooistra & Pulleman 2010). Subsequently in historic to more recent times, there is the suggestion

of irregular and mixed pulses of eroded soil material derived from all the geological substrates in the valley system, which reflects increasing disruption in the landscape associated with agricultural activities and probably also terrace construction (see Chapters 7 & 8).

At several of the core sites, there is at least one main phase of humic silt mud accumulation, pointing to a major change in the depositional environment and therefore the nature of human activity in each valley and potentially also slight differences in the wider climatic regime. The very fine and relatively minor minerogenic components of these phases of organic accumulation under shallow standing water conditions, point to a wider stability in the landscape, and greater catching of soil surface run-off water in the valley bottoms. Nonetheless, the humification of these humic silts points to strong seasonal drying. At Xemxija, the onset of these paludal, shallow freshwater, conditions at the mouth of the valley occurred from c. 4326–4053 cal. BC at a depth of 5.7 m, ceasing some two millennia later by c. 2198–1985 cal. BC at a depth of 4.6 m. This period of water run-off capture appears to bracket the whole Neolithic Temple Period and into the Early Bronze Age (see Chapters 2 & 4). In the Wied Żembaq core, the thickness of similar deposits is much reduced with two episodes of c. 40 cm of accumulation, which both probably occurred within the fourth millennium BC. These observations point to variation in periodicity, time-line and duration of periods of landscape stability and disruption occurring in each valley catchment. Indeed, the Xemxija core location may be quite different than the others, since it is captured behind a near-shore dune system on an uplifted part of the northern coastline of Malta (C.O. Hunt, pers. comm.), and this may explain its lengthy time-depth and apparent uniqueness as a potentially wet refugium resource.

In each core, the enormous volume of eroded soils from each valley catchment that has been on the move and accumulating in the valley bottoms is significant, certainly in earlier prehistoric (pre-c. 4000 cal. BC), later prehistoric (post-c. 2000 cal. BC), historic times (from the mid-first millennium BC), and more recent times in the last 100–150 years. These hillwash derived, alluvial accumulations range from at least 2.5–9 m to as much as 25 m in thickness. They are typified by the reddish brown silty clay loams and calcitic fine sandy/silty loams of Marsaxlokk and Xemxija/Salina, respectively. These re-deposited soils then remain stable for sufficient periods of time to form and exhibit a good soil structure, which suggests relatively lengthy periods of landscape stability punctuated by episodes of alluvial deposition with an almost continual slight input of fine wind-blown material. This

major landscape transformation process can only be directly associated with de-vegetation and physical disruption of the watershed valleys, and the associated Upper Coralline Limestone upper slopes and plateaux where present. The combined effects of soil disturbance through agricultural use, xerification and periodic rainfall events made the earlier-mid-Holocene highly mobile soils when they were either de-vegetated and/or with bare soil surfaces after any crop harvest. How much the investment in time, labour and energy of making the terrace systems that cover this landscape today served to halt or slow this twin process of soil erosion and alluviation remains as yet unanswered, but, at face value, does not appear to have been overtly successful until relatively recent times.

5.4. The Holocene landscapes of Gozo and Malta

The flat-topped limestone mesas of Gozo that are not occupied by towns and villages today are highly denuded of soil and vegetation. These 'garrigue' areas are characterized by shallow eroded remnants of earlier soils called Luvisols or shallow A/C type Leptosols (WRB 2014) with large areas of exposed bedrock and sparse scrub and grass vegetation (Fig. 5.23). Springs tend to emanate from just below the mesa plateau

zone, often at the Upper Coralline–Greensand/Blue Clay boundary, leading to lateral flush wet zones immediately down-slope. These are often occupied by modern cisterns and small reservoirs built by present day farmers to enhance water capture. Down the variable degrees of slope into the valleys below, it is common to see extensive exposed areas of grey silty clay on Blue Clay geology across the mid-upper slopes, situated between the Upper Coralline and Globigerina Limestones, such as occurs in the Ramla valley. Thin and variable Greensand exposures often emerge at the transition boundary between the upper part of the Blue Clay and the base of the Upper Coralline Limestone formations, usually about two-thirds of the way up-slope towards the mesa plateaux. Springs often emerge at these geological boundaries. These transitional Upper Coralline/Greensand and Blue Clay valley slope areas are commonly used for arable cereal crops today as they are relatively moisture and nutrient retentive, even if the Blue Clays in particular are 'heavy' soils that require a plough. In many valleys such as the lower Ramla and Wied il-Kibr, the limestone bedrock (of both Upper Coralline and Globigerina) outcrops in a series of low steps or inset plateaux which are all farmed today, usually with wheat, barley or vine crops (Fig. 5.24). The valley bottoms have a varied



Figure 5.23. *Scrub woodland on an abandoned terrace system and garrigue plateau land on the north coast of Gozo (C. French).*

geomorphology, but are often narrow and meandering, often scoured out and incised into the limestone bedrock through water action, and/or infilled with thick combinations of eroded coarse to fine hillwash material derived from the soils and geology upslope, with inset low plateau areas in the lower parts of the valleys, often composed of Globigerina Limestone.

In general, hillwash accumulation on the lower Blue Clay slopes is relatively thin and variable, whereas there may be up to c. 10–12 m of aggraded hillwash-derived material captured in the base of the valleys dominated by limestone bedrock, especially towards the sea. Several of the deep cores contain a distinctive captured record of soil erosion from the different geological and slope components of the valley systems (see Chapter 2 and §5.3.8 & 5.3.9). As best expressed in the Xemxija core in northeastern Malta, fine soil erosion and aggradation had begun by at least c. 7000 cal. bc with indications represented from its mineral suite and size classes that this material was at least initially derived from the upper slopes of the valley inland at the Blue Clay/Greensand geological transition. Within the Neolithic period of temple building in the fourth millennium bc this initial trend gave way to eroded red silty clay soil material derived from the Upper Coralline Limestone plateaux and other upper slopes areas of the valley.

Moving into post-Neolithic times, the erosion sequences commonly become dominated by more massive silt-sized calcitic sediments associated with the erosion and aggradation of dry, de-vegetated and degraded soils, interrupted by occasional influxes of coarse gravelly material indicative of more major erosive events. These fine/coarse calcitic sediments are commonly found aggrading in great thicknesses in valley bottoms towards the sea in most of the deep cores investigated such as Xemxija, Wied Żembaq, Marsaxlokk and Salina (see Chapter 2). In the upper Marsalforn valley this material was on the move from the mid-second millennium bc with a basal phase of relative stability dated to c. 1560–1480 bc and a middle zone of lengthier stability and soil formation dated to before c. 760 bc. In the lower Ramla valley, soil erosion accumulating in the lower valley bottom was much more recent (mid-nineteenth–early twentieth century ad) with relatively short phases of temporary soil stability and soil formation, interrupted by phases of renewed soil run-off and re-deposition. In contrast, the lower slope erosion profiles on the Blue Clay and Globigerina Limestone geologies in the Ramla valley are rarely deeper than c. 70–80 cm, and tend to be characterized by A/C type soil profiles (or Leptosols) with or silty clay or fine sandy silt soils, respectively, which have been completely homogenized by recent

ploughing activity. There is considerable modern down-cutting by flash-flood streams generated from thunderstorm events, often cutting into the bedrock by 1–1.5 m such as occurs in the Wied ta'Xhajma valley of the upper Ramla valley to the east of the In-Nuffara plateau. In many cases, land-owners have attempted to prevent further valley incision by building sets of walls at different heights and times to contain soil erosion at the base of the valley slopes, but in each case the flood event flows have continued episodically to down-cut into the Globigerina Limestone bedrock below.

In the geoarchaeological survey of the Ramla and Marsalforn valleys, very few pre-hillwash erosion buried soils were in evidence. Indeed, the best preserved earlier Holocene soils were found directly associated with the Neolithic temple sites investigated and on several modern construction sites on the Xagħra mesa. These soils were characterized by a two-horizon, well developed sub-angular to columnar blocky structured, strong red to purplish red, silty clay loam soil. This typical Luvisol or red Mediterranean soil type was probably formed under a wetter pedo-climatic regime leading to clay illuviation down-profile during the earlier Holocene, which subsequently became subject to long-term drying out and predominant secondary iron formation (Gvirtzman & Wieder 2001). It is the very eroded and transformed version of this type of soil which is now commonly found on the mesas and around their margins, such as around the margins of the Xagħra plateau.

A completely different 'brown to red' Mediterranean soil was revealed at Santa Verna beneath the earthen *torba* floors within the temple and in Test Trench B just outside the temple to the northeast (Figs. 3 & 10). In each case, these soils were thicker (c. 50–60 cm) and exhibited much better development characteristics than in the buried soils found elsewhere on the Xagħra plateau and at Ġgantija temple. Two horizons are visible, a lower more reddish brown to purply brown horizon and a slightly browner but still reddish brown upper horizon, which is indicative of both B and A horizon survival. The pelley crumb structure of the upper horizon is indicative of the base of a mollic or mull horizon of a brown earth type of soil (Gerasimova & Lebedeva-Verba 2010, 354; Goldberg & Macphail 2006, 65). In addition, the upper parts of all the profiles analysed contained significantly enhanced phosphorus values. Both inside and outside the Santa Verna and Ġgantija monuments, the transition from this lower A horizon to the B horizon is marked by a very mixed fabric of pelley/aggregated silty clay and varying admixtures of micritic calcium carbonate, which can more or less predominate. This is essentially acting as a depleted and oxidized, calcium

carbonate dominated eluvial Eb horizon. Below this, and especially in the Ashby and Trump Sondages within the interior of the temple, there is c. 20–40 cm of a clay-enriched B horizon present. This is primarily composed of a silty clay with greater/lesser degrees of striation with pure to slightly dusty clays evident, and a well developed, small blocky to columnar ped structure. This is indicative of a stable, well drained and organized, illuvial, clay enriched or argillic (or Bt) horizon (Bullock & Murphy 1979; Fedoroff 1968; Kuhn *et al.* 2010, 233ff). This type of argillic brown earth soil no longer appears to exist in present day Malta and Gozo, and its presence in a pre-early fourth millennium BC buried context at Santa Verna on the Upper Coralline Limestone of the Xagħra plateau is therefore of great significance. Importantly also, this same type of soil material was present in a very thick cumulative exposure (up to 1.1 m) in the base of the Xemxija 1 core in northern Malta, dated from about 8780–8452 cal. BC (UBA-25001) at its base to 6000–5840 cal. BC (UBA-31706) at its upper surface (see Chapter 2).

This type of palaeosol or red-brown Mediterranean soil (or Orthic Luvisol) was probably formed under a well vegetated and moister pedo-climatic regime in the earlier Holocene (Fedoroff 1997; Yaalon 1997). OSL dating of this primary soil at Ġgantija and Skorba suggests that this soil had begun to form by at least the ninth millennium BC (see Chapter 2). It is characterized first by the weathering of the limestone substrate and then by clay illuviation down-profile creating a clay enriched lower Bt or agric horizon (Verhaye & Stoops 1973). In all the buried soil profiles there is also a considerable component of aeolian dust, contributing to the ubiquitously high silt component of these soils, a feature that is widespread across the Mediterranean region (Yaalon & Ganor 1973). Strong reddening or rubification of the Xagħra palaeosols probably occurred hand-in-hand with the process of clay illuviation (Fedoroff 1997; Yaalon 1997) and rapid bio-degradation of organic material, as well as increasing calcification with time. These latter processes are probably associated with the removal and disturbance of the vegetative cover and a marked, lengthy dry season (Goldberg & Macphail 2006, 70; Gvirtzman & Wieder 2001; Yaalon 1997). It is the very eroded, disturbed and highly weathered thin base of this type of soil which is now commonly found on and around the margins of the limestone plateaux of Gozo, such as at Xagħra.

Nonetheless, this buried soil does not exhibit or preserve an upper organic litter horizon (Ah/l). The surviving A horizon and upper part of the B horizon has been disturbed and mixed throughout, largely by the soil fauna, and considerably affected by the

secondary formation of calcium carbonate and iron oxides/hydroxides. This soil mixing aspect is more evident and to a much greater depth in the profiles at Ġgantija and Skorba than at Santa Verna. These soils may also have been disturbed by physical mixing as there is often a mix of fine crumbs and small irregular blocky peds of soil in the same soil horizon, and probably also truncated by subsequent human activities associated with constructing the temples. In addition, the strong reddening or rubification (or ferrallitization) with iron oxide depletion hypo-coatings (Bridges 1978, 33; Gerasimova & Lebedeva-Verba 2010, 357), and indeed the ubiquitous formation of common micro-sparitic calcium carbonate, especially in the upper half of the profiles, suggests that this soil became open and largely devegetated, and subject to evapo-transpiration and oxidation processes (Lindbo *et al.* 2010). At Santa Verna and Skorba, this occurred just before burial by monument construction in the earlier fourth millennium BC. Nonetheless, the very high phosphorus values and fine included anthropogenic debris do suggest that there has been some kind of management of these soils in the past, undoubtedly associated with manuring and probably also the deliberate re-deposition of settlement derived refuse.

The buried soils discovered to either side of the viewing terrace on the southern side of Ġgantija temple revealed another variation in the soil story on the Xagħra plateau. On the western side beneath the late Neolithic temple blocks and a thick agricultural soil in Test Pit 1, there is a complete Ah/Bwt/C horizon brown loam soil (or Luvisol) developed on the Upper Coralline Limestone bedrock (Fig. 5.7). This soil must have formed under moister, organic, nutrient-rich conditions, unlike the present day pedo-climatic regime of dry Mediterranean with seasonal rains and a marked and lengthy dry season (Fedoroff 1997; Yaalon 1997). Nonetheless, it is exhibiting signs of fines (of silt and clay) depletion and secondary calcification and amorphous iron formation, and therefore marking a change in soil formation conditions to one that is more disturbed and xeric. Before burial by the terrace soil above, this soil has therefore become subject to evapo-transpiration and the formation of secondary calcium carbonate and to a lesser extent amorphous sesquioxides. This suggests that it had been an earlier Holocene soil similar to that which was observed beneath the nearby Santa Verna temple. It has also seen some anthropogenic influence and disturbance in terms of opening-up its vegetated surface and greater humification and transpiration processes. But at the same time, there appears to have also been some management in terms of organic input and the incorporation of later Neolithic pottery, bone, charcoal and

humic material to amend or enhance the fertility and stability of this soil. These suggestions are corroborated by the palynofacies analyses of the buried soils at both Santa Verna and Ġgantija which point to highly biologically active soils that were enriched with organic and charred material, most probably derived from settlement activity nearby (see Volume 2). Standing water bodies were probably also present nearby during the later Neolithic at Ġgantija (Ruffell *et al.* 2018), and in the very early Neolithic phase at Santa Verna, and the micro-plankton observed in the buried soils at both sites suggest the ‘slubbing-out’ of organic mud from the base of these pools of water and its addition to these soils as well as molluscan evidence from several deep valley cores such as Xemxija on Malta during the Temple period for marshy and standing water areas (see Chapters 3 & 4).

On the southeastern side of Ġgantija in the WC Trench there is a well preserved variant of this same soil profile. Here the buried soil is buried by thick mixed soil-midden deposits with plentiful included Neolithic artefactual material with a radiocarbon date suggestive of burial by *c.* 2580–2300 cal. BC (UBA-33707). The soil itself has a similar Ah/Bwt/C profile to that observed in TP1, although it is just beginning to show signs of reddening with depth and calcification through drying

effects. Thus both these Ġgantija profiles appear to be a ‘half-way’ soil-type in development terms between a brown and a red Mediterranean soil, with the Ġgantija soil formation sequence more altered as a result of a longer period of continuing human use and disturbance, in contrast to the Santa Verna palaeosol which was buried about 1000–1300 years earlier. A similar sequence of formation events was also evident in the buried soil profiles at Skorba, although it was occurring much earlier in the early fourth millennium BC as at Santa Verna.

The variable expression of mixing, oxidation and secondary calcium carbonate and amorphous iron forming processes imply that the original thick and well developed soils at Santa Verna are on the cusp of major pedogenic change from a brown to red Mediterranean soil. This change is best seen in its early onset form at Santa Verna in the Ashby and Trump sondages, and is much more advanced in both the Skorba and Ġgantija buried soil profiles. This transitional process of soil change is no doubt associated and aggravated by the human use of this part of the Xagħra plateau, in terms of clearance and temple construction, and undoubtedly also associated settlement and agricultural activities. Significantly, this major soil change may also be reflective of a wider change in the moisture and vegetational



Figure 5.24. Terracing within land parcels (defined by modern sinuous lanes) on the Blue Clay slopes of the Ramla valley with Xagħra in the background on the Upper Coralline Limestone plateau, probably established by the Order of St John in the sixteenth century AD (C. French).

regime, from a moister and well vegetated landscape to one with a low but periodic rainfall, poor moisture retention and general aridification or xeric processes, which are all at work by the time of temple construction from about 3800 cal. bc onwards and through the first half of the third millennium bc. Nonetheless, there are clear signs of management of these soils in this same time frame through the addition of settlement derived midden debris in an attempt to enhance these soils, most probably for arable agricultural use.

In the valley bottom about 500 m to the south of Ta Marżiena, there was a well preserved reddish brown silty clay loam preserved beneath about 90 cm of silty clay loam, possibly of colluvial origin derived from the silty clay shallow slopes to the north. The presence of a buried soil here as well as on the mesa top at Xagħra and Santa Verna strongly suggests a once greater ubiquity of red/brown Mediterranean soils in this landscape, based on the observation of other capture zones of eroded earlier Holocene soils in the Xemxija and Wied Żembaq cores for example.

One notable land-use feature was observed in the Ramla valley between Ġgantija and In-Nuffara, especially on the southeast-facing slope of the valley. Large rectilinear parcels of land, probably dating from the knights of the Order of St John 'colonization' of this area from the sixteenth century AD (see Chapters 9 & 10), occupy the exposed Blue Clay geology valley slopes (Fig. 5.24) (Alberti *et al.* 2018). This is notable in that this geology now supports thick, homogeneous, silty clay vertisols with a groundwater table close to the surface in many places, making these soils both moisture retentive as gleys but at the same time relatively intractable in terms of ease of ploughing until the arrival of machinery. This could imply that these clay valley slope zones were the last to be cleared and taken into private ownership as it was relatively hard land to farm (but not nutrient poor), requiring either metal-tipped ploughs and/or animal-drawn or mechanized ploughs.

5.5. A model of landscape development

On the basis of the geoarchaeological survey and the buried soil analyses, it is now possible to propose the following model of landscape soil development and land-use for the central area of Gozo around Xagħra as well as in the north/northeastern part of Malta around Skorba during the Holocene.

The thick purplish red, columnar to sub-angular blocky ped silty clay soil with distinct clay-enrichment that is observed deeply set into fissures in the Upper Coralline Limestone on the Xagħra town mesa conforms to classic *terra rossa* of the soil classification

systems (Bridges 1978, 69). These soils may have their origins to be in the last interglacial period (van Andel 1998; Catt 1990), but are generally understood to be the climax soil type present for this parent material in a strongly seasonal, semi-arid Mediterranean landscape (Bridges 1978; Duchaufour 1982; Durn 2003; Lang 1960; Yaalon 1997). The geoarchaeological and micromorphological study presented here strongly supports this to be the case with well developed brown luvisolic soils developed by the early Neolithic or the seventh–fifth millennia bc on the Upper Coralline Limestone geology on Gozo and Malta. These soils slowly but surely degraded to become thin red, calcitic soils through the combined effects of human intervention and xerification during the Neolithic and later prehistoric periods.

This earlier Holocene brown Mediterranean soil was thick (up to c. 80 cm), had a higher percentage of soil organic matter, was well structured (blocky or columnar) and multi-horizonal (Ah/Eb/Bwt/C) loam, with evidence of clay illuviation in a clay-enriched Bt or argillic horizon towards its base. It was undoubtedly associated with a moister climate with higher annual precipitation which supported an increased biomass, a sparse, scrubby woodland vegetation, all leading to good stability and reasonable moisture retention. The palynological and molluscan studies of the *FRAGSUS Project* appear to corroborate this theme of relatively sparse, scrubby woodland cover for much of Gozo/Malta in earlier Neolithic times with a greater availability of freshwater in many of the valley systems (see Chapters 3 & 4). This soil type appears to have been largely confined to the upper third of the valley slopes and on the mesa plateaux, and directly associated with the Upper Coralline Limestone geology. It is suggested that this soil was just beginning to become transformed by the time that the Santa Verna temple was being built in the early fourth millennium bc, and indeed the buried soil at Santa Verna exhibited characteristics that indicate that it was buried right at the cusp of change. This same trajectory of change was slightly further developed at Skorba by the same period of the early fourth millennium bc. In contrast, the buried soils present at Ġgantija temple indicate that this soil had become fully transformed to a calcitic, poorly structured soil by the middle of the third millennium bc. But at both Skorba and Ġgantija, the soils were already being amended and improved through the deliberate addition of settlement-derived organic waste during the Temple period, and subsequently at Ġgantija became subject to terrace soil aggradation by the mid-/later second millennium bc.

In some valleys, there are very early signs of landscape disruption and soil erosion taking place from

the Blue Clay/Greensand boundary zone of the upper valley slopes from the early Neolithic if not before. By the time of the main development of the Neolithic Temple Period, this erosion signature was shifting to the erosion of the well developed soils derived from the Upper Coralline Limestone. Moreover, there is a much greater influence of freshwater in the valley bottoms at the same time, suggesting that there may have been contemporary greater rainfall and greater spring activity in the valley landscapes during the same period. These features are best expressed in the Xemxija core and associated valley system as well as at Wied Żembaq on Malta.

In contrast to Xemxija and Wied Żembaq, the slopes of the Ramla and Marsalforn valleys on Gozo were initially quite stable, possibly associated with scrub woodland on the Blue Clay geology and vertisol exposures in the middle-lower slope zones. Streams/rivers in the valley bottoms were quite small, meandering and relatively stable. The upper-middle parts of the valleys appear to have suffered from hillwash erosion and aggradation such as observed at Marsalforn where there was significant erosion off the Coralline Limestone upper slopes throughout much of the second and first millennia BC. In contrast, the lower clay slopes of the Ramla valley appear not to have been subject to any significant colluvial aggradation through hillwash and slope processes, whereas there are several metres of relatively recent/last century coarse/fine colluvial aggradational fills in the valley bottom towards the sea, occasionally interrupted by variable lengths of relative stability and incipient soil formation. These more aggressive erosional features appear to be a much later feature of the last couple of centuries, and are undoubtedly associated with agricultural activities on the upper and lower slopes, in spite of terracing. In contrast, in several places within the lower Ramla valley for example, there are very fine silt-rich (or loessic) soils on low upstanding mesa exposures of Globigerina Limestone at about c. 5–20 m above the valley floor. These naturally very fertile silt soils are where modern vineyards are situated which would have provided a long-term nutrient-rich resource for arable farming in the past as well. The evident variation in soil and erosion histories from valley to valley suggests that there is no one synchronous sequence of erosion across the Maltese Islands in prehistoric times, rather multiple variations in time, space and characteristics, dependent on the human–landscape interactions in each valley system.

The one consistent feature which is absolutely clear is that the well structured, clay-enriched brown soil-type observed repeatedly on several of the limestone mesa plateaux was probably the climax Holocene

soil type for the Gozo and Malta islands by the early Neolithic period/sixth millennium BC, as previously hypothesized for many parts of the Mediterranean region (Bridges 1978; Lang 1960; van Andel 1998). Through a combination of human activities associated with clearance and agriculture, it is very clear that soil type change had begun during the Neolithic period. Soils on the mesa plateaux became characterized by a reddish brown, secondary amorphous iron oxide and calcium carbonate dominated, fine sandy/silt loam soil, as seen today in the fields outside the temple areas at Ġgantija, Ta Marżiena, Santa Verna and Skorba. This soil type change was occurring in the fourth and third millennia BC just before and during the Temple Period. Importantly, the continuing human exploitation of these soils, combined with drier climatic conditions from at least 2300 cal. BC and certainly from the second millennium BC onwards (Carroll *et al.* 2012; Magny *et al.* 2011; Sadori *et al.* 2013) (see Chapters 2 & 3) led to significant secondary soil formation and erosion processes taking precedence. Initially this was marked by clay and iron movement via the soil water system and their redeposition down-profile, but then increasingly the formation of silt-sized calcium carbonate associated with xerification. In combination, these now organic depleted and poorly structured soils became thin, single horizon, highly iron impregnated and calcium carbonate dominated, xeric red or pale grey soils (Aguilar *et al.* 1983). As an associated consequence, these thin and poorly structured soils also became very prone to erosion especially without well vegetated ground cover (Butzer 1982; Kwaad & Mucher 1979).

This model of soil change is the most probable scenario, and there is excellent corroborative soil evidence at both Santa Verna and Ġgantija on the western part of the Xagħra plateau, and at Skorba in northern Malta. At Santa Verna, the buried soil found beneath the *torba* floors is a dark brownish red reflecting the down-profile illuvial movement of clay creating a stable and well structured, clay enriched soil that soon becomes dominated by the secondary formation of iron oxides. This is the type of soil change trajectory that occurs when a well vegetated, moist, humic brown soil becomes subject to some disturbance and oxidation. This soil appears to be a precursor soil to the calcitic reddish brown soils observed at Skorba and Ġgantija, but not necessarily for the off-site, Xagħra red soils. In many respects, it appears that the soil development catenas between Santa Verna and Ġgantija, and also at Skorba, are tracing the beginnings of soil change associated with use and disruption of this landscape that began to occur just before the main construction of these temples in the early fourth millennium BC.

The slightly different development trajectories of the buried soils present at each Neolithic site investigated could be associated with the building chronologies of these temple sites. From the comprehensive new set of AMS radiocarbon dates made available by the *FRAGSUS Project*, the Santa Verna and Skorba temples began construction much earlier at about 3800 cal. BC as opposed to c. 3400–2500 cal. BC at recently excavated areas of what may be the later phases of Ġgantija (see Chapter 2 & Volume 2, Chapters 4, 5 & 7). This apparent time-depth differential and lengthier exposure may explain the greater xeric qualities of the Ġgantija profiles versus the better developed earlier buried soil profiles present at Santa Verna and Skorba for example, and indeed the unknown longer potential exposure of the Xagħra house construction site profiles and the Taċ-Ċawla settlement site in Rabat.

The observed soil formation sequence at these temple/mesa plateaux sites suggests that the single horizon, dry, red calcitic soils with thin organic A horizons (or Leptosols) were becoming the norm on the Upper Coralline Limestone geology of the mesa plateaux areas of Gozo and Malta from at least beginning of the fourth millennium BC, and were very well established by the third millennium BC. Associated and subsequent over-use for arable and grazing land, de-vegetation and disruption of the landscape led to gradual and continuing denudation and depletion, coincident with the widespread soil erosion and the establishment of an impoverished garrigue flora, thus creating the landscape we see today.

Later prehistoric and early historic agriculture in combination with the dry Mediterranean climate kept these thin xeric soils ubiquitously present on most of the higher/upper parts of the Gozo/Malta landscape, ostensibly associated with the Upper Coralline Limestone. These red soils probably thinned with time and became less moisture retentive, more iron- and calcite-rich, and less fertile, unless subject to continual amendment with household waste and domestic livestock manure, and/or a mixed pasture, fruit tree and arable use. At Ġgantija for example, there does appear to have been a concerted attempt at amending and enhancing the fertility and thickness of the later Neolithic topsoil with domestic refuse. Nonetheless from at least the Neolithic period (or fourth–third millennium BC), soil erosion has also been a factor in causing slope erosion and valley infill processes in many parts of Malta/Gozo (see Chapter 2) as well as Europe more broadly (*cf.* Bevan & Conolly 2013; Brandt & Thornes 1996; Grove & Rackham 2003; Hughes 2011; Imeson *et al.* 1980; Kwaad & Mucher 1979; Thornes 2007). Stratigraphic records recovered from a number of valley sites in Malta in the *FRAGSUS Project* (see

Chapter 2) and through earlier palynological work on Malta (Carroll *et al.* 2012) and similar intensive studies in this volume (see Chapter 3) suggest continuing disruption of the landscape associated with agricultural exploitation from at least the sixth millennium BC, and especially from c. 2300 cal. BC with increasing aridification. In addition, recent palynological work on Malta suggests coincident disruption of the landscape as marked by a gradual decline in the scrub and tree vegetation (and see Chapter 3), which became more pronounced from c. 4000 cal. BC onwards and especially from c. 2300 cal. BC, and perhaps even the relative ‘abandonment’ of arable agriculture in the late third millennium BC with an associated greater emphasis on pastoral activities (Carroll *et al.* 2012; Djamali *et al.* 2013). Together these evident signals of deterioration in the landscape could have prompted the development and onset of terrace construction, especially on the Coralline Limestone upper slopes, in an effort to slow landscape degradation, but secure archaeological evidence remains far from convincing (and see Chapter 11).

The human exploitation of these transitional brown to red soils during the Late Neolithic period was followed by drier climatic conditions probably from the late third millennium BC onwards, a consistent feature also observed across much of the Mediterranean area (Carroll *et al.* 2012; Magny *et al.* 2011; Morris 2002; Sadori *et al.* 2013), and in the palynological and molluscan studies conducted in this project (see Chapters 2–4). It is the xeric moisture regime of strong seasonal winter/summer rainfall contrasting with winter rainfall in excess of evapo-transpiration versus a lengthy period of the drying out of the root zone in the soil over the summer months which defines the climatic constraints on soil formation in Malta and elsewhere in the Mediterranean region (Yaalon 1997). In combination with human use of the mesa plateaux and the coincident removal of vegetation, there were the associated processes of soil moisture loss, de-stabilization and humic and fines depletion. Consequently, a number of significant secondary soil processes then took precedence, predominantly the bio-degradation of the humic components and the common formation of silt-sized calcium carbonate, as well as clay and iron movement and their re-deposition down-profile leading to finer and denser soil fabrics and strong soil reddening. These combined processes resulted in the development of thin, organic depleted, highly iron oxide impregnated xeric soils which were becoming increasingly dominated by secondary calcium carbonate formation (Aguilar *et al.* 1983). These secondary processes changed the earlier Holocene soil type and moisture-vegetation balance once and for all.

From the evidence gleaned in the geoarchaeological survey, valley slope hillwash deposits range from slight to substantial. For example, earlier Neolithic soil erosion is evident in the deep Xemxija core from the seventh millennium BC and at Wied Żembaq in the mid-fourth millennium BC, but much of the valley fill in the Marsalforn valley is of later prehistoric age (mid-second to first millennium BC), and in the Ramla valley of the late nineteenth–early twentieth century AD. Moreover, most of the deep valley cores show a major step increase in erosion from after about 2000 cal. BC (see Chapter 2). Thus it is suggested that exploitation of the wider landscape became more and more extensive during later prehistoric times, with greater and lesser phases of major intensity, a feature corroborated by the deep valley core stratigraphic records and palynological analyses (see Chapters 2 & 3).

In the Marsalforn valley, thick hillwash accumulations of highly calcitic, rubbly, fine sandy and silty soils have continued for some time, undoubtedly associated with arable agricultural activities upslope. This was taking place long after the major soil and climatic changes in the mid-/later Neolithic, from at least the mid-second millennium BC and throughout much of the first millennium BC (Table 12). The already calcitic/xeric soils that are on the move down-slope as overland flow imply substantial and severe disruption on the hill-slopes above, and strongly suggest the physical disruption of bare soils. This could well have been associated with the construction of terrace systems in this valley. In many respects, the Marsalforn sequence is probably more typical of the island, where the original soils are either long gone through down-slope erosion, and/or so deeply buried and present only as remnants such that it is extremely difficult to discover and recover them.

In contrast, the largely silty clay loam dominated Ramla valley slope soils appear to have remained relatively stable at the time that the soils on the Upper Coralline Limestone geology were being transformed during the Neolithic and later prehistoric times. In addition, the intractability of these clay and silt dominated vertisols developed on the Blue Clay geology valley slopes (Vella 2003) meant that they were best avoided for arable agriculture until the arrival of metal-shod, mould-board ploughs, at least from Roman times onwards (Margaritis & Jones 2008). Despite some indications of initial erosion from the Blue Clay/Greensand zone of the upper valley slopes in some valley sequences, it is suggested that the Blue Clay slope areas would have probably largely remained as scrub woodland and/or grassland for grazing for most of prehistoric times. There are also numerous springs emanating from the upper and lower contacts of the clay with the limestone

geology which would have provided natural water sources and wet areas for reed and sedge growth (as they still do today), all suitable as roofing/building materials for example. There are also hints of Roman period settlement activity towards the base of slope down-valley, such as at Ramla Bay (Ashby 1915), which was undoubtedly utilizing similar landscape features.

Finally, there were many landscape modifications occurring from the later medieval period (mid-sixteenth century AD) onwards (Blouet 1997; Carroll *et al.* 2012; Wettinger 2011). Certainly the Ramla valley slopes become systematically exploited in the sixteenth century AD crusader Order of St John period and again in the mid-nineteenth century AD (Alberti *et al.* 2018; Blouet 1997) with two sets of superimposed systems of field boundaries and sinuous property boundaries located up/down the slopes (Fig. 24) (see Chapters 8–10). This combined extensification and intensification of landscape development may well have been associated with pressure on land to enable more sustainable arable agriculture to support the island population (see Chapters 7 & 8), but was also related to the use of better plough machinery and importantly the presence of reliable water sources from the natural spring lines in each valley.

There has been significant exploitation of the valley slopes and Blue Clay geology areas over the last five centuries or so (Grima 2008a), and as seen in the *Cabreo* maps of AD 1861 (Alberti *et al.* 2018). This agricultural expansion has undoubtedly led to increased down-slope erosion off the clay slopes and mixed accumulations of limestone rubble, sand and silty clay materials as hillwash in the valley bottoms such as in the lower Ramla, and confirmed by later nineteenth to early twentieth centuries AD OSL dates (Table 2.6). Nonetheless, there is some degree of balance and resilience in this landscape imposed through the widespread remodelling of the landscape with terrace systems. Today, this apparent landscape stability is interrupted by intense individual thunderstorm events which remove any easily erodible soils out to sea and contribute to continuing incision into the bedrock basement of the valleys by 1.5 m or more.

Since the 1960s, there has been continuing transformation of the Gozitan and Maltese landscapes with widespread clearance and uptake of arable land in the valleys and slope areas and expanding town-scapes on the limestone plateaux (Vella 2003). There has been soil removal and re-deposition as deliberate amendment of the thin red soils around the mesa margins using silty clay soil taken from the mid-/upper slope area on Blue Clay geology. For example, this occurred in the fields on the eastern side of Ġgantija temple in 1961 and again in 1985. At the same time, many of

the mesa plateaux areas have become more and more occupied by urban development, especially since the 1980s, perhaps as a corollary of the poor state of soil development on these plateaux.

Today, the landscape is extensively terraced and farmed for arable cash crops, olives and vines. In contrast, pastoral use for sheep/goat has largely recently disappeared, a casualty of EU marketing regulations. The natural springs at the upper Blue Clay/Greensand–Upper Coralline Limestone contacts survive, and the landscape is also relatively stable, although heavy rainfall events still lead to surface water and soil run-off to the sea that can be severe.

5.6. Conclusions

Geoarchaeological fieldwork on the island Gozo focused on the Ramla and Marsalforn valleys and the associated Neolithic archaeological sites at Ġgantija and Santa Verna, the Taċ-Ċawla settlement site, Ta' Marżiena temple and the Skorba temple as well as a number of deep valley sites such as Xemxija and Wied Żembaq on Malta. This study has suggested a new model of soil development for the early to mid-Holocene which especially shows the impact of Neolithic and later historic period communities on the soil/landscape system. It is suggested that a well developed, thick, moist, vegetated and clay-enriched brown soil or Luvisol had developed on several of the limestone plateaux areas of the Maltese Islands in the earlier Holocene. Similar brown argillic soils were

probably once more widespread in the Maltese Islands and indeed the wider Mediterranean region (cf. Yaalon 1997). This soil type exhibited signs of disturbance from at least the earlier Neolithic period at some notable locations on both Gozo and Malta, but then witnessed the beginnings of major soil changes associated with both aridifying and de-vegetation trends trend from at least the beginning of the fourth millennium BC. This trend intensified throughout the third millennium BC and the later prehistoric periods, with soil erosion and its re-deposition being major factors in modifying the plateaux and valley landscapes, especially taking place from the mid-second millennium BC. These transformations set the scene for the subsequent palaeoenvironmental record characterized by thin, dry, calcitic soils and open xeric landscapes from the late third millennium BC onwards. Of course, these soil development trajectories need not have occurred everywhere on the Maltese Islands in the same manner, nor over the same time frames. Although there are repeated signs of fine soil erosion from the Blue Clay, Greensand and Upper Coralline Limestone geologies as exposed in most of the valleys on Malta from at least the beginning of the seventh millennium BC, it was probably not until post-mid-sixteenth century AD times that the Blue Clay, or silty clay vertisol, valley slope landscapes began to be exploited for agriculture in any intensive and extensive way, and especially during the second half of the nineteenth century AD, leading to later erosional aggradation in the lower valleys such as the Ramla in northern Gozo.

Temple landscapes

The ERC-funded *FRAGSUS Project (Fragility and sustainability in small island environments: adaptation, cultural change and collapse in prehistory, 2013–18)*, led by Caroline Malone (Queens University Belfast) has explored issues of environmental fragility and Neolithic social resilience and sustainability during the Holocene period in the Maltese Islands. This, the first volume of three, presents the palaeo-environmental story of early Maltese landscapes.

The project employed a programme of high-resolution chronological and stratigraphic investigations of the valley systems on Malta and Gozo. Buried deposits extracted through coring and geoarchaeological study yielded rich and chronologically controlled data that allow an important new understanding of environmental change in the islands. The study combined AMS radiocarbon and OSL chronologies with detailed palynological, molluscan and geoarchaeological analyses. These enable environmental reconstruction of prehistoric landscapes and the changing resources exploited by the islanders between the seventh and second millennia BC. The interdisciplinary studies combined with excavated economic and environmental materials from archaeological sites allows *Temple landscapes* to examine the dramatic and damaging impacts made by the first farming communities on the islands' soil and resources. The project reveals the remarkable resilience of the soil-vegetational system of the island landscapes, as well as the adaptations made by Neolithic communities to harness their productivity, in the face of climatic change and inexorable soil erosion. Neolithic people evidently understood how to maintain soil fertility and cope with the inherently unstable changing landscapes of Malta. In contrast, second millennium BC Bronze Age societies failed to adapt effectively to the long-term aridifying trend so clearly highlighted in the soil and vegetation record. This failure led to severe and irreversible erosion and very different and short-lived socio-economic systems across the Maltese islands.

Editors:

Charles French is Professor of Geoarchaeology in the Department of Archaeology, University of Cambridge.

Chris O. Hunt is a Professor in the School of Biological and Environmental Sciences, Liverpool John Moores University, Liverpool.

Reuben Grima is a Senior Lecturer in the Department of Conservation and Built Heritage, University of Malta.

Rowan McLaughlin is Senior Researcher in the Department of Scientific Research at the British Museum and honorary research scholar at Queen's University Belfast.

Caroline Malone is a Professor in the School of Natural and Built Environment, Queen's University Belfast.

Simon Stoddart is Reader in Prehistory in the Department of Archaeology, University of Cambridge.

*Published by the McDonald Institute for Archaeological Research,
University of Cambridge, Downing Street, Cambridge, CB2 3ER, UK.*

Cover design by Dora Kemp and Ben Plumridge.

ISBN: 978-1-902937-99-1



UNIVERSITY OF
CAMBRIDGE

